1-1-2011

Compensatory renal hypertrophy, mitochondria and redox status

Bavneet Benipal
Wayne State University,

COMPENSATORY RENAL HYPERTROPHY, MITOCHONDRIA AND REDOX STATUS

by

BAVNEET BENIPAL

DISSERTATION

Submitted to the Graduate School

of Wayne State University,

Detroit, Michigan

in partial fulfillment of the requirements

for the degree of

DOCTOR OF PHILOSOPHY

2011

MAJOR: PHARMACOLOGY

Approved by:

Advisor Date

DEDICATION

I dedicate this work to my family and friends that helped me in reaching my academic goals and become the person I am today. I would like to give the most recognition to the following people:

My parents, Sukhpal and Lakhbir Benipal who have been my role model for hard work throughout my whole life. I deeply appreciate their love, support, encouragement and faith in me. My grandfather, Raghbir Benipal who always emphasized the importance of education and provided me unconditional encouragement and support.

ACKNOWLEDGMENTS

My deepest gratitude is to my mentor, Dr. Lawrence H. Lash. I have been fortunate to have an advisor who provided me an independent environment to develop my project and at the same time the guidance and support to overcome many challenges and finish this dissertation.

I would also like to thank my committee members, Dr. Thomas Kocarek, Dr. Todd Leff, Dr. Roy McCauley and Dr. Julie Boerner for their valuable advice and constructive criticism at different stages of my research. I would also like to acknowledge David Putt for his invaluable assistance and long discussions that helped me improve my knowledge and sort out the technical details of my work. I truly appreciate his encouragement, supervision, patience and most importantly, his friendship over the last few years.

Finally and most importantly, I would like to express my gratitude to my family, who has been a constant source of love, support and strength all these years.

TABLE OF CONTENTS

Dedication ……..…..…… ii

Acknowledgments ……..…….. iii

List of Tables …… x

List of Figures ……..……. xi

List of Abbreviations ……..……. xiii

CHAPTER I. INTRODUCTION …….. 1

Reduction in functional renal mass ……. 1

Compensatory renal hypertrophy: Cellular and molecular events underlying compensatory renal hypertrophy ……. 5

Compensatory renal hypertrophy, mitochondria, nephrotoxicity and clinical complications ……. 7

Function and importance of thiol redox status in renal function in proximal tubules .. 10

Pathways of glutathione transport in renal proximal tubule ……. 18

Mitochondrial GSH status, transporters, and mechanisms of renal mitochondrial GSH transport …… 23

Significance of mitochondrial GSH transport in protection from oxidative stress … 27

Goals of present study ……..... 29

CHAPTER II. MATERIALS AND METHODS ……..... 33

Animals ……..…….……..... 33

II-1 RENAL FUNCTION AND MITOCHONDRIAL STATUS …… 34

Chemicals …….…… 34

Methods ……..... 34

In vivo assessment of renal physiological parameters ……..…. 34

Determination of protein expression of renal plasma membrane organic anion transporters by Western blot analysis ……. 35

Determination of protein expression of renal mitochondrial GSH transporters and redox status proteins by Western blot analysis …….…… 36

Analysis of gene expression by real-time PCR ……..…….. 37

Determination of mitochondrial GSH status …….. 37

Enzyme assays and protein expression ……...…… 37

GSSG reductase assay ……. 38

GSH peroxidase assay ……..……..……... 38

GSH *S*-transferase assay …….……. 38

Glutamate dehydrogenase assay ….....……. 38

Malic dehydrogenase assay …..……..……..... 39

Succinate: cytochrome c oxidoreductase assay ……..... 39

Protein determination ……... 39

Mitochondrial oxygen consumption ……. 40

Mitochondrial proteomics …… 40

Assessment of basal and toxicant-induced mitochondrial oxidative stress …… 41

Lipid peroxidation by malondialdehyde assay …….. 41

Lipid peroxidation by cis-parinaric acid fluorescence assay …… 41

Mitochondrial aconitase activity …….. 42

Analysis of oxidative stress markers by Western blot analysis …… 42

Effect of toxicant (tBH) on mitochondrial protein expression during compensatory renal hypertrophy …… 43

Data analysis ……. 43

II-2 STUDIES IN PROXIMAL TUBULAR CELL PRIMARY CULTURES …… 44

Chemicals …….. 44

Culture of rat proximal tubular cells …… 44

MitoTracker™ orange staining ..…….. 46

JC-1 (5,5',6,6'-tetrachloro-1,1',3,3'-tetraethylbenzyimidazolyl-carbocyanine iodide staining .…….. 47

DNA fluorescence assay …….. 47

Mitochondrial protein assay ……..... 48

Transfection ……. 48

Gene expression by real-time PCR ……. 49

Assay for assessment of cytotoxicity …….. 49

Data analysis ……..…… 50

CHAPTER III. RENAL FUNCTION …… 51

Renal physiological parameters *in vivo* …….. 51

Results ……. 51

Discussion …… 54

Protein and gene expression analysis of renal plasma membrane organic anion

transporters ……..... 56

Results …….. 56

Discussion …… 61

CHAPTER IV. MITOCHONDRIAL STATUS ……. 63

Mitochondrial redox status …….. 63

Results ……..…… 63

Discussion …… 70

Impact of compensatory hypertrophy on functional characteristics of renal mitochondria 72

Enzyme results ……. 72

Respiration results …… 75

Proteomics results …… 77

Discussion …… 81

Assessment of basal and toxicant-induced oxidative stress in renal mitochondria .. 83

Results …….. 83

Discussion …… 93

Effect of compensatory renal hypertrophy on mitochondrial size, number and membrane potential ……. 96

Results …….. 96

Discussion …… 104

CHAPTER V. MODULATION OF MITOCHONDRIAL REDOX STATUS IN PROXIMAL TUBULAR CELLS TO REDUCE THE RISK OF SUSCEPTIBILTY TO NEPHROTOXICANTS …… 105

Influence of overexpression of the DIC on susceptibility to chemically induced toxicity by mitochondrial toxicants …… 105

Results ……. 105

Influence of overexpression of the OGC on susceptibility to chemically induced toxicity by mitochondrial toxicants ……. 110

Results ……. 110

Discussion …….. 115

CHAPTER VI. SUMMARY AND CONCLUSIONS …… 119

CHAPTER VII. OVERALL SIGNIFICANCE AND FUTURE DIRECTIONS … 125

References ……... 129

Abstract ……... 151

Autobiographical Statement ……..... 153

LIST OF TABLES

Table 1-1. Mitochondrial anion transporters ……..... 26

Table 3-1. Physiological parameters of renal function *in vivo* ……..... 52

Table 3-2. Real-time quantitative PCR analysis of Oat1 and Oat3 mRNA expression in renal cortex of control and NPX rats ……..
60

Table 4-1. GSH and GSSG concentrations in renal mitochondria from control and NPX rats ……..
64

Table 4-2. Real-time quantitative PCR analysis of DIC and OGC mRNA expression in renal cortex of control and NPX rats ……
67

Table 4-3. Effects of compensatory renal hypertrophy on GSH-dependent and mitochondrial enzymes……
73

Table 4-4. Effects of compensatory renal hypertrophy on mitochondrial respiration .. 76

Table 4-5. Mitochondrial proteomics ……..…….. 78

Table 4-6. Effect of toxicant (tBH) on mitochondrial protein expression during compensatory renal hypertrophy ……
88

Table 5-1. Analysis of DIC gene overexpression by RT-PCR in renal proximal tubular cells from NPX rats ……
106

Table 5-2. Analysis of OGC gene overexpression by RT-PCR in renal proximal tubule cells from NPX rats ……....
111

LIST OF FIGURES

Figure 1-1. Kidney structure …….. ……..... 3

Figure 1-2. From blood filtrate to urine: A closer look 4

Figure 1-3. Glutathione (GSH) structure ……... 12

Figure 1-4. Functions of glutathione (GSH) ……..... 13

Figure 1-5. Glutathione synthesis …….……. 16

Figure 1-6. Interorgan transport and metabolism of GSH ……....... 17

Figure 1-7. Pathways for GSH transport and metabolism in renal proximal tubular cells 20

Figure 1-8. Schematic summary of renal plasma membrane transporters 21

Figure 1-9. Mitochondrial GSH content and transport …… 25

Figure 3-1. Effect of compensatory renal growth on protein expression of renal plasma membrane organic anion transporters and the (Na^+ + K^+)-stimulated ATPase ……. 58

Figure 4-1. Effect of compensatory renal growth on protein expression of renal mitochondrial GSH transporters .……..... 65

Figure 4-2. Effect of compensatory renal growth on protein expression of renal mitochondrial Sod2 and Trx2 …….....**.....** 68

Figure 4-3. Assessment of effects of compensatory renal growth on basal and toxicant induced oxidative stress in renal mitochondria ……..... 86

Figure 4-4. MitoTracker^{TM} staining …… 98

Figure 4-5. Mitochondrial DNA ……. 100

Figure 4-6. Mitochondrial protein ……..…… 101

Figure 4-7. Measurement of mitochondrial membrane potential in PT cells from control and NPX rats …… 102

Figure 5-1. Effect of overexpression of the DIC on sensitivity to chemical-induced toxicity ……..…… 107

Figure 5-2. Effect of overexpression of the OGC on sensitivity to chemical-induced toxicity …… 112

Figure 5-3. Mitochondrial toxicants ……..... 118

Figure 6-1. Summary scheme ……..... 124

LIST OF ABBREVIATIONS

AA	Antimycin A
Acivicin	L-(αS,5S)-α-amino-3-chloro-4,5-dihydro-5-isoxazoleacetic acid;
BBM	Brush-border plasma membrane
BLM	Basolateral plasma membrane
CM	canalicular membrane;
Cys	Cysteine
DIC	Dicarboxylate carrier
GAPDH	glyceraldehyde 3-phosphate dehydrogenase
GCS	L-γ-glutamyl-L-cysteine synthetase
GGT	γ-glutamyltransferase
GLRX	Glutaredoxin
GPX	glutathione peroxidase
GRD	glutathione disulfide Reductase
GS	GSH synthetase

GS^-	Thiolate anion of glutathione
GSH	Glutathione
GS–R	GSH conjugate
GSSG	Glutathione disulfide
GST	Glutathione S-transferase
HNE	4-Hydroxy-2-nonenal
LDH	Lactate dehydrogenase
MDA	Malondialdehyde
MDH	Malic dehydrogenase
Mrp	Multidrug resistance protein
MVK	Methyl vinyl ketone
NaC3	Sodium-dicarboxylate 3 carrier
NAG	N-Acetyl-β-D-glucosaminidase
NHE	Sodium-hydrogen exchanger
NPX	Uninephrectomized
NT	3-Nitrotyrosine
OA^-	Organic anion

Oat1/3	Organic anion transporters 1 and 3
Oat-k1/k2	Kidney specific organic anion transporter
Oatp1	Organic anion transporting polypeptide 1
OC^{+}	Organic cation
Oct	Organic cation transporter
OG^{2-}	2-Oxoglutarate
OGC	2-Oxoglutarate carrier
OPT	o-Phthalaldehyde
Pi^{2-}	Inorganic phosphate
PRX	Peroxiredoxin
PT	Proximal tubular
RCR	Respiratory control ratio
ROH	Lipid alcohol
ROOH	Lipid peroxide
ROS	Reactive oxygen species
SDH	Succinate: cytochrome c oxidoreductase
SM	Sinusoidal membrane

Sod2	Superoxide dismutase 2
tBH	tert-Butyl hydroperoxide
Trx2	Thioredoxin 2
VDAC	Voltage-dependent anion channel (porin)

CHAPTER I. INTRODUCTION

Reduction in functional renal mass

Renal function is critical to life as the kidneys are responsible for filtering wastes, toxins and fluids from the blood stream. The ability of the organ to function is a result of the collective effort of a number of different types of kidney cells. As shown in **Figures 1-1 and 1-2**, the outer section of the kidney is called the renal cortex and the inner section is called the medulla. The kidneys are covered by a layer called the capsule. The nephron, the primary structural unit of the kidneys, is comprised of specialized epithelial cells, including those of the glomerulus, proximal tubule, the loop of Henle, distal tubules, and collecting duct, each with its own distinctive morphology, physiology and biochemistry. Kidney cells display a higher susceptibility to several toxicants due to physiological and biochemical reasons (Lash and Cummings, 2010). Physiological factors include the fact that the kidneys receive 25% of the cardiac output, which ensures that high levels of toxicants are delivered to renal cells. The kidneys also have a tremendous ability to concentrate solutes, which results in high concentrations of toxicants in the medullary lumen and interstitium. Biochemical factors include the presence of several biotransformation enzymes that catalyze the formation of toxic metabolites and reactive intermediates such as cytochrome P450 monooxygenases, glutathione S-transferases and flavin-containing monooxygenases. In addition, the high metabolic rate and workload of renal cells also increases their sensitivity to toxicants.

It is well known that reductions in functional renal mass occur in humans during aging and severe kidney damage from diseases, injuries, infections and congenital conditions and after nephrectomy. Nephrectomy, or surgical removal of a kidney or a section of a kidney, is performed for treatment of unilateral, secondary renal cancer, infections and for kidney transplantation. The incidence of reductions in renal mass is increasing in the U.S. and represents a significant challenge to public healthcare. The number of patients treated with dialysis or kidney transplantation was projected to increase from 340,000 in 1999 to 651,000 in 2010 (Holcomb, 2005). Reduction of renal mass due to nephrectomy results in increases in the size (hypertrophy) and function of the remnant kidney cells, most prominently in the proximal tubular (PT) region (Meyer et al., 1996), and this multistep adaptive process is called compensatory renal hypertrophy.

Studies have shown that surgical removal of one kidney in experimental animals and patients was performed in the nineteenth century and led to the observation that the remaining kidney subsequently undergoes compensatory renal growth (Nowinski, 1969). In adult animals, 80% of compensatory renal growth following uninephrectomy is reportedly due to hypertrophy, an increase in cell size predominantly of proximal tubules, whereas 15-30% of growth can be ascribed to hyperplasia, an increase in cell number (Johnson and Vera, 1966; Johnson, 1969).

Figure 1-1. Kidney Structure.

From Campbell and Reece (2005).

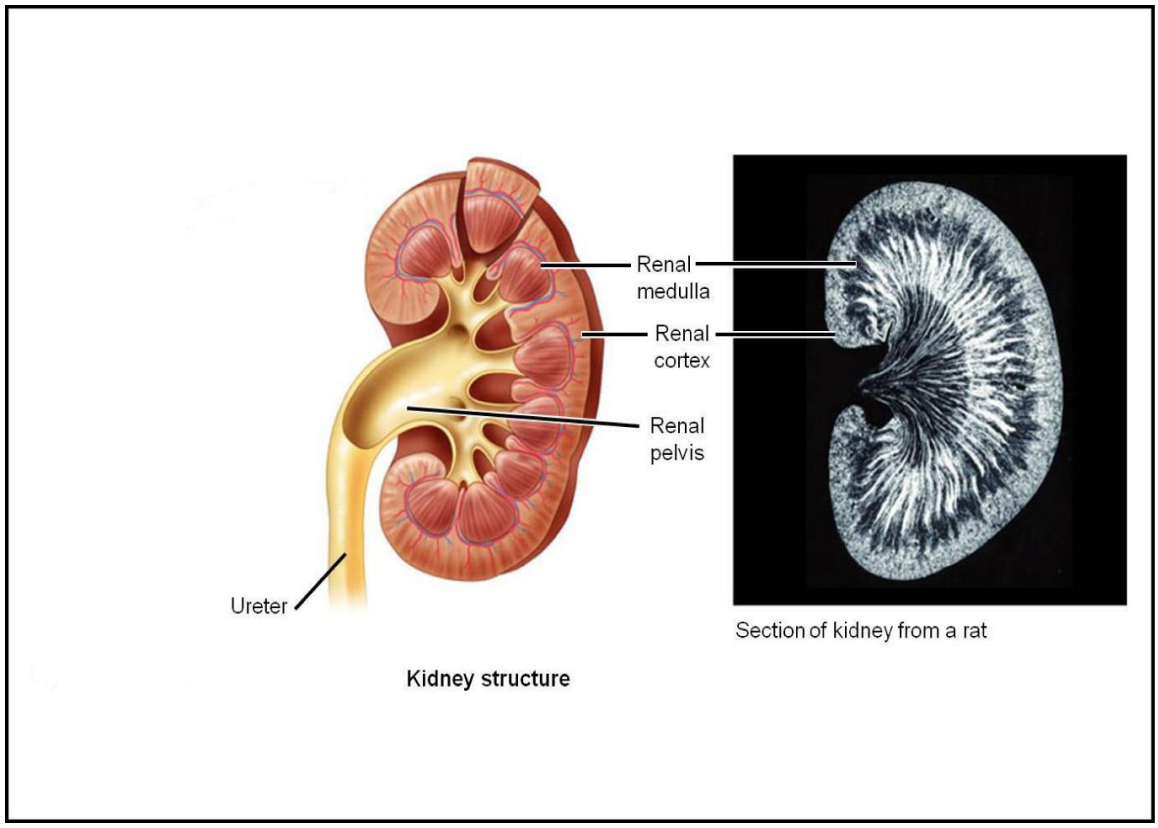

Figure 1-2. From blood filtrate to urine: A closer look.

From Campbell and Reece (2005).

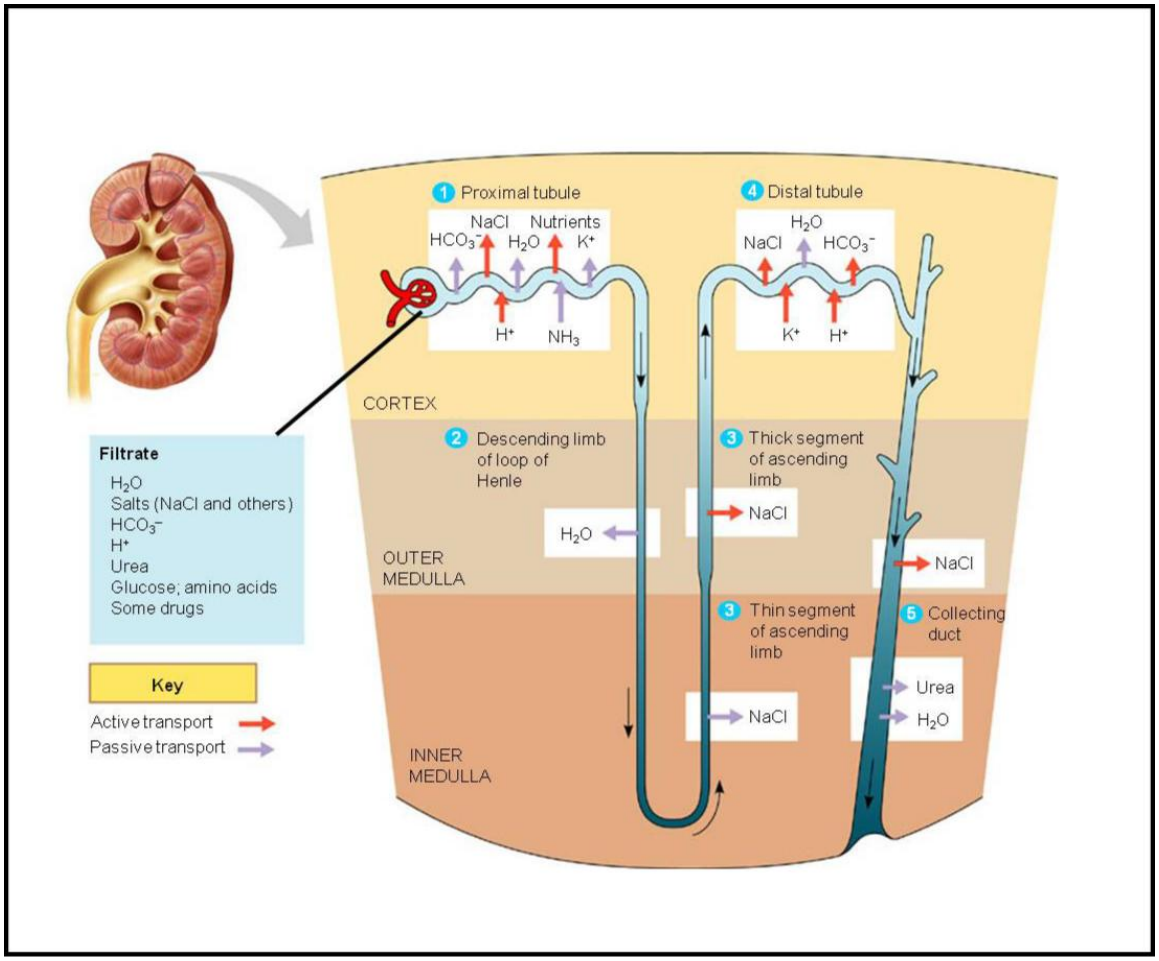

Compensatory renal hypertrophy: Cellular and molecular events underlying compensatory renal hypertrophy

Although the phenomenon of compensatory renal hypertrophy is well known and despite extensive research over the past century, the mechanism of this process still remains unclear. After the removal of one kidney, the remaining kidney exhibits a hyperfiltration state and changes in glomerular hemodynamics that activate a series of growth events leading to compensatory growth of the remaining kidney (Wesson, 1989; Fine and Norman, 1992). This compensatory hypertrophy response is mediated by vasoactive molecules, cytokines, growth factors and increases in glomerular capillary pressure and flow (Holcomb, 2005; Meyer et al., 1996; Fine, 1986; Shirley and Walter, 1991).

The cellular characteristics of hypertrophy include increases in cellular volume, area and surface density of the basolateral (BLM) and brush-border plasma membranes (BBM), increases in cellular synthesis and content of glutathione (L-γ-glutamyl-L-cysteinyl-glycine, GSH) (Zalups and Lash, 1990), and mitochondrial proliferation within renal PT cells (Johnson and Amendola, 1969). Physiological changes consist of increased glomerular filtration rate (GFR), renal blood flow (RBF) and water and electrolyte transport (Shirley and Walter, 1991; Wolf and Neilson, 1991; Zalups and Henderson, 1992). Biochemical changes include increases in renal protein content (Coe and Korty, 1967; Halliburton and Thomson, 1967), rates of renal protein synthesis (Johnson and Vera Roman, 1966) and RNA synthesis (Johnson and Vera Roman, 1966; Ouellette, 1983) and increased mitochondrial metabolism in proximal and distal tubules (Harris et al., 1988; Nath et al., 1990; Shapiro et al., 1994).

Additionally, activities of most renal enzymes increase in the hypertrophied kidney. For example, increased activity of enzymes that are involved in excretion of solutes, such as the (Na^++K^+)-stimulated ATPase (Mujais and Kurtzman, 1986; Scherzer et al., 1985) and enzymes that contribute to cell growth, such as ornithine decarboxylase (Brandt et al., 1972; Humphreys et al., 1988), guanylate cyclase, protein kinase C, enzymes of the pentose phosphate pathway (Schlondorff and Weber, 1976; Caramelo et al., 1988; Steer et al., 1982), choline kinase and choline phosphotransferase (Toback et al., 1974; Hise et al., 1984), are observed.

The sequential production of different growth factors is also required to achieve coordinated growth of kidney cells after growth has been triggered by some unidentified kidney-specific signal. There is also strong evidence that a large number of factors promote kidney growth in cultured PT cells, including insulin, insulin-like growth factor (IGF-1), epidermal growth factor (EGF), hepatocyte growth factor (HGF), platelet-derived growth factor, prostaglandin E2, and hormones including hydrocortisone, thyroxine, arginine vasopressin and angiotensin (Fine, 1986; Caramelo et al., 1988; Igawa et al., 1991). Moreover, recent studies suggest that transforming growth factor-β (TGF-β) is one of the most important factors causing tubular cell hypertrophy (Franch et al., 1995; Fujita et al., 2004; Wolf et al., 1993; Sinuani et al., 2006). TGF-β induces hypertrophy of tubular cells through a cell cycle-dependent mechanism that involves entry of cells into the G_1 phase, initiating G_1-related events, and arresting cell cycle progression prior to the G_1/S restriction point (Franch et al., 1995, 1997; Nagahara et al., 1999).

The toxicological implications of compensatory renal growth are higher susceptibility to nephrotoxicants such as inorganic mercury, analgesics and cadmium metallothionein (Henry et

al., 1983; Houser and Berndt, 1986; Lash and Zalups, 1992; Lash et al., 1999, 2006; Molland, 1976; Zalups, 1997; Zalups and Diamond, 1987; Zalups et al., 1992). Furthermore, previous studies from our lab showed that cellular GSH content was significantly higher in renal homogenates (whole kidney, cortex and outer stripe of the outer medulla) from uninephrectomized (NPX) rats, suggesting that increased GSH content is an adaptive response to enhanced oxidative stress (Zalups and Lash, 1990).

It has been further shown that there are many factors that influence the compensatory renal growth response. For example, feeding a protein-rich diet increased kidney weight in NPX rats (Hostetter et al., 1986), administration of androgens increased kidney weight in mice and rats (Schlondorff et al., 1977; Blantz et al., 1988), and a greater growth response after uninephrectomy was observed in young rats as compared to older rats (Barrows et al., 1962). Conversely, starvation, protein depletion and endocrine abnormalities retard growth (Hayslet, 1979).

Compensatory renal hypertrophy, mitochondria, nephrotoxicity and clinical complications

The mitochondria are the primary organelle for production of ATP. Reducing equivalents from malate and glycerol phosphate are transported from the cytoplasm into mitochondria by the NADH shuttle system. Pyruvate, which is a product of glycolysis, enters mitochondria and is metabolized by the citric acid cycle to produce NADH and $FADH_2$. NADH and $FADH_2$ further go through the electron-transport chain located on the inner mitochondrial membrane to synthesize ATP. The electron-transport chain consists of four enzyme complexes, denoted as complexes I, II, III and IV. Complex I is the NADH:ubiquinone oxidoreductase. Complex II is

the succinate:ubiquinone oxidoreductase. Complex III is the ubiquinol:cytochrome c oxidoreductase, which is a ubisemiquinone radical-generating Q cycle and can be a site at which 1% to 2% of total oxygen consumption leaks to generate superoxide anion ($O_2^{\cdot -}$). Complex IV is the cytochrome c oxidase.

Under normal conditions, mitochondrial reactive oxygen species (ROS) produced in the course of metabolism are contained by the natural antioxidant system that protects cells from ROS-mediated modifications. The main mitochondrial antioxidants are GSH, manganese superoxide dismutase and thioredoxin systems. The antioxidant capacity of mitochondria is limited compared to the cytoplasm and mitochondria depend on GSH transporters for their GSH supply. The various antioxidants play a crucial role in protection from oxidative stress, which can be caused by an increase in ROS or an impaired antioxidant defense system. Under various abnormal conditions, the rate of ROS production may exceed the natural antioxidant capacity, leading to oxidative stress. The primary ROS produced in the course of mitochondrial oxygen metabolism is superoxide anion, which is a highly reactive and cytotoxic ROS.

Mitochondria are not only the main organelle that produces superoxide anion but are also the main targets of ROS, leading to mitochondrial dysfunction. It has been shown that compensatory renal hypertrophy results in increased energy demands on PT cells. To accommodate these energy demands, there are increased rates of mitochondrial electron transport, which produces a hypermetabolic state (Harris et al., 1988; Shapiro et al., 1994) that can lead to mitochondrial dysfunction. In addition, our previous studies also showed in isolated mitochondria from hypertrophied PT cells that although intramitochondrial GSH contents and activity are increased,

these mitochondria exhibit an enhanced basal oxidative stress and greater sensitivity to mitochondrial toxicants (Lash et al., 2001a). There is increasing evidence that in experimental animals, compensatory renal hypertrophy increases risk for later toxicological complications due to increased renal oxidative stress. For example, uninephrectomy and compensatory renal hypertrophy result in markedly altered susceptibility to injury from a broad variety of nephrotoxicants, including heavy metals, analgesics, and antibiotics (Zalups et al., 1992; Lash and Zalups, 1992; Lash et al., 1999, 2006; Molland, 1976; Zalups, 1997; Zalups and Diamond, 1987).

There is also strong evidence in experimental animals that significant reduction in renal mass leads to proteinuria, systemic and glomerular hypertension, glomerular hyperfiltration and progressive renal damage (Hostetter et al., 2001; Remuzzi et al., 2006; Santos et al., 2006). Studies also suggest this glomerular hypertension and glomerular hyperfiltration lead to pathogenesis of proteinuria and progressive glomerulosclerosis (Hostetter et al., 2001). Ever since the recognition of hyperfiltration injury in animals undergoing renal ablation, there has been concern over the extended outcome after kidney donation. There is also strong clinical evidence that suggests short and long-term medical risks of human renal donor nephrectomy for transplantation purposes. The human clinical studies that investigated the quality of life of renal donors found early and late health complications such as hypertension, microalbumiuria, hematuria and proteinuria (Azar et al., 2007; Berber et al., 2008).

Function and importance of thiol redox status in renal function in proximal tubules

Due to high rates of aerobic metabolism in the proximal tubules and high exposure to a broad and diverse range of chemicals and drugs, the kidneys are highly dependent on adequate supply of the thiol-disulfide redox protectant GSH to maintain proper function. Besides the GSH system, there are other renal protective systems, including thioredoxin and low-molecular-weight thiols such as N-acetyl-L-cysteine (NAC) (Lash, 2010). Several signaling pathways also function in nephroprotection, such as the epidermal growth factor (EGF), mitogen activated protein kinase (MAPK), protein kinase B (PKB/Akt), protein kinase C (PKC), heat shock proteins (HSPs), and nuclear factor kappa-B (NF-κB) pathways; these act through modulation of redox status or by altering cellular pH (Lash, 2010). Small amino acids, such as glycine, are also nephroprotective.

GSH is the most abundant non-protein thiol (SH) in mammalian cells. As shown in **Figure 1-3**, GSH is a tripeptide composed of the amino acids L-glutamate, L-cysteine and glycine. Glutathione can exist in two major forms: the antioxidant 'reduced glutathione' tripeptide is called glutathione and abbreviated GSH; the oxidized form is a sulfur-sulfur linked compound known as glutathione disulfide or GSSG (Kidd, 1997). The GSH/GSSG ratio may be a sensitive indicator of oxidative stress. The high electron-donating capacity of GSH due to its sulfhydryl (-SH) group combined with its high intracellular concentration endow GSH with great reducing power, which is used to regulate a complex thiol-exchange system (Franco, 2007). Glutathione is present inside cells mainly in its reduced GSH form. Intracellular GSH status appears to be a sensitive indicator of the overall health of the cell and of its ability to resist toxic challenges.

As shown in **Figure 1-4**, the primary, critical processes involving GSH are peroxide reduction, electrophile conjugation, glutathionylation and action as a coenzyme in detoxification, metabolism and hormone biosynthesis. GSH is considered the most important antioxidant in the human body. GSH recycles other antioxidants, such as vitamins A, C and E, keeping them in an active state longer and helping to prevent oxidative stress and inflammation. GSH is often called 'the master antioxidant.' GSH acts as a main detoxifier by binding to toxins such as heavy metals, solvents and pesticides, allowing them to be excreted in urine or bile. GSH strengthens the immune system by boosting production of T cells that fight viral and bacterial infections. Elevated GSH levels help the body to produce more white blood cells. White blood cells are the most important cells for maintaining sterility of body fluids by serving as garbage collectors for the body. In other words, healthy growth and activity of white blood cells depend on availability of GSH. It is widely accepted that GSH also acts as a mediator of many other physiological reactions, including cellular signaling, metabolism of xenobiotics, thiol-disulfide exchange reactions, and as an important reservoir of cysteine (Franco, 2007).

Figure 1-3. Glutathione (GSH) structure.

The L-glutamyl and L-cysteinyl residues are linked through the γ-carboxyl group of L-glutamate, making the isopeptide bond resistant to most proteases. The tripeptide thiol glutathione (GSH) has facile electron-donating capacity, linked to its sulfhydryl (–SH) group.

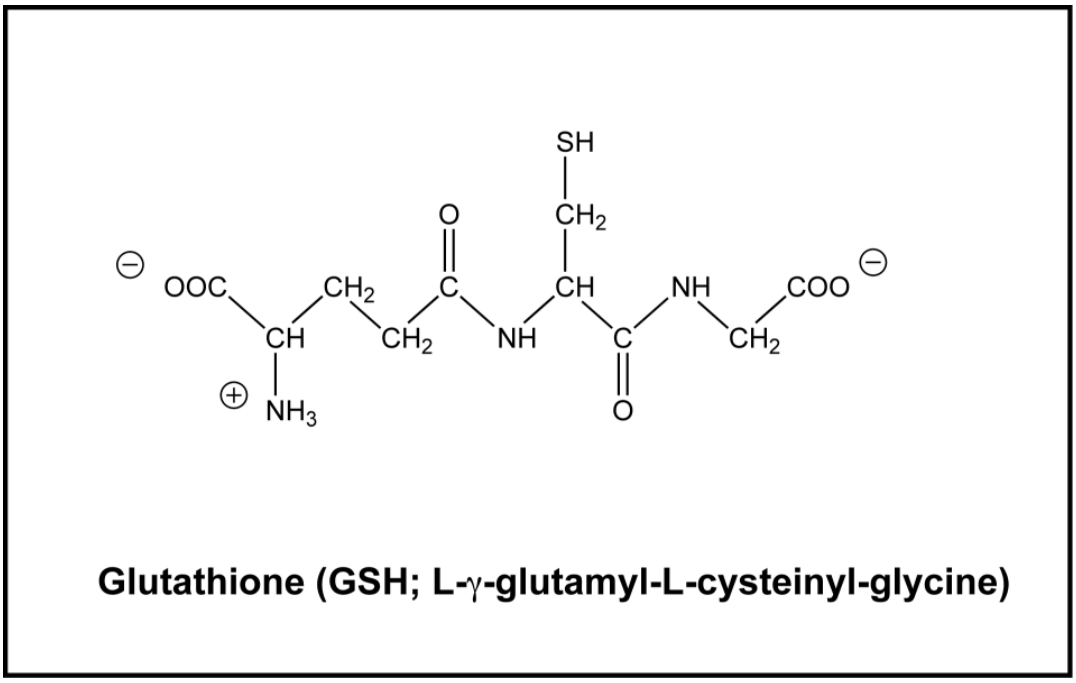

Figure 1-4. Functions of glutathione (GSH).

The basic types of functions for GSH in cytoprotection are mentioned.

Abbreviations: E, electrophile; GLRX, glutaredoxin; GPX, GSH peroxidase; GRD, glutathione disulfide reductase; GS–R, GSH conjugate; GSSG, glutathione disulfide; PRX, peroxiredoxin; ROH, lipid alcohol; ROOH, lipid peroxide.

From Lash (2010).

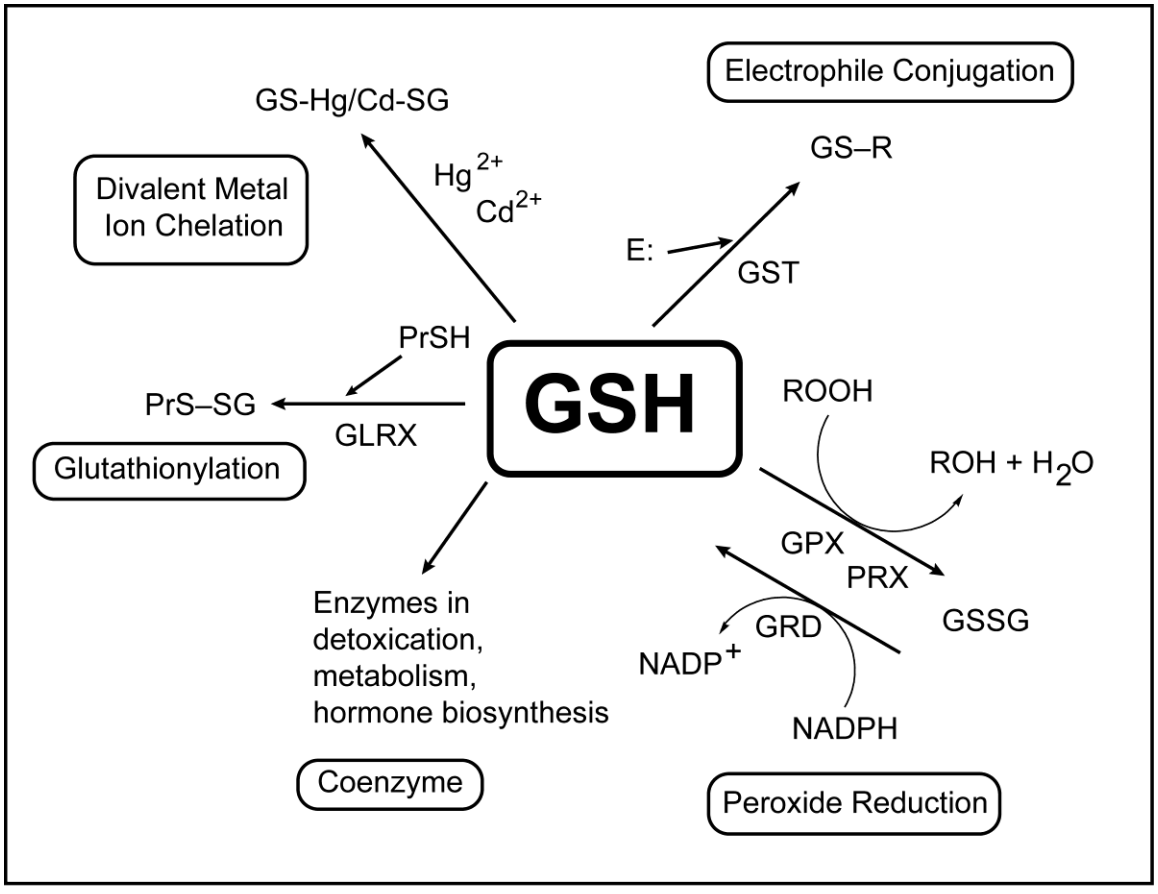

As shown in **Figure 1-5**, GSH is synthesized in the cytoplasm by two ATP-dependent reactions, the glutamate-cysteine ligase (GCL) [also called γ-glutamyl cysteine synthetase (γ-GCS)] and GSH synthetase (GS). In the first reaction, L-cysteine and L-glutamate are combined by γ-glutamyl cysteinyl synthetase. In the second reaction, GSH synthetase combines γ-glutamyl-cysteine with glycine to generate GSH. Reduced glutathione (GSH) is oxidized to glutathione disulfide (GSSG) in a reaction catalyzed by glutathione peroxidase and GSSG is reduced to regenerate GSH by glutathione reductase, which uses NADPH as a hydrogen donor. GSH degradation is mediated by either a hydrolysis or transpeptidation reaction catalyzed by γ-glutamyltransferase (GGT), followed by hydrolysis catalyzed by dipeptidase (DP) activity. The major difference between synthesis and degradation is that whereas degradation occurs extracellularly, as both GGT and DP face the external side of the BBM and GGT is selectively localized on the BBM, GSH synthesis occurs in the cytoplasm as GCL and GS are found exclusively in the cytoplasm.

The highest concentration of GSH is found in the liver, which is the principal organ involved in the detoxification and elimination of toxic materials. As shown in **Figure 1-6**, the process by which GSH circulates throughout the body, which involves transport across plasma membranes and translocation between tissues, is called 'Interorgan metabolism' (Anderson et al., 1980; Griffith and Meister, 1979a; Lash et al., 1988; McIntyre and Curthoys, 1980). Hepatic GSH is transported out of the liver by transport across either the sinusoidal or canalicular plasma membranes to plasma and bile, respectively (Ballatori and Dutczak, 1994; Kaplowitz et al.,

1985). Biliary GSH is degraded to constituent amino acids in either the bile or small intestine and the enterohepatic circulation returns these amino acids to the liver for resynthesis of GSH.

Figure 1-5. Glutathione Synthesis.

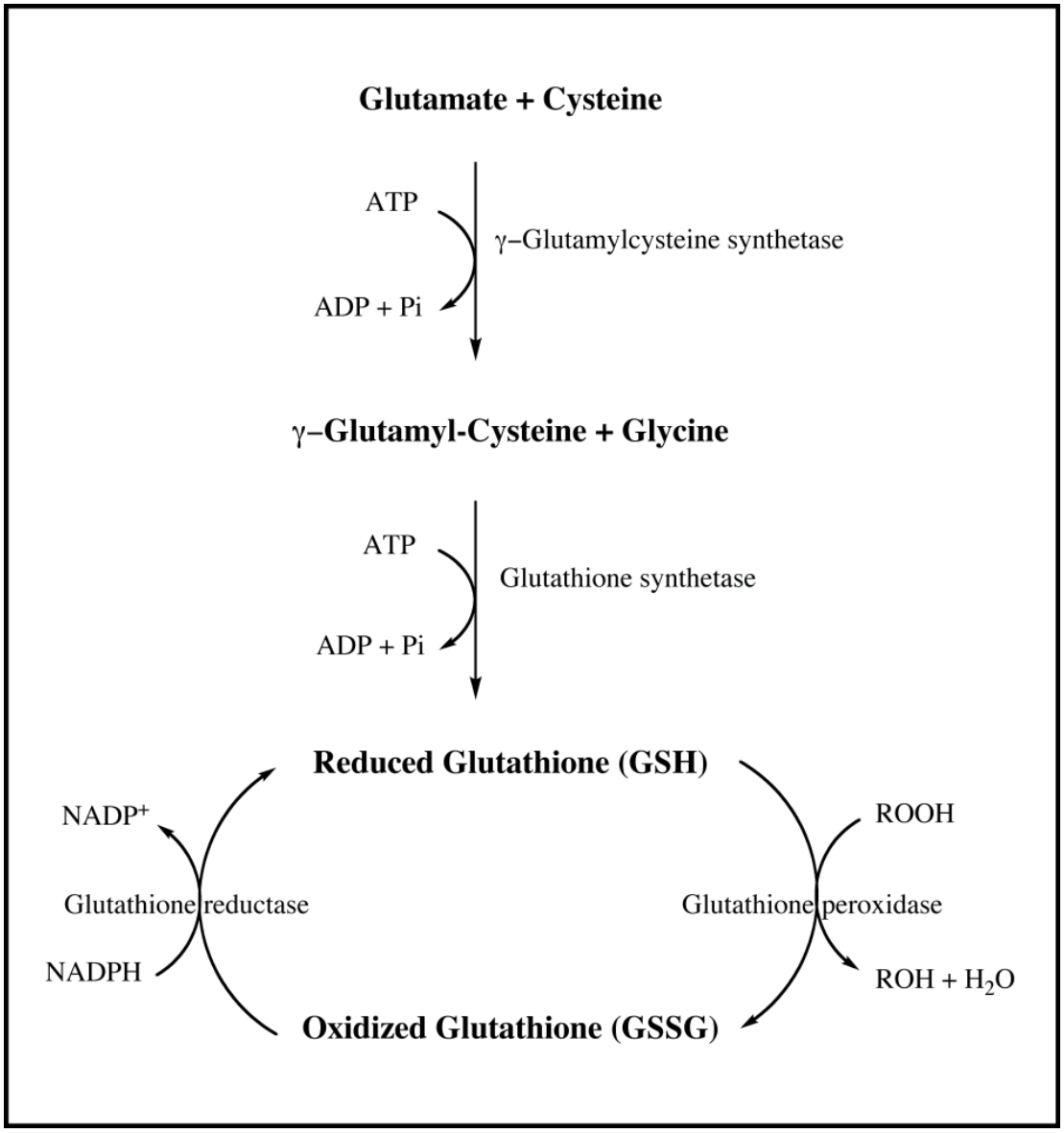

Figure 1-6. Interorgan transport and metabolism of GSH.

This scheme summarizes the pathways for transport, translocation between tissues and metabolism of GSH and its metabolites involving the liver, kidneys, small intestine, bile and plasma.

Abbreviations: BBM, brush-border membrane; BLM, basolateral membrane; CM, canalicular membrane; SM, sinusoidal membrane.

From: Lash (2010).

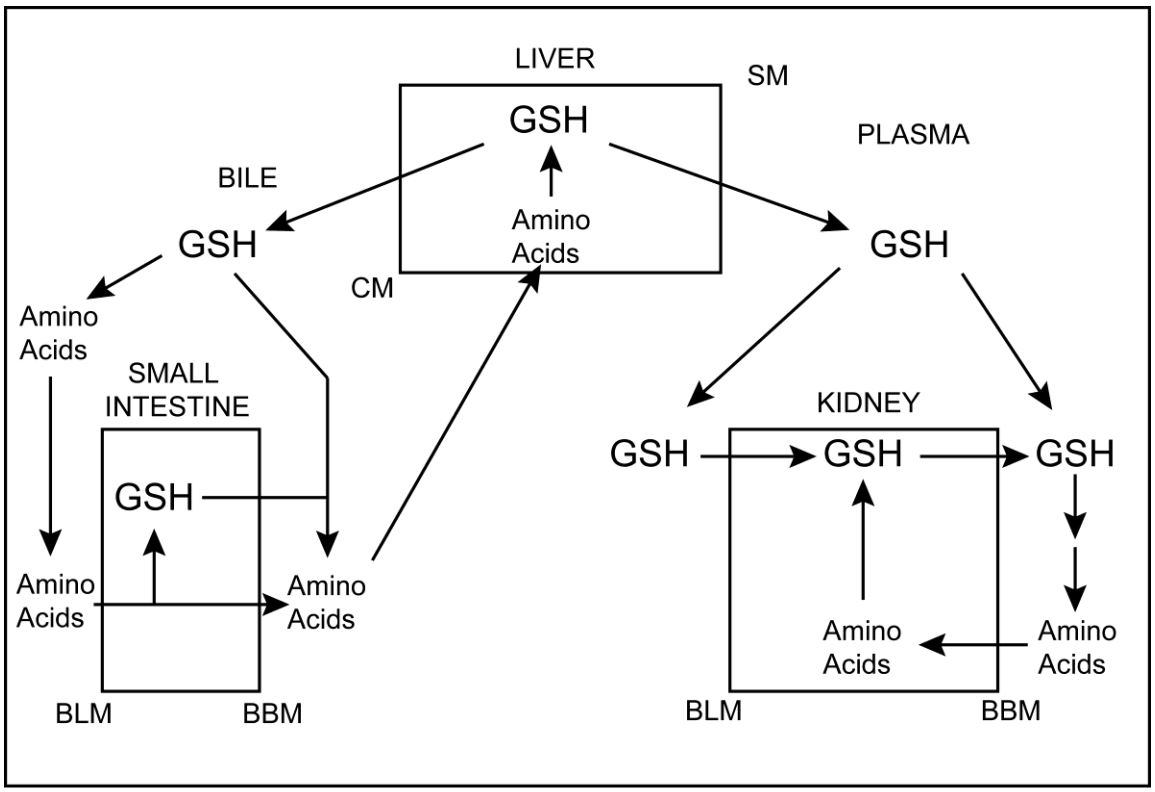

Plasma GSH is extracted by the kidneys by either glomerular filtration or basolateral uptake. Even though liver is the primary source of GSH, the kidneys (predominantly PT cells) are the major site for metabolism of GSH in the body. The kidneys play a central role in the overall disposition of GSH in the body. Whereas the liver exhibits low activities of GSH uptake and GGT for degradation of GSH, the kidneys play the major role in uptake and efflux of GSH, synthesis of GSH from precursors, degradation of GSH and uptake of constituent amino acids (Lash et al., 1988). The kidneys extract approximately 80% of the plasma GSH pool during a single pass of the blood through the renal circulation (Griffith and Meister, 1979a; Haberle et al., 1979). As shown in **Figure 1-7**, 50% of the GSH extracted occurs by a basolateral route whereas 30% of the extraction occurs by glomerular filtration.

Pathways of glutathione transport in renal proximal tubule

Plasma membrane GSH transport systems: Basolateral membrane (BLM) and brush border membrane (BBM) transport

Basolateral plasma membrane transport: Renal PT cells obtain GSH from both extracellular spaces by transport across the BLM and intracellular synthesis from precursor amino acids.

GSH uptake across the BLM of renal PT cells comprises two transport processes, a Na^+-coupled and a Na^+-ion independent pathway. Current data suggest the potential involvement of three carriers in the transport of GSH across the BLM of renal PT cells, the organic anion transporter 1 (Oat1; *Slc22a6*), organic anion transporter 3 (Oat3; *Slc22a8*), and the sodium-dicarboxylate

carrier 3 (NaC3; *Slc13a3*; formerly known as sodium-dicarboxylate transporter 2 or SDCT-2). As described in **Figure 1-8**, Oat1 and Oat3 function in the uptake of GSH in exchange for 2-oxoglutarate ($2\text{-}OG^{2-}$) and NaC3 functions in the co-transport of GSH with at least two Na^+ ions. Both Oat1 and Oat3 are broad-substrate specific organic anion transporters that are highly expressed on the renal BLM. The functions of Oat1 and Oat3 account for the sodium-independent uptake of GSH (Lash and Jones, 1983, 1984; Lash et al., 2007) and that of NaC3 accounts for the sodium-coupled uptake of GSH across the renal BLM. The (Na^++K^+)-stimulated ATPase provides the Na^+ ion gradient for transporters such as NaC3, thereby helping to provide the driving force for uptake of GSH and other organic anions. Two multidrug resistance proteins, Mrp5 (*Abcc5*) and Mrp6 (*Abcc6*), function in the ATP-dependent efflux of organic anions. In addition to organic anion transporters, there are also organic cation transporters, such as Oct2 (*Slc22a3*) and Oct3 (*Slc22a3*) present on the BLM. Both Oct2 and Oct3 are uniporters for uptake of organic cations (OC^+).

Brush border plasma membrane transport: As shown in **Figure 1-8**, unlike BLM GSH transport, the BBM process is not mediated by coupling to transport of any ion such as protons or Na^+ ions and is predominantly efflux of intracellular GSH into the tubular lumen rather than uptake of extracellular GSH into the cell. At the outer surface of the BBM, GSH is rapidly degraded to its constituent amino acids such as cysteine, which is the rate-limiting component. Cysteine is taken up by carriers on the BBM and is used for protein or GSH synthesis.

Although no direct evidence for a role for any specific carrier in the efflux of GSH across the BBM has been demonstrated, the proposed carriers as mediators of GSH efflux are the organic

Figure 1-7. Pathways for GSH transport and metabolism in renal proximal tubular cells.

Abbreviations: Cys, cysteine; DIC, dicarboxylate carrier; GCS, g-glutamylcysteine synthetase; GSH, glutathione; GS, GSH synthetase; Oat1/3, organic anion transporters 1 and 3; DIC, dicarboxylate carrier; OGC, oxoglutarate carrier.

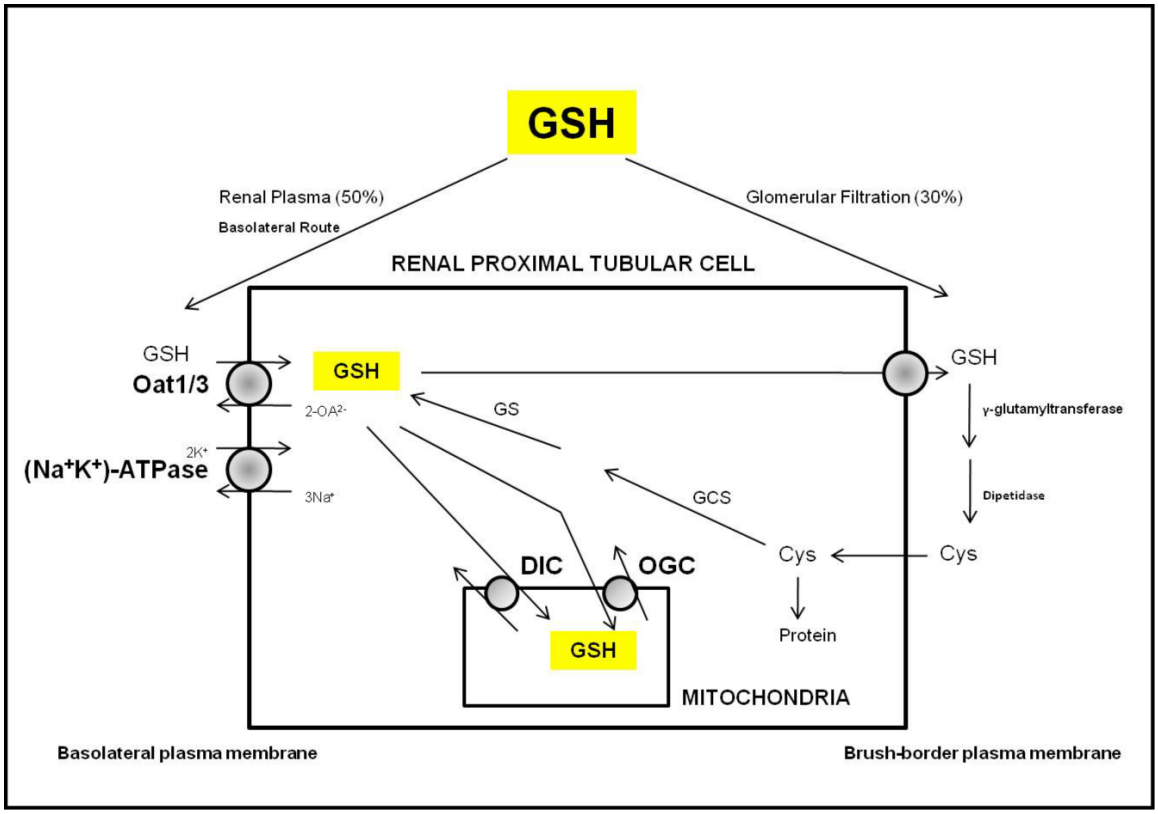

Figure 1-8. Schematic summary of renal plasma membrane transporters.

Major transporters for the uptake or efflux of OA^- or OC^+ on the BLM and BBM of PT cells are illustrated. There are also the $(Na^+ + K^+)$-ATPase on the BLM and NHE on the BBM, which provide ion or co-substrate gradients.

Abbreviations: BLM, basolateral membrane; BBM, brush-border membrane; Oat, organic anion transporter; Mrp, multidrug resistance protein; Oct, organic cation transporter; Oat-k1/k2, kidney specific organic anion transporter; NHE, sodium-hydrogen exchanger; GS^-, Thiolate anion of glutathione; OA^-, organic anion; OC^+, organic cation; $2\text{-}OG^{2-}$, 2-oxoglutarate; NaC3, sodium-coupled carboxylate transporter; Oatp1, organic anion transporting polypeptide 1.

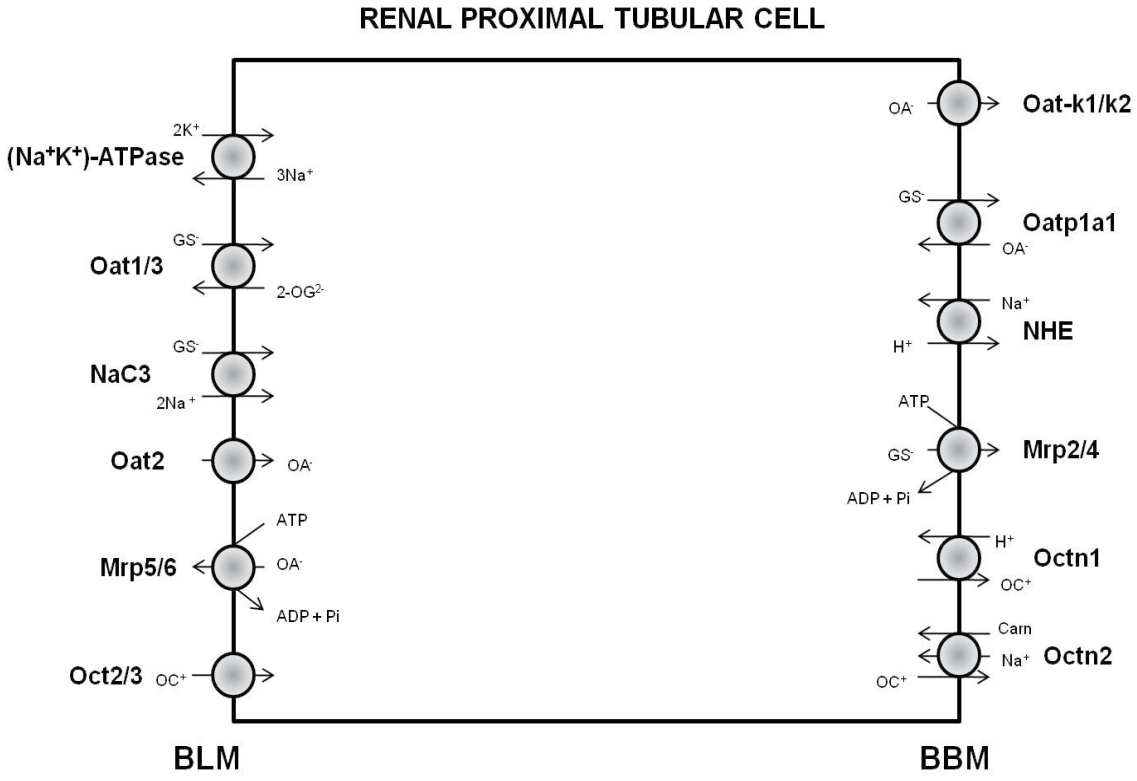

anion transporting polypeptide 1 (Oatp1; *Slco1a1*) and two isoforms of the ATP-dependent multidrug resistance proteins, Mrp2 (*Abcc2*) and Mrp4 (*Abcc4*). As described in **Figure 1-8**, Oatp1, which is highly expressed on the BBM of the rat proximal tubule, has been shown in other systems to mediate the efflux of GSH (Li et al., 1998; Mittur et al., 2002) and both Mrp2 and Mrp4 have been demonstrated to transport GSH (Evers et al., 2000; Gotoh et al., 2000; Lou et al., 2003; Paulusma et al., 1999; Rebbeor et al., 2002 Rius et al., 2003). The BBM also expresses three major carriers that function in the secretion of organic cations (OC^+): Octn1 (*Slc22a4*), Octn2 (*Slc22a5*) and P-glycoprotein [P-gp]. Octn1 is an electroneutral exchanger of OC^+ with protons. Octn2 can function in either the facilitated efflux of OC^+ or as a Na^+ ion/carnitine uptake cotransporter.

Significance of BLM and BBM GSH transport: Based on pharmacological and toxicological studies, there are several potential functions for GSH transport across renal plasma membranes. Previous studies provided *in vivo* evidence for renal tissue GSH uptake by orally administered GSH (Aw et al., 1991; Flagg et al., 1994; Hagen et al., 1990). In addition, *in vitro* studies with isolated renal PT cells showed that exogenous GSH increases intracellular GSH levels by BLM transport and protected against various oxidants (Hagen et al., 1988; Lash and Tokarz, 1990; Lash et al., 1996), suggesting significance of BLM GSH uptake in nephroprotection against toxicants.

Even though there is some uncertainty in the literature regarding the precise physiological function of GSH uptake across the renal BLM, the critical physiological importance of GSH efflux across the renal BBM has been long appreciated (Lash, 2005, 2009). The BBM GSH

transport process is critical for turnover of whole body GSH as efflux of GSH into the lumen mediates delivery of GSH to the active site of GGT on the surface of the BBM. The transport of GSH across the BBM occurs with favorable driving forces including an outwardly-directly GSH electrochemical gradient and high GGT activity on the BBM. Furthermore, previous studies showed that inhibition of renal GGT activity in mice causes glutathionuria, suggesting the importance of BBM efflux and GGT activity in GSH turnover (Griffith and Meister, 1979b).

Mitochondrial GSH status, transporters, and mechanisms of renal mitochondrial GSH transport

There are two main cellular pools of GSH, one in the cytoplasm and the other in mitochondria (Franco, 2007). The pH of cytoplasm is approximately 7.0 and that of the mitochondrial matrix is approximately 7.8. Hence, the GSH pools are likely to each have a net charge of between -1 and -2. As shown in **Figure 1-9**, GSH is synthesized in the cytoplasm and the predominant, if not exclusive, location of enzymes catalyzing synthesis of GSH is the cytoplasm, suggesting that the transport of GSH from the cytoplasm to mitochondria must occur to supply mitochondria with GSH. We have shown previously that renal concentrations of GSH increase significantly after uninephrectomy (Zalups and Lash, 1990). Because mitochondria lack enzymes for the synthesis of GSH, what may cause an increase in mitochondrial GSH in PT cells from NPX rats? We attempted to answer this question in two ways: First, by measuring rates of synthesis of GSH in the cytoplasm and second, by measuring rates of transport of GSH from cytoplasm into mitochondria. Our data showed that GCS activity was significantly higher in PT cells from NPX rats than in PT cells from SHAM-operated (or control) rats (Lash and Zalups, 1994). These data suggest that compensatory renal growth causes increases in the intracellular concentration of

GSH by inducing synthesis from its precursors by GCS, which is the rate-limiting enzyme involved in GSH biosynthesis. After the synthesis of GSH in cytoplasm, GSH is then transported across the mitochondrial inner membrane into the matrix.

Mitochondria possess a membrane potential with the matrix space negative relative to the cytoplasm and GSH is a negatively charged molecule at physiological pH. These facts suggest that GSH must be transported actively or in exchange for another anion by mitochondrial anion carriers. There are eight known anion carriers present in the mitochondrial inner membrane that could play a role in the uptake of GSH from the cytoplasm **(Table 1-1)**. These carriers are highly active in cells such as those of the renal proximal tubule because of high rates of mitochondrial respiration, active transport and gluconeogenesis (Lash, 2006). These mitochondrial carriers are electroneutral in the sense that they mediate exchange of anions so that there is no net transfer of charge across the inner mitochondrial membrane. Substrate specificity and energy dependence studies in isolated rat kidney mitochondria (McKernan et al., 1991; Chen and Lash, 1998) showed that two electroneutral anion exchange carriers, the dicarboxylate carrier (DIC, *Slc25a10*) and 2-oxoglutarate carrier (OGC, *Slc25a11*) mediate most of the GSH uptake into mitochondria. The function of each of these carriers is electroneutral, catalyzing the exchange of anions across the inner membrane without any net transfer of charge. Furthermore, at least 80% of GSH transport across the inner membrane of kidney mitochondria is due to the function of the DIC and OGC (Chen and Lash, 1998, Chen et al., 2000). The function of these carriers in transport of citric acid cycle intermediates suggests further that mitochondrial GSH status is regulated by mitochondrial energetics.

Figure 1-9. Mitochondrial GSH content and transport.

DIC, Dicarboxylate carrier; GS^-, thiolate anion of glutathione; $2\text{-}OG^{2-}$, 2-oxoglutarate; OGC, oxoglutarate carrier; Pi^{2-}, inorganic phosphate.

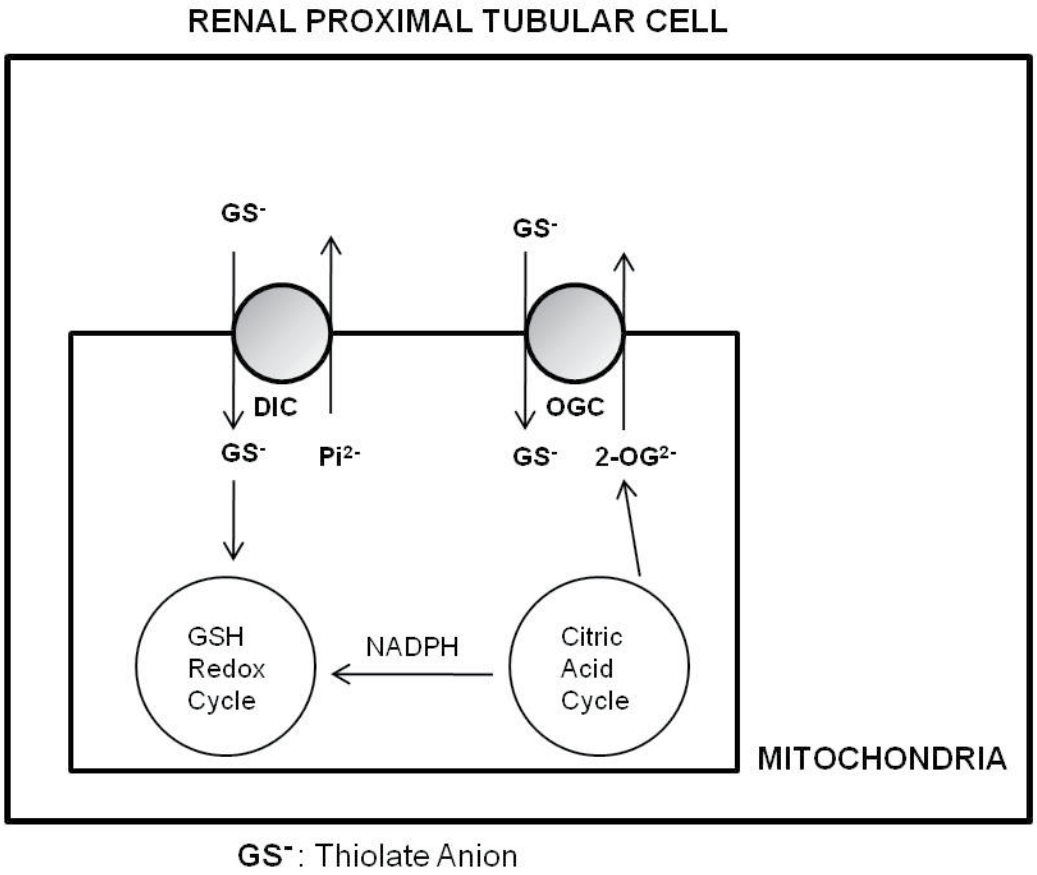

Table 1-1. Mitochondrial anion transporters.

From Lash (2006).

Mitochondrial anion transporters

Carrier	Function	Charge transfer
Adenine nucleotide translocase (AAC1-3; *Slc25a4–6*)	ADP^{3-} in, ATP^{4-} out	Electrogenic
Phosphate (PiC; *Slc25a3*)	$H_2PO_4^-$ in, OH^- out	Electroneutral
Dicarboxylate (DIC; *Slc25a10*)	$Malate^{2-}$ in, HPO_4^{2-} out	Electroneutral
2-Oxoglutarate (OGC; *Slc25a11*)	$2\text{-}Oxoglutarate^{2-}$ in, $malate^{2-}$ out	Electroneutral
Glutamate–aspartate (AGC1/2; *Slc25a12/13*)	$Glutamate^- + H^+$ in, $Aspartate^-$ out	Electrogenic
Glutamate-hydroxide (GC1/2; *Slc25a22/18*)	$Glutamate^-$ in, OH^- out	Electroneutral
Tricarboxylate/citrate (CIC; *Slc25a1*)	$Citrate^{3-} + H^+$ in, $malate^{2-}$ out	Electroneutral
Monocarboxylate (MCC)	$Pyruvate^-$ in, OH^- out	Electroneutral

A generalized scheme illustrating the functions of the DIC and OGC in GSH transport and their relationship to both the citric acid and GSH redox cycles is shown in **Figure 1-9**. These two carriers mediate the electroneutral exchange of GSH (in the form of GS^{2-}) with inorganic phosphate and 2-OG, respectively. As both carriers are also involved in the transport of citric acid cycle intermediates, amino acids and gluconeogenesis precursors (Klingenberg 1979; Palmieri, 2004; Palmieri et al., 1996), this indicates that mitochondrial GSH status is influenced by mitochondrial energy status. Both the DIC and OGC belong to a superfamily of mitochondrial inner membrane transporters with similar three-dimensional structures as predicted by the TMpred program. According to data from the TMpred program, the members of this superfamily have three trans-membrane domains (TMDs). Each TMD is composed of two hydrophobic stretches that span the membrane as α-helices, each separated by hydrophilic loops. Both the N- and C-terminals are in the cytoplasm. Both DIC and OGC are similar in size, with the DIC containing 286 or 287 amino acids with a molecular weight of ~31 kDa and the OGC containing 314 to 322 amino acids with a molecular weight of 34-37 kDa, depending on species.

Significance of mitochondrial GSH transport in protection from oxidative stress

Mitochondria maintain redox balance and serve as the primary intracellular sites of generation of reactive oxygen species (ROS). The redox status of mitochondrial GSH is known to be critical for proper mitochondrial function. Alterations in GSH concentration and redox status are associated with oxidative stress induced by peroxides and other oxidants in mitochondria from kidney, liver, brain, tumor cells and activation of signaling pathways. In addition, previous studies have shown that decreased concentration of mitochondrial GSH is associated with acute toxicity (Lash and Anders, 1987) and apoptosis (Chen et al., 2001) in renal mitochondria and

renal PT cells and depletion of the mitochondrial pool of GSH leads to several types of chemical-induced toxicity such as oxidative stress (Shan et al., 1993; Fernandez-Checa et al., 1993). Thus, maintenance of adequate concentrations of GSH within the mitochondrial matrix is essential for regulation and proper function of many critical processes.

To explore the physiological and toxicological importance of mitochondrial GSH transport in a well-defined renal cellular model system, the influence of modulation of mitochondrial GSH status on cellular function and susceptibility to toxicants was studied in NRK-52E cells, an immortalized cell line derived from normal rat kidney (Lash et al., 2002a). Our previous studies showed that two mitochondrial carriers, the DIC and OGC, are responsible for at least 80% of total transport of cytoplasmic GSH across the renal mitochondrial membrane (Chen and Lash, 1998; Chen et al., 2000). To further explore the role of these two carriers in GSH transport, NRK-52E cells were transfected with cDNA for rat DIC, OGC and a double-cysteine mutant of the OGC (Xu et al., 2006; Lash et al., 2002b). Overexpression of the DIC or OGC resulted in 5.5-fold and 6.1-fold increases in rates of mitochondrial GSH transport, respectively, as compared to wild-type cells. In contrast, cells overexpressing the mutant OGC exhibited a marked reduction in GSH transport as compared to wild-type cells.

To investigate the toxicological consequences of alterations in mitochondrial GSH transport, NRK-52E cells were transfected with either nothing (WT) or cDNAs for the rDIC, rOGC or rOGC-Mutant (Xu et al., 2006; Lash et al., 2002b). NRK-52E cells were incubated with either of two mitochondrial toxicants, 10 µM tert-butyl hydroperoxide (tBH) and 50 µM *S*-(1,2-dichlorovinyl)-L-cysteine (DCVC), to determine the fraction of cells undergoing apoptosis.

Although both tBH and DCVC exhibit distinct mechanisms of action, both can cause lipid peroxidation, GSH oxidation in mitochondria and apoptosis under appropriate conditions (Lash et al., 2001a). The results showed that NRK-52E-DIC or NRK-52E-OGC cells exhibited resistance to cell injury whereas NRK-52E-OGC-M cells exhibited similar sensitivity to tBH or DCVC as the NRK-52E-WT cells. These results suggest that higher GSH transport activity by overexpression of DIC and OGC markedly protected against apoptosis induced by either DCVC or tBH, indicating the significance of mitochondrial GSH transport in determining susceptibility to cytotoxic chemicals.

Goals of present study

Compensatory renal hypertrophy caused by a reduction in functional renal mass is associated with a series of physiological, morphological and biochemical changes that also have toxicological implications. As mentioned above, human clinical data also suggest health complications due to reduced renal mass caused by renal donor nephrectomy. One of the simplest experimental models for compensatory renal hypertrophy is the uninephrectomy rat model (NPX model). In this NPX rat model, the right kidney is removed and compensatory renal hypertrophy response is completed within 7-10 days and is maintained for at least 30 days thereafter.

Previous studies showed that compensatory renal hypertrophy increases energy demand on PT cells by increasing oxygen consumption and glucose production, leading to a hypermetabolic state (Harris et al., 1988) that is associated with alterations in renal function and mitochondrial status. Furthermore, previous studies showed that increased renal GSH content (Zalups and Lash,

1990) and higher susceptibility to nephrotoxicants (Lash et al., 2006) follow nephrectomy. These observations suggest that increased renal GSH content is an adaptive response to an enhanced basal oxidative stress that results from compensatory renal hypertrophy and susceptibility to oxidant-induced injury increases because the increase in renal GSH content is insufficient to maintain redox balance in the hypertrophied kidney cells. Interestingly, in 2002 and 2006 our lab also showed that in NRK-52E cells, overexpression of mitochondrial GSH transporters protected against nephrotoxicants (Lash et al., 2002b; Xu et al., 2006). These data suggested a possibility that this approach can be used to protect hypertrophied kidney cells by further increasing renal mitochondrial GSH content. Based on all these previous studies, we hypothesize that compensatory renal hypertrophy after uninephrectomy alters renal function *in vivo* and mitochondrial status. Further, we hypothesize that modulation of mitochondrial redox status alters susceptibility to nephrotoxicants and oxidative stress in hypertrophied kidney cells. To study these hypotheses, three specific aims of this study were conducted:

Aim 1. Determine the effect of compensatory renal hypertrophy on renal function including physiological parameters and renal plasma membrane transporters.

Aim 2. Determine the effect of compensatory renal hypertrophy on mitochondrial status including mitochondrial redox status, function, energetics, oxidative stress, size, number and membrane potential.

Aim 3. Manipulation of mitochondrial glutathione (GSH) by overexpression of mitochondrial GSH carriers, DIC and OGC, to provide sustained increases in mitochondrial GSH content and reduce susceptibility to nephrotoxicants in hypertrophied kidney cells.

Studies in Aim 1 and Aim 2 were conducted *in vivo, in vitro* and *ex vivo* to study renal function and mitochondrial status. Studies in Aim 3 were done *ex vivo* using a primary cell culture model with molecular approaches to study the effect of mitochondrial redox status on susceptibility of PT cells to nephrotoxicants. In the nephron, glomerular and proximal tubular epithelium are the most prominent sites that exhibit the various morphological, biochemical and functional changes seen after uninephrectomy and compensatory renal growth. Our studies focus on the PT cells because these cells play a major role in metabolite absorption and secretion and drug metabolism. As a result, these PT cells are also a major target cells for drug-induced nephrotoxicity and are most prominently affected in acute renal failure. Even though there are numerous parameters of toxicity, changes in mitochondrial energetics and redox status appear to be prominent components of the compensatory renal hypertrophy response. Hence, we primarily focused on mitochondrial function and redox status.

Overall, our proposed research plan provides integrated approaches with *in vivo*, *in vitro* and *ex vivo* models to further study renal function and mitochondrial energetics status, including redox status and oxidative stress, and the influence of mitochondrial GSH on susceptibility to chemically induced cytotoxicity. The significance of the present study lies in the occurrence of reduction in functional kidney mass due to numerous diseases, surgery, aging and substantial evidence that compensatory renal hypertrophy also increases the risks for development of health

complications, renal insufficiency or renal failure from other diseases or environmental exposures.

CHAPTER II. MATERIALS AND METHODS

Animals

Surgical Procedures. Male Sprague-Dawley rats (150-175g) were used in the present study. Animals that underwent surgical nephrectomy (removal of right kidney) were allowed a minimum 10-day recovery period prior to experiments (Zalups and Lash, 1990). Right-side nephrectomized rats were purchased from Harlan (Indianapolis, IN). The procedure they used is as follows: Each rat was anesthetized with sodium pentobarbital (50 mg/kg i.p.) before surgery. Unilateral nephrectomy was performed by making a 2.5-cm flank incision on the right side of the body with a No. 11 scalpel blade, beginning at erector spinae muscles and continuing along the angle of the 12^{th} rib. The incision was made through the skin and underlying fascia. The abdominal muscles were then incised along the same plane as the skin was cut to expose the retroperitoneal region where the right kidney is situated. With blunt dissection, the right kidney was exteriorized from the animal and the renal blood vessels and ureter were ligated with sterile 2.0 silk suture. The right kidney was then excised distal to the ligature. The abdominal muscles were sewn together with 4.0 sterile silk suture and the opposite ends of the incised skin and fascia were brought together with sterile 9-mm would clips. Control rats were surgically naïve, because previous studies showed that sham surgery has no apparent effect on the compensatory growth response (Zalups and Lash, 1990; Zalups, 1997; Lash et al., 1999). Control and NPX rats were age-matched for all studies.

Uninephrectomized Rat Model

In the uninephrectomized rat (NPX) model, the right kidney is removed and the compensatory hypertrophy response is completed within 7-10 days after surgery (Zalups and Diamond, 1987; Meyer et al., 1996). The experiments are done between day 10 and 30.

II-1 RENAL FUNCTION AND MITOCHONDRIAL STATUS

Chemicals

Cis-parinaric acid was purchased from Molecular Probes (Eugene, OR). Rotenone, tert-butyl hydroperoxide (tBH), hemin and 1-methyl-2-phenylindole were purchased from Sigma-Aldrich (St. Louis, MO). All other chemicals were of the highest purity available and were purchased from commercial sources.

Methods

In vivo assessment of renal physiological parameters

Rats were kept in metabolic cages and urine samples were collected every 24 h for one week. Basic parameters of renal function, including urine volume (U-Vol), urinary protein (U-Pr), urinary-glutathione (U-GSH) and urinary glutathione disulfide (U-GSSG), urinary and serum creatinine (U-Cr, S-Cr), urinary albumin (U-Alb), urinary *N*-acetyl-β-D-glucosaminidase (U-NAG) and urinary γ-glutamyltransferase (U-GGT) were measured.

U-Pr (BCA protein assay kit from Pierce, Milwaukee, WI, U.S.A.), U-Cr and S-Cr (Quantichrom^{TM} creatinine kit from BioAssay Systems, Hayward, CA, U.S.A.), U-Alb (Nephrat ii kit from Exocell, Philadelphia, PA, U.S.A.), U-GSH and U-GSSG (GSH-Glo® kit from Promega, Madison, WI, U.S.A.), and U-NAG (NAG assay kit from Diazyme, Poway, CA, U.S.A.) were measured using commercial kits. U-GGT was measured by a spectrophotometric assay (Orlowski and Meister, 1963).

Determination of protein expression of renal plasma membrane organic anion transporters by Western blot analysis

Crude plasma membrane fractions were isolated according to the method of Scalera et al. (1981) using a sucrose-triethanolamine (0.25 mM sucrose, 10 mM triethanolamine/HCl, pH 7.6, 0.1 mM phenylmethylsulfonyl fluoride) buffer. Protein expression of organic anion transporters was determined in isolated plasma membranes from kidney cortex derived from control and NPX rats using commercially prepared antibodies. Polyclonal antibodies to organic anion transporter 1 and 3 (Oat1 and Oat3; *Slc22a6* and *Slc22a8*, respectively) were purchased from Alpha Diagnostic International (San Antonio, TX, U.S.A.). Monoclonal antibodies against multidrug resistance-associated protein 2 and 5 (Mrp2 and Mrp5; *Abcc2* and *Abcc5*, respectively) were purchased from Abcam (Cambridge, MA, U.S.A.). Monoclonal antibody against Na^+K^+ATPase α1 subunit was purchased from Affinity Bioreagents, Inc. (Golden, CO, U.S.A.). Secondary antibodies (anti-rat, anti-rabbit, and anti-mouse) were purchased from Jackson ImmunoResearch (West Grove, PA, U.S.A.). Polyclonal anti-actin antibody was purchased from Cell Signaling Technology (Danvers, MA, U.S.A.) for use as a control for loading of total cellular protein.

Determination of protein expression of renal mitochondrial GSH transporters and redox status proteins by Western blot analysis

Suspensions of isolated mitochondria were prepared from renal cortex from control and NPX rats by differential centrifugation as follows: Rat kidneys were decapsulated and the medulla removed. Kidneys were then placed in 15 ml of ice-cold buffer (225 mM sucrose, 10 mM potassium phosphate, pH 7.4, 5 mM $MgCl_2$, 20 mM KCl, 20 mM triethanolamine, pH 7.4, 0.1 mM phenylmethylsulfonyl fluoride, and 2 mM EGTA), homogenized, and centrifuged in 50 ml polycarbonate centrifuge tubes at 600 x *g* (2250 rpm) for 10 min in a Sorvall SS34 rotor in a Sorvall RC2B centrifuge. Supernatant was decanted and saved. The pellets containing tissue fragments and mitochondria were washed with 30 ml of buffer and the resuspended material centrifuged at 600 x *g* for 10 min. The supernatant fractions were combined and centrifuged at 15,000 x *g* for 5 min. The resultant pellet was resuspended in 2 ml of buffer without EGTA. Protein expression of mitochondrial GSH transporters and redox enzymes were determined in isolated mitochondria with commercially prepared antibodies. Specific proteins were visualized by Enhanced Chemiluminescence (Pierce; Rockford, IL, U.S.A.). Monoclonal antibodies against the 2-oxoglutarate carrier (OGC; *Slc25a11*) and prohibitin and polyclonal antibodies against the dicarboxylate carrier (DIC; *Slc25a10*), superoxide dismutase 2 (Sod2) and the voltage-dependent anion channel (VDAC or porin) were purchased from Abcam (Cambridge, MA, U.S.A.). Polyclonal antibody against thioredoxin 2 (Trx2) was purchased from Santa Cruz Biotechnology (Santa Cruz, CA, U.S.A.). Expression of VDAC or prohibitin was used as mitochondrial loading controls.

Analysis of gene expression by real-time PCR

Total RNA from the renal cortex was isolated using Trizol® (Invitrogen; Carlsbad, CA, U.S.A.). First-strand cDNA was made from the isolated total RNA using a multiscribe reverse transcriptase with random hexamers from Applied Biosystems (Foster City, CA, U.S.A.). TaqMan Gene Assay kits containing primer/probe sets for Oat1 (GenBank accession no. **NM_017224**), Oat3 (GenBank accession no. **NM_031332**), DIC (GenBank accession no. **NM_133418**), OGC (GenBank accession no. **NM_022398**), and glyceraldehyde 3-phosphate dehydrogenase (GAPDH; loading control; GenBank accession no. **NM_017008.3**) were purchased from Applied Biosystems. All reactions were performed in triplicate. The relative amounts of mRNA were calculated by using the comparative C_T method.

Determination of mitochondrial GSH status

A fluorometric method (Hissin and Hilf, 1976) was used for determination of GSH and GSSG in mitochondrial suspensions. GSH content was measured by the fluorescent product formed on reaction with *o*-phthalaldehyde (OPT) with excitation at 350 nm and emission at 420 nm. GSSG content was measured after treatment with *N*-ethylmaleimide, followed by reduction with dithiothreitol and measurement of the fluorescent product formed with OPT.

Enzyme assays and protein determination

Activities of several GSH- and energy metabolism-related enzymes were measured in cytoplasm and/or mitochondria from renal cortical homogenates from control and NPX rats.

GSSG reductase assay:

GSSG reductase (GRD) activity was measured as NADPH oxidation by monitoring the decrease in absorbance at 340 nm (ε = 6,220 $M^{-1}cm^{-1}$) as described by Bellomo et al. (1987).

GSH peroxidase assay:

GSH peroxidase (GPX) activity was measured with 25 mM H_2O_2 as substrate and was equated to NADPH oxidation as detected by the decrease in absorbance at 340 nm (ε = 6,220 $M^{-1}cm^{-1}$) according to Lawrence and Burk (1976).

GSH *S*-transferase assay:

GSH *S*-transferase (GST) activity was measured with 1-chloro-2,4-dinitrobenzene as substrate and quantitation of *S*-2,4-dinitrophenyl-GSH formation by the increase in absorbance at 340 nm (ε = 9,600 $M^{-1}cm^{-1}$) as described by Habig et al. (1974).

Glutamate dehydrogenase assay:

Glutamate dehydrogenase (GDH) activity was measured spectrophotometrically by coupling 2-oxoglutarate reduction to NADH oxidation as described by Schmidt and Schmidt (1983). The oxidation of NADH was coupled to the reduction of 2-oxoglutarate to glutamate according to the following reaction:

$$\text{2-oxoglutarate} + \text{NADH} + NH_4 \longleftrightarrow \text{glutamate} + NAD^+ + H_2O$$

The activity was quantified by determining the consequent decrease in absorbance at 340 nm using an extinction coefficient of 6,220 $M^{-1}cm^{-1}$ for NADH.

Malic dehydrogenase assay:

Malic dehydrogenase (MDH) activity was measured as described by Ochoa (1955). The oxidation of NADH was coupled to the reduction of oxaloacetate to malate according to the following reaction:

$$\text{Oxaloacetate} + \text{NADH} + H^+ \longleftrightarrow \text{L-Malate} + NAD^+$$

The activity was determined by monitoring the decrease in absorbance at 340 nm (ε = 6,220 $M^{-1}cm^{-1}$).

Succinate: cytochrome c oxidoreductase assay:

Succinate: cytochrome c oxidoreductase (SDH) activity was measured as described by Fleischer and Fleischer (1967). The oxidation of succinate to fumarate was coupled to reduction of ferricytochrome c to ferrocytochrome c according to the following reaction:

$$\text{Succinate} + \text{2- ferricytochrome c} \rightarrow \text{fumarate} + \text{2-ferrocytochrome c}$$

The activity was quantified by determining the increase in absorbance at 550.5 nm using an extinction coefficient of 18,500 $M^{-1}cm^{-1}$ for reduced cytochrome c.

Protein Determination:

Protein content of samples was determined by the bicinchoninic acid (BCA) protein assay method using bovine serum albumin as a standard (Bradford, 1976).

Mitochondrial oxygen consumption

Oxygen consumption was measured in suspensions of isolated renal cortical mitochondria from control and NPX rats with a Gilson 5/6H Oxygraph in a thermostated, air-tight, 1.6 ml chamber at 25˚C (Lash et al., 2001a). State 3 rates of oxygen consumption were measured by the addition of 0.3 mM ADP and respiratory substrate (3.3 mM succinate in the presence of 5 μM rotenone) for coupling site II to the chamber containing 0.5 ml of mitochondrial sample and 1 ml mitochondrial buffer. State 4 rates of oxygen consumption were measured after depletion of ADP. Respiratory control ratio (RCR = State 3/State 4) was then calculated.

Mitochondrial Proteomics

Two mitochondrial samples of renal cortical homogenates from control and NPX rat group were used. An aliquot (100 μg) of each mitochondrial extract was reduced with DTT, alkylated with iodoacetamide and digested with trypsin overnight at 37˚C. Each of the samples was labeled with a unique isobaric iTRAQ tag (Applied Biosystems): Control-114 (tag), NPX-115 (tag). The samples were combined and purified by strong cation exchange chromatography using the SCX Methods Development Kit (Applied Biosystems). Each sample was dried and resuspended in water (2 cycles), then dried and resuspended in 2% acetonitrile, 0.1% TFA.

Peptides were separated by reverse phase chromatography (Magic C18 column, Michrom). Peptides were ionized with the ADVANCE ion source (Michrom) and introduced into a LTQ-XL mass spectrometer (Thermo Fisher Scientific). Abundant species were fragmented in Pulsed-Q Dissociation mode (PQD). 5 LC/MS/MS runs were performed, 3 short and 2 long, on the same

sample. Data analyses were performed twice using SEQUEST, X!Tandem and Mascot search engines. A rat protein database (IPI ver 3.47) was used for the analysis.

Relative quantitation:

115/114: average signal intensity (NPX) / average signal intensity (Control)

The proteomics work was done at the Proteomics Core Facility of the Institute of Environmental Health Sciences at Wayne State University, School of Medicine.

Assessment of basal and toxicant-induced mitochondrial oxidative stress

Lipid peroxidation by malondialdehyde assay

One method for assessment of lipid peroxidation was measurement of malondialdehyde (MDA) formation using 1-methyl-2-phenylindole (Gérard-Monnier et al., 1998). Mitochondrial suspensions (200 µl) were treated with tBH (500 µM) or buffer for 1 h at 37˚C and then hydrolyzed using 0.1 M HCl and incubated for 60 min at 60˚C. An aliquot (200 µl) of the resulting supernatant was then incubated with 650 µl 1-methyl-2-phenylindole and 150 µl 37% HCl. After incubating the mixture for 30 min at 45˚C, absorbance at 586 nm was determined.

Lipid peroxidation by cis-parinaric acid fluorescence assay

Cis-parinaric acid is considered a very sensitive marker for the initial stages of lipid peroxidation (Tribble et al., 1994). Isolated mitochondria (1 mg protein/ml) were incubated on ice with 6.4 µM cis-parinaric acid for 15 min. After pelleting mitochondria (11,200 g x 5 min) and discarding

the supernatant, mitochondria were resuspended (0.5 mg protein/ml) in mitochondrial buffer. For anaerobic conditions, mitochondria were resuspended in mitochondrial buffer (prepared with nitrogen sparging) and treated with 5 μM hemin (Fe^{2+}). Samples were then added to a 24-well plate and incubated at room temperature for 10 min before treatment with tBH or buffer. Lipid peroxidation was measured as the loss of cis-parinaric acid fluorescence (excitation 324 nm, emission 413 nm) over time using a fluorescence plate reader (Tribble et al., 1994; Murphy et al., 2003).

Mitochondrial aconitase activity

Aconitase activity was assayed by following formation of NADPH at 340 nm at 25˚C, as described by Han et al. (2003). The reaction mixture contained 30 mM Tris-HCl, pH 7.4, 30 mM sodium citrate, 0.6 mM $MnCl_2$, 0.2 mM $NADP^+$, 1 U/ml isocitrate dehydrogenase and 0.1 mg of mitochondrial protein.

Analysis of oxidative stress markers by Western blot analysis

Proteins modified with 3-nitrotyrosine (3-NT) or 4-hydroxy-2-nonenal (HNE) were also assessed as markers of oxidative alterations in renal mitochondria. Monoclonal antibody to 3-NT was purchased from Abcam (Cambridge, MA, U.S.A.). Polyclonal antibody to HNE was purchased from Calbiochem (La Jolla, CA, U.S.A.).

Effect of toxicant (tBH) on mitochondrial protein expression during compensatory renal hypertrophy

Mitochondrial samples from control and NPX groups were treated with 10 μM tBH for 1h at 37^{o}C. Each of the samples was labeled with a unique isobaric iTRAQ tag (Applied Biosystems): Control-116 (tag), NPX-117 (tag). The samples were processed as described previously in the mitochondrial proteomics section.

Relative quantitation:

117/115: average signal intensity (NPX-tBH) / average signal intensity (NPX)

116/114: average signal intensity (Control-tBH) / average signal intensity (Control)

117/116: average signal intensity (NPX-tBH) / average signal intensity (Control-tBH)

Data analysis

Data for enzyme assays were normalized to the content of cellular protein. All measurements were performed at least 3 to 5 times. Results are expressed as means ± SEM unless specified. Densitometry of bands on Western blots were performed using GelEval 1.22 software for Mac OS X. When two or more parameters were varied and compared (e.g., tBH treatment vs. buffer in control and NPX rats), significant differences among means for data were first assessed by a one-way analysis of variance. When significant "F values" were obtained, the Fisher's protected least significance *t* test was performed to determine which means were significantly different from one another, with two-tail probabilities < 0.05 considered significant. Otherwise, Student's *t*-test was performed to determine which means were significantly different from one another, using a two-tail probability of $P < 0.05$ as the criteria for significance.

II-2 STUDIES IN PROXIMAL TUBULAR CELL PRIMARY CULTURES

Chemicals

Percoll, collagenase (type I; EC 3.4.24.3), type I collagen, bovine serum albumin (fraction V), penicillin G, streptomycin, amphotericin B, insulin (from bovine pancreas), human transferrin, sodium selenite, hydrocortisone, epidermal growth factor (EGF; from mouse submaxillary glands), and 3,3',5-triiodo-DL-thyronine (T3) were purchased from Sigma Chemical Co. (St. Louis, MO). Dulbecco's modified Eagle's medium/Ham's F-12 (DMEM/F-12, 50/50, 1X) was purchased from Mediatech Inc. (Herndon, VA). Polystyrene tissue culture dishes were purchased from Corning Inc. (Corning, NY). Polypropylene micromesh (210 µm pore size) was purchased from SpectraPor Inc. (Rancho Dominguez, CA).

Culture of rat proximal tubular cells

Isolated renal cortical cells were obtained by collagenase perfusion (Jones et al., 1979). A day before perfusion, all the glassware and surgical tools were sterilized in an autoclave. On the day of perfusion, Hank's concentrate (5X) containing 137 mM NaCl, 5.4 mM KCl, 0.81 mM $MgSO_4.7H_2O$, 0.42 mM Na_2HPO_4, 0.44 mM KH_2PO_4 and 25 mM $NaHCO_3$ was used to make Hank's I (25 mM Hepes, 0.5 mM EGTA and 2% (w/v) BSA) and Hank's II (4 mM $CaCl_2$ and 0.15% (w/v) collagenase) buffers. Krebs-Henseleit Concentrate #1 (2X) containing 118 mM NaCl, 4.8 mM KCl, 0.96 mM KH_2PO_4, 1.2 mM $MgSO_4.7H_2O$, 25 mM $NaHCO_3$ and 2.55 mM $CaCl_2.2H_2O$ was used to make KHB-1 buffer. Krebs-Henseleit Concentrate #2 (10X) containing

118 mM NaCl, 4.8 mM KCl, 0.96 mM KH_2PO_4, 1.2 mM $MgSO_4.7H_2O$ and 25 mM $NaHCO_3$ and 25 mM Hepes was used to make KHB-II buffer. All buffers were bubbled with 95% O_2/5% CO_2 for 30 min and adjusted to pH 7.40.

Rats were anaesthetized with an intraperitoneal injection of sodium pentobarbital (50 mg/kg body weight) and injected with 0.3 ml heparin into the tail vein. After sterilizing abdominal walls with 70% (v/v) ethanol, the peritoneal cavity was opened by a midventral incision and the aorta was freed below and above the renal arteries. One ligature with 4-O silk was placed below the renal arteries and a second one was placed right below the liver. To avoid leakage of the perfusion fluid, mesenteric arteries (coeliac and superior) are ligated. A small incision is made in the aorta above the lower ligature and a 19-gauge conical probe cannula is inserted and closed with a clamp and a ligature. The perfusion of kidneys is started *in situ* using Hank's I buffer maintained at 37°C. Once kidneys become pale, Hank's I buffer is replaced by Hank's II buffer maintained at 37°C. After a few minutes of perfusion, the kidneys are excised from the posterior abdominal wall and transferred to beaker containing Hank's II buffer.

After circulating the buffer for 20 min at a flow rate of 5 ml/min, the kidneys are dispersed with a pair of forceps into KHB-1 buffer containing 25 mM Hepes and 2% (w/v) BSA. The digested renal mixtures were filtered through a 210 μm polypropylene micromesh from SpectraPor Inc. (Rancho Dominguez, CA), and then the filtrates were centrifuged for 2 min at 50 rpm at room temperature. The pellets were resuspended in KHB-II buffer and 5 ml of cortical cells were

layered on 35 ml of Percoll solution in 50-ml polycarbonate centrifuge tubes. After centrifuging both tubes at 4°C for 30 min at 12,900 rpm in a SS34 rotor in a Sorvall RC2B centrifuge, the upper layers of cells, which are PT cells, were taken out. The PT cells were diluted with DMEM/F-12 (50/50, 1X) media supplemented with 5 µg/ml insulin, 100 ng/ml Hydrocortisone, 100 ng/ml EGF, 5 µg/ml transferrin, 30 nM sodium selenite, 7.5 pg/ml triidothyronine, 100x antibiotics (penicillin, streptomycin and amphotericin B). The cells were seeded onto collagen-coated, 35-mm polystyrene tissue culture dishes at a density of 2 to 4 x 10^6 cells/ml. Media were changed the next day and every other day thereafter. On day 4 of culture, the cells were processed.

MitoTracker™ orange staining

On day 4 of primary culture, the PT cells were stained with MitoTracker™ orange (50 nM) for 30 min. The cells were viewed with a Zeiss LSM-510 META NLO Laser Scanning Confocal Microscope at 554 nm excitation and 576 nm emission using 630x magnification. Three images of each group were quantitated by using Metamorph 7.1.7.0 Offline (Molecular Devices, Sunnyvale, CA) with measurement of integrated intensity of the entire image. Average intensity (intensity/µm) of three confocal images from each group was then calculated.

JC-1 (5,5',6,6'-tetrachloro-1,1',3,3'-tetraethylbenzyimidazolyl-carbocyanine iodide) staining

On day 4 of primary culture, PT cells were stained with JC-1 (5 µg/ml) for 30 min. The cells were analyzed with a LSM-510 META NLO Laser Scanning Confocal Microscope using an overlay of images in red (488 nm excitation, 590 nm emission, polarization) and green (488 nm excitation, 525 nm emission, depolarization) using 630x magnification. Three images of each group were quantitated by using Metamorph 7.1.7.0 Offline (Molecular Devices, Sunnyvale, CA) with measurement of integrated intensity of the entire image. Average intensity (intensity/µm) of three confocal images from each group was then calculated.

Confocal Microscopy

The confocal work was done at the Microscopy, Imaging and Cytometry Resources Core at Wayne State University, School of Medicine (Detroit, MI).

DNA fluorescence assay

DNA was purified from renal mitochondria from control and NPX rats using the SV genomic DNA purification system (Promega, Madison WI). Mitochondrial DNA was measured by a DNA fluorescence assay (Sorger and Germinario, 1983). Relative fluorescence of the DNA-DAPI complex was measured with a SpectraMax M2 plate reader set to 360 nm excitation and 450 nm emission. A concentrated DAPI stock solution (1 mg/ml in water) was wrapped in foil and stored

at 0-4˚C. A DAPI working solution (2.5 µg/ml) was prepared by bringing 1 ml of DAPI stock solution (1 mg/ml) to 400 ml with assay buffer (18 mM Na_2SO_4 in 50 mM Hepes, pH 7.0).

Standards were prepared containing 0.25-2.5 µg DNA/ml, 200 µg BSA/ml and 10 µl/ml of 1 M NaOH in 0.2% Triton X-100. Aliquots of standards and mitochondrial samples were added to disposable glass tubes and 2.5 ml of DAPI reagent (0.4 volumes of DAPI working solution (2.5 µg/ml), 3.6 volumes of assay buffer, 6 volumes of water) was added to each tube. After 90 min of incubation at room temperature, relative fluorescence was measured.

Mitochondrial protein assay

Protein content of renal mitochondrial samples was determined by the bicinchoninic acid (BCA) protein assay method using bovine serum albumin as a standard (Pierce Rockford, IL).

Transfection

DIC cDNA that was cloned into pcDNA 3.1/V5-His-TOPO vector (Lash et al., 2002b) and cDNA encoding OGC that was cloned into pcDNA 3.1/V5-His-TOPO vector (Xu et al., 2006) were purified using Maxiprep (Promega, Madison WI).

On day 3 of primary culture, cells were transfected with purified DIC and OGC plasmids with final concentration of 800 ng plasmid DNA/well of Dulbecco's modified Eagle's medium using Lipofectamine^{TM} and PLUS^{TM} reagents (Invitrogen; Carlsbad, CA, U.S.A.).

Gene expression by real-time PCR

Total RNA was isolated on day 6 of cell culture (72 h post-DIC transfection) from cell culture of rat PT cells using Trizol$^{®}$ (Invitrogen; Carlsbad, CA, U.S.A.). First-strand cDNA was made from the isolated total RNA using a multiscribe reverse transcriptase with random hexamers from Applied Biosystems (Foster City, CA, U.S.A.). Taq Man gene assay kits containing primer/probe sets for DIC (GenBank accession no. NM 133418), OGC (GenBank accession no. NM 022398) and glyceraldehyde 3-phosphate dehydrogenase (GAPDH, GenBank accession no. NM 017008.3) were purchased from Applied Biosystems. The fold change of genes was calculated by the $2^{\Delta CT}$ formula where 2 is used assuming a doubling in every cycle.

Assay for assessment of cytotoxicity

Necrotic cell death was measured in PT cells by measurement of lactate dehydrogenase (LDH) release. On day 6, suspensions of PT cells were treated with either antimycin A (1 μM, 10 μM), tBH (100 μM, 200 μM) or MVK (100 μM, 200 μM) for 4 h with or without an overnight preincubation with 5 mM GSH. After 4 h, aliquots were removed and LDH activity was measured. LDH activities in supernatant and cells were measured spectrophotometrically as

NADH oxidation at 340 nm after addition of 3 mg/ml pyruvate and 3 mg/ml NADH. Percentage of LDH release was calculated using the formula:

% LDH release = [LDH activity in media/(LDH activity in media + LDH activity in cells)] x 100%

Data analysis

Results are expressed as means ± SE values of measurements from the indicated number of cell preparations. Significant differences among selected mean values were calculated using Student's t-test with P values ≤ 0.05 as the criteria for significance.

CHAPTER III. RENAL FUNCTION

Renal physiological parameters *in vivo*

Results

Examination of basic parameters of renal function indicates that there are some discernable changes in rats post-nephrectomy compared to age-matched control rats (**Table 3-1**). After uninephrectomy and a 10-day period to allow for completion of the acute phase of compensatory growth, the remaining kidney weighs significantly more than a single kidney from control rats. NPX animals had markedly higher urine volume, indicating an increase in renal function to compensate for the loss of a kidney. However, we also observed increases in total urinary protein (U-Pr), urinary albumin (UAlb), serum creatinine (S-Cr), urinary N-acetyl-β-D-glucosaminidase (U-NAG), urinary γ-glutamyltransferase (U-GGT) and urinary glutathione disulfide (U-GSSG), but lower urinary creatinine (U-Cr) over a 24-h period and lower creatinine clearance (CCr), indicating significant impairment of renal function.

Table 3-1. Physiological parameters of renal function *in vivo*.

Parameters were measured in uninephrectomized (NPX) rats at 10 days post-surgery and in age-matched control rats. Results are means ± SEM of measurements from the indicated number of rats from each group.

Parameter (units; n)	Control	NPX
Kidney Weight (g; 10)	0.95 ± 0.04	1.51 ± 0.06*
U-Vol (ml; 6)	3.08 ± 0.47	8.43 ± 1.63*
U-Pr (mg/24 h; 6)	11.1 ± 1.5	34.9 ± 3.2*
S-Cr (mg/dl; 3)	0.09 ± 0.04	0.24 ± 0.06*
U-Cr (mg/dl; 3)	168 ± 7	93.6 ± 11.2*
U-Cr (mg/24 h; 3)	7.63 ± 0.48	5.43 ± 0.30*
CCr (ml/min; 3)	6.67 ± 0.80	2.00 ± 0.54*
U-Alb (mg/24 h; 3)	150 ± 10	860 ± 110*
U-GSSG (nmol/24 h; 6)	1.53 ± 0.73	9.51 ± 0.32*
U-NAG (U/24 h; 9)	0.07 ± 0.01	0.14 ± 0.03*
U-GGT (mU/24 h; 6)	197 ± 9	327 ± 30*

Abbreviations: U-Vol, urinary volume; U-Pr, urinary protein; S-Cr, serum creatinine; U-Cr, urinary creatinine; CCr, creatinine clearance; U-Alb, urinary albumin; U-GSSG, urinary

glutathione disulfide; U-NAG, urinary N-acetyl-β-D-glucosaminidase; U-GGT, urinary γ-glutamyltransferase. *Significantly different ($P<0.05$) from the corresponding value in control rats.

Discussion

The major underlying hypothesis to explain the physiological and pathological changes that occur in remnant renal tissue as a consequence of compensatory renal hypertrophy begins with the increased need for renal function requiring increased mitochondrial electron transport to generate ATP (Meyer et al., 1996; Harris et al., 1988; Nath et al., 1990; Shapiro et al., 1994). As a consequence of this increase in mitochondrial function, more reactive oxygen species are generated, which in turn leads to a higher level of renal oxidative stress, further leading to increased susceptibility of renal PT cells from NPX rats to nephrotoxicants.

The present study not only confirmed the increase in kidney weight and urine production that accompany the compensatory response of the remnant kidney after uninephrectomy, but also provided evidence at the *in vivo* level that this compensation is associated with some degree of renal damage. Several markers, which are all considered diagnostic for renal function, were uniformly altered in a manner consistent with mild renal injury. Evidence for renal injury at the level of the PT cell was also observed by the increases in U-NAG and U-GGT. We also observed a 6.2-fold increase in U-GSSG, which may indicate some amount of oxidative damage in the kidneys. Compared to normal conditions in which creatinine is filtered and proteins usually do not cross the glomerular membrane, compensatory renal hypertrophy decreases creatinine clearance but increases protein secretion. Previous studies have shown that proteinuria is also correlated with intrinsic renal toxicity and contributes to progression of renal damage (Bertani et al., 1986). The compensatory renal hypertrophy also decreases the ability to conserve ions, bicarbonate and water, leading to increases in urine volume. This suggests increased renal function to compensate for the reduction in nephron mass.

Our data are also consistent with previous animal studies that suggested that glomerular hypertension and glomerular hyperfiltration lead to pathogenesis of proteinuria and progressive glomerulosclerosis (Hostetler et al., 2001). Overall, our data also suggest some clinical implications such as proteinuria, microalbuminuria and hypertension, which is consistent with data from human clinical studies that are investigating the quality of life of renal transplant donors (Berber et al., 2008; Tellioglu et al., 2008; Azar et al., 2007).

Protein and gene expression analysis of renal plasma membrane organic anion transporters.

Results

Based on previous observations of increases in intracellular GSH concentrations and GSH transport activity after compensatory renal hypertrophy (Zalups and Lash, 1990; Lash et al., 2001b), we hypothesized that these increases were due, at least in part, to increases in gene and/or protein expression of carriers involved in GSH transport across renal plasma membranes. To test this, we determined mRNA and protein expression of four renal plasma membrane transporters that are known or thought to be involved in GSH transport. Real-time PCR analysis of Oat1 and Oat3 mRNA expression (**Table 3-2**) revealed no differences between control and NPX rats. In contrast, Western blot analyses of Oat1 and Oat3 protein levels showed nearly 2-fold increases in protein expression for both carriers in kidneys of NPX rats as compared to those of control rats (**Figure 3-1**).

Additionally, expression of two Mrp carriers that can transport GSH were examined. Whereas protein expression of Mrp2, which is localized to the BBM, was increased by approximately 30% in NPX rat kidneys as compared to that in control rat kidneys, expression of Mrp5, which is localized to the BLM, was unchanged. Inasmuch as both Oat1 and Oat3 are believed to mediate uptake of GSH into the renal PT cell whereas both Mrp2 and Mrp5 mediate efflux from the cell, the larger increase in Oat1/3 compared to that for Mrp2 are consistent with higher intracellular accumulation of GSH. We also examined protein expression of the $(Na^+ + K^+)$-ATPase, which

provides the major driving force for many secondary active transport carriers; its expression was also found to be significantly higher (1.4-fold) in kidneys of NPX rats as well.

Figure 3-1. Effect of compensatory renal growth on protein expression of renal plasma membrane organic anion transporters and the (Na^+ + K^+)-stimulated ATPase.

Protein expression of Oat1, Oat3, Mrp2, Mrp5 and the (Na^+ + K^+)-stimulated ATPase were determined by Western blot analysis as described in Section 2. β-Actin protein was used as a loading control. Blots were scanned and quantified by densitometry using GelEval 1.22 software. Data represent means ± SEM of measurements from renal homogenates from three control and three NPX rats. *Significantly different ($P < 0.05$) from corresponding control sample.

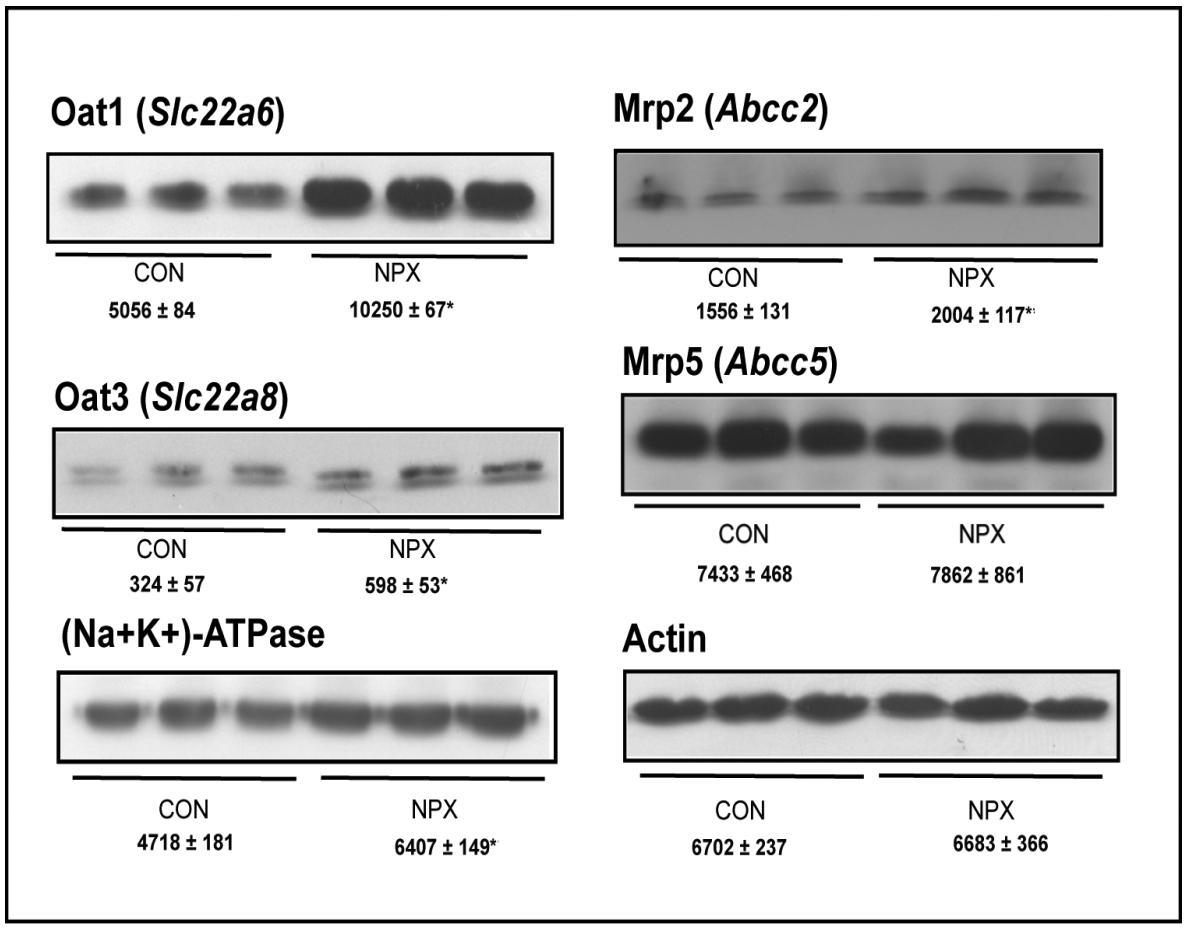
Oat1 (Slc22a6)
CON
NPX
5056 ± 84
10250 ± 67*
Mrp2 (Abcc2)
CON
NPX
1556 ± 131
2004 ± 117*
Oat3 (Slc22a8)
CON
NPX
324 ± 57
598 ± 53*
Mrp5 (Abcc5)
CON
NPX
7433 ± 468
7862 ± 861
(Na+K+)-ATPase
CON
NPX
4718 ± 181
6407 ± 149*
Actin
CON
NPX
6702 ± 237
6683 ± 366

Table 3-2. Real-time quantitative PCR analysis of Oat1, Oat3 mRNA expression in renal cortex of control and NPX rats.

Primers were designed with the aid of Oligo 6.76 and the cDNA sequences published in GenBank™. Primer and labeled probe sets were from Applied Biosystems. An optimum cDNA concentration of 30–300 ng DNA/well was determined for each gene. All C_T values are based on the measurements of total RNA samples from kidney cortex of both control and NPX rats and are means ± SEM. GAPDH C_T values were used for correction: For Oat1 and Oat3 samples, GAPDH C_T values = 30.3 ± 0.2 for control rats and 30.4 ± 0.3 for NPX rats. Relative gene expression values were calculated by the formula: $2^{-\Delta CT\ (NPX)} / 2^{-\Delta CT\ (Control)}$, ΔC_T value is the difference between the C_T value for the gene of interest and that of GAPDH.

Gene	**Control**	**NPX**	**Relative Expression**
	C_T mean ± SE	C_T mean ± SE	(NPX / Control)
Oat 1 (Slc22a6)	31.4 ± 0.3	32.0 ± 0.8	0.75
Oat 3 (Slc22a8)	32.4 ± 0.1	32.8 ± 0.5	0.86

Discussion

A longstanding observation is that compensatory renal hypertrophy is associated with a significant increase in total cellular GSH content compared to that in kidneys from control rats, particularly in the PT region of the nephron (Zalups and Lash, 1990). We previously showed that compensatory renal hypertrophy is associated with higher activity of γ-glutamylcysteine synthetase (GCS) (Lash and Zalups, 1992, 1994; Lash et al., 2001b). While higher GCS activity could certainly be one mechanism for the increase in the cytoplasmic pool of GSH, increased transport across the BLM of plasma or renal periplasma GSH is also another potential mechanism. Thus, increase in the activity and/or expression of the plasma membrane carrier proteins that are responsible for GSH transport into the PT cell may also help explain some of the data.

Despite the lack of a clear understanding of the physiological role(s) for uptake of GSH into the renal PT cell, several candidate carrier proteins have been identified (Lash, 2005, 2009; Lash et al., 2007). These include Oat1, Oat3, and the sodium-dicarboxylate 3 (NaC3; *Slc13a3*) carriers on the renal BLM. Additionally, both Mrp2 and Mrp5 can mediate efflux of GSH out of the renal PT cell across the BBM and BLM, respectively. The present study demonstrated significantly higher protein expression (~ 2-fold increases) for both Oat1 and Oat3 in renal homogenates from NPX rats. Whereas no difference was observed between Mrp5 expression in renal homogenates from control and NPX rats, Mrp2 protein expression was modestly (~ 50%) higher in renal tissue from NPX rats. Thus, although there is higher efflux by Mrp2, the increases in uptake by Oat1 and Oat3 would seem to predominate, thereby leading to higher intracellular accumulation of

GSH. These results are consistent with our previous finding of higher activity of both Oat1 and Oat3 in renal BLM vesicles from NPX rats as compared to those from control rats (Lash et al., 2005).

Expression of these Oat carriers at the mRNA level was also determined by real-time PCR. Despite our expectation that mRNA levels of the Oat carriers would be higher in kidneys of NPX rats, we found no differences between kidneys of the two groups of rats. This indicates that the changes in the plasma membrane carriers that occur as a consequence of compensatory renal growth are post-transcriptional and/or post-translational, and probably involve a combination of effects, including increased mRNA translation, increased protein stability, and/or decreased protein degradation.

CHAPTER IV. MITOCHONDRIAL STATUS

Mitochondrial redox status

Results

To determine whether or not compensatory renal hypertrophy causes alterations in renal mitochondrial redox status, we first measured mitochondrial GSH (reduced glutathione) and GSSG (glutathione disulfide) levels in renal mitochondria from both control and NPX rats. Modest, but significant increases were observed in concentrations of both GSH and GSSG in renal mitochondria from NPX rats as compared to those from control rats (**Table 4-1**).

Inasmuch as GSH status in renal mitochondria is determined primarily, if not entirely, by the function of two inner membrane carrier proteins, the DIC and OGC (Chen and Lash, 1998; Chen et al., 2000), we next determined gene and protein expression of these carriers. Because previous work (Lash et al., 2001a) showed markedly higher rates of GSH uptake by renal mitochondria from NPX rats as compared to those from control rats, we expected to see increases in expression of these carrier proteins. Despite this expectation, neither mRNA (**Table 4-2**) nor protein (**Figure 4-1**) expression of either the DIC or OGC were elevated in renal mitochondria from NPX rats as compared to those in renal mitochondria from control rats. Besides the GSH system, redox status in mitochondria is also regulated by two other enzymes, superoxide dismutase 2 (Sod2) and thioredoxin 2 (Trx2). Measurements of protein expression of Sod2 and Trx2 (**Figure 4-2**), however, showed no significant differences between renal mitochondria of control and NPX rats.

Table 4-1. GSH and GSSG concentrations in renal mitochondria from control and NPX rats.

Mitochondrial GSH and GSSG levels were measured in suspensions of isolated mitochondria from rat renal cortex from control and NPX rats using a fluorometric method. Results are nmol/mg protein and are means ± SEM of measurements from three rats from each group.

Parameter	Control	NPX
GSH	1.67 ± 0.08	1.97 ± 0.05*
GSSG	0.90 ± 0.04	1.05 ± 0.02*

* Significantly different ($P<0.05$) from the corresponding value in control rats.

Figure 4-1. Effect of compensatory renal growth on protein expression of renal mitochondrial GSH transporters.

Mitochondrial samples were isolated from rat kidney cortex of control (CON) and uninephrectomized (NPX) rats and subjected to immunoblotting with anti-DIC, -OGC and -VDAC. The VDAC protein served as a mitochondrial loading control. Note that the OGC protein was detected as both monomers (M_r = 32.5 kDa) and a dimer (M_r = 65 kDa). Blots were scanned and quantified by densitometry using GelEval 1.22 software. Data represent means ± SEM of measurements from renal mitochondrial samples from three CON and three NPX rats. No significant differences were detected between corresponding CON and NPX samples.

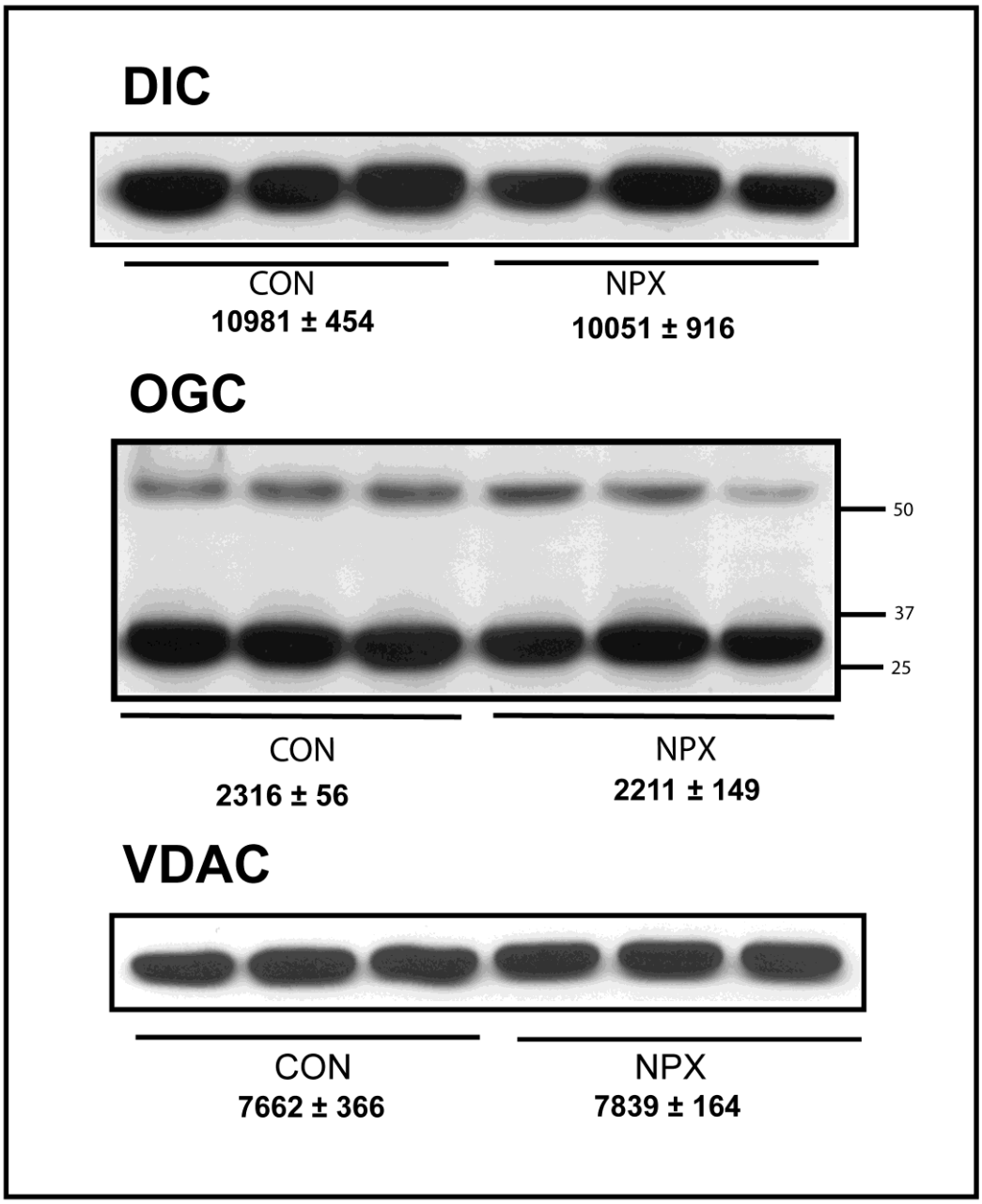
DIC
CON
10981 ± 454
NPX
10051 ± 916
OGC
50
37
25
CON
2316 ± 56
NPX
2211 ± 149
VDAC
CON
7662 ± 366
NPX
7839 ± 164

Table 4-2. Real-time quantitative PCR analysis of DIC and OGC mRNA expression in renal cortex of control and NPX rats.

Primers were designed with the aid of Oligo 6.76 and the cDNA sequences published in GenBank™. Primer and labeled probe sets were from Applied Biosystems. An optimum cDNA concentration of 30–300 ng DNA/well was determined for each gene. All C_T values are based on the measurements of total RNA samples from kidney cortex of both control and NPX rats and are means ± SEM. GAPDH C_T values were used for correction: For DIC and OGC samples, GAPDH C_T values = 30.3 ± 0.2 for control rats and 30.4 ± 0.3 for NPX rats. Relative gene expression values were calculated by the formula: $2^{-\Delta CT\ (NPX)} / 2^{-\Delta CT\ (Control)}$, ΔC_T value is the difference between the C_T value for the gene of interest and that of GAPDH.

Gene	**Control**	**NPX**	**Relative Expression**
	C_T mean ± SE	C_T mean ± SE	(NPX / Control)
DIC (Slc22a10)	32.9 ± 0.2	33.4 ± 0.4	0.78
OGC (Slc22a11)	33.6 ± 0.3	33.9 ± 0.1	0.89

Figure 4-2. Effect of compensatory renal growth on protein expression of renal mitochondrial Sod2 and Trx2.

Mitochondrial samples were isolated from rat kidney cortex of control (CON) and uninephrectomized (NPX) rats and subjected to immunoblotting with anti-Sod2, anti-Trx2, and anti-prohibitin. The prohibitin protein served as a mitochondrial loading control. Blots were scanned and quantified by densitometry using GelEval 1.22 software. Data represent means ± SEM of measurements from renal mitochondrial samples from three CON and three NPX rats. No significant differences were detected between corresponding CON and NPX samples.

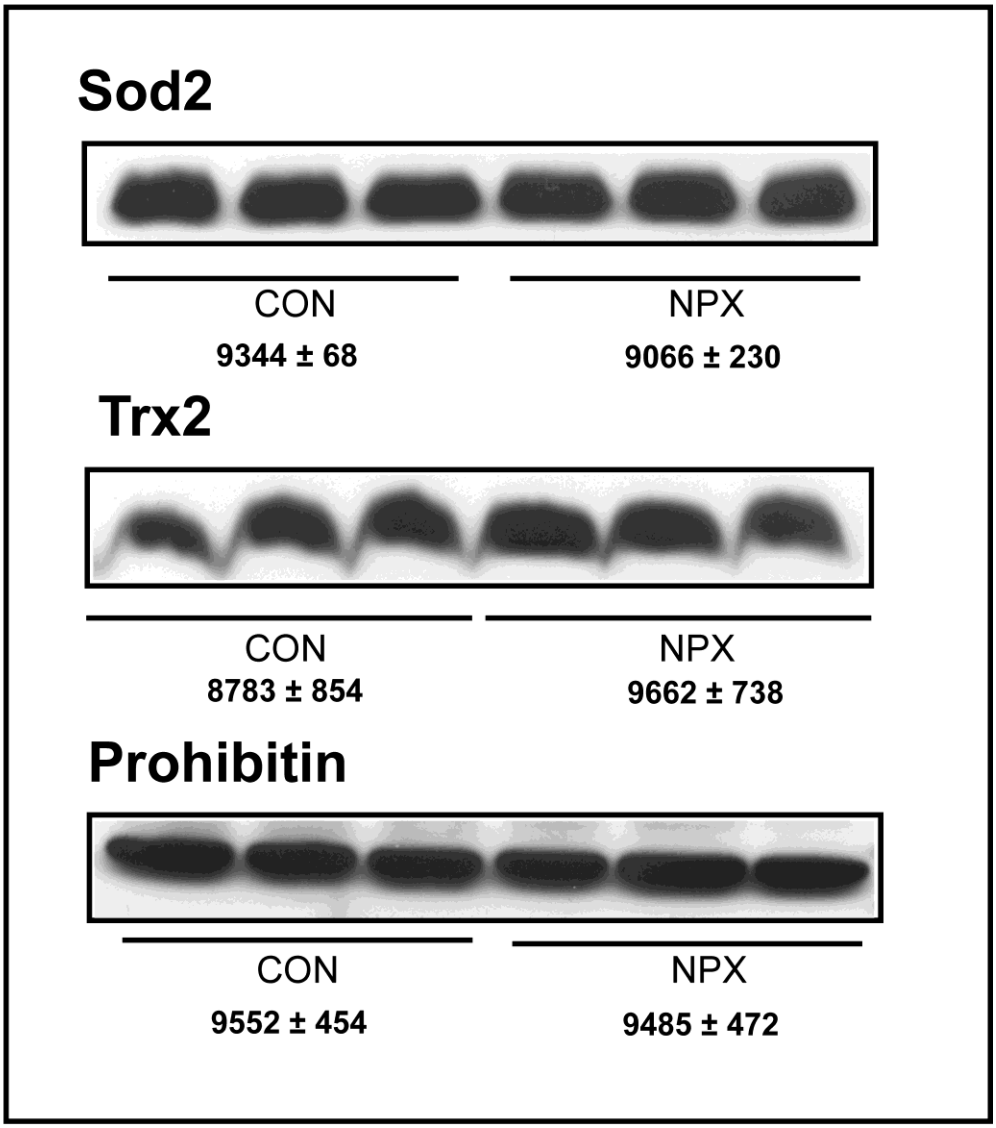
Sod2
CON
NPX
9344 ± 68
9066 ± 230
Trx2
CON
NPX
8783 ± 854
9662 ± 738
Prohibitin
CON
NPX
9552 ± 454
9485 ± 472

Discussion

Although most of the GSH detected when one measures total cellular content resides in the cytoplasm, changes in the status of GSH in the mitochondrial pool would also be expected to occur. Such changes in mitochondrial GSH content have important impacts on mitochondrial function, cellular energetics, and ultimately cell viability (Lash et al., 1998). The present study demonstrated a significantly higher level of GSH specifically in renal mitochondria from NPX rats as compared to those from control rats. Because GSH synthesis in the renal PT cell only occurs in the cytoplasm (McKernan et al., 1991), transport of GSH across the mitochondrial inner membrane would appear to be the sole source of GSH for the mitochondrial matrix. In the renal cortex and PT cell, the DIC and OGC are the two carriers we identified as being responsible for this transport process (Chen and Lash, 1998; Chen et al., 2000). The functional importance of this renal mitochondrial GSH pool has been demonstrated in studies in which genetic manipulation of DIC or OGC expression markedly altered redox status and susceptibility to oxidants and other nephrotoxicants (Lash et al., 2002a 2002b; Xu et al., 2006).

Besides showing an increase in mitochondrial GSH content, we previously found markedly increased rates of GSH uptake into renal mitochondria (Lash et al., 2001a). While this suggested to us that expression of the DIC and/or the OGC might be up-regulated in compensatory renal hypertrophy, measurements of both mRNA and protein expression for the two mitochondrial carriers showed no differences between control and NPX rats. To understand, then, what is responsible for the increased content of GSH in renal mitochondria from NPX rats, one has to consider the functions of the DIC and OGC in dicarboxylate transport and the observations that activities of several mitochondrial dehydrogenases and succinate-dependent respiration were

significantly higher in renal mitochondria from NPX rats. The increased mitochondrial uptake of GSH in compensatory renal hypertrophy, therefore, is likely due to kinetic or mass action effects resulting from the hypermetabolic state. In other words, the higher supply of dicarboxylate substrate for the two carriers drives the uptake of GSH into the mitochondria.

Impact of compensatory hypertrophy on functional characteristics of renal mitochondria

Enzyme results

Activities of several enzymes that are indicative of cellular energetics and redox status were measured in preparations of mitochondria and cytoplasm from renal cortex of control and NPX rats (**Table 4-3**). With the exception of small decreases in mitochondrial GPX and cytoplasmic GST in kidneys of NPX rats, there were no significant differences in activities of GSH-dependent detoxification enzymes between control and NPX rat kidneys. In contrast, activities of malic dehydrogenase, glutamate dehydrogenase and succinate: cytochrome c oxidoreductase were significantly higher in renal mitochondria from NPX rats as compared to those from control rats. These increases in key enzymes of mitochondrial intermediary metabolism without corresponding changes in mitochondrial GSH-dependent enzymes are consistent with there being changes in mitochondrial redox status in kidneys of NPX rats.

Table 4-3. Effect of compensatory renal hypertrophy on GSH-dependent and mitochondrial enzymes.

Enzyme activities were measured in cytoplasm or mitochondria isolated from kidney(s) of uninephrectomized (NPX) rats at 10 days post-surgery and age-matched control rats. Results are expressed as mU/mg protein and are means ± SEM of measurements from six rats from each group.

Enzyme	**Control**	**NPX**
	mU/mg protein	mU/mg protein
GSSG Reductase		
Mitochondria	16.5 ± 1.8	19.9 ± 0.9
Cytoplasm	21.1 ± 0.8	19.6 ± 0.8
GSH peroxidase		
Mitochondria	12.6 ± 0.5	9.69 ± 0.06*
Cytoplasm	11.7 ± 0.9	10.9 ± 0.8
GSH S-transferase		
Mitochondria	4.91 ± 0.97	2.71 ± 0.31*
Cytoplasm	34.1 ± 0.7	25.6 ± 0.2*
Malic dehydrogenase		
Mitochondria	27.1 ± 1.7	38.3 ± 1.4*
Glutamate dehydrogenase		
Mitochondria	57.7 ± 4.2	77.5 ± 6.1*

Succinate: cytochrome c oxidoreductase		
Mitochondria	28.7 ± 1.1	56.7 ± 4.2*

*Significantly different ($P < 0.05$) from the corresponding value in control rats.

Respiration results

Succinate-stimulated (complex II) state 3 respiration was also higher in renal mitochondria from NPX rats than in those from control rats (**Table 4-4**). Similarly, the RCR value, which gives an indication of how well oxygen consumption is coupled to ADP phosphorylation, was significantly elevated with succinate (complex II) as respiratory substrate in renal mitochondria from NPX rats relative to that in renal mitochondria from control rats. This significant acceleration of mitochondrial respiratory activity after compensatory renal cellular hypertrophy is consistent with the increased activities of mitochondrial dehydrogenases noted above and the general hypothesis that renal mitochondria from NPX rats are in a hypermetabolic state.

Table 4-4. Effects of compensatory renal hypertrophy on mitochondrial respiration.

Mitochondrial succinate-dependent State 3 and State 4 respiration were measured in suspensions of isolated mitochondria from kidney(s) of control and NPX rats. Rates of oxygen consumption were determined in an Oxygraph with a Clark-type electrode using 3.3 mM succinate as respiratory substrate in the presence of 5 μM rotenone. Results are means ± SEM of measurements from six separate mitochondrial preparations from each group.

RCR= respiratory control ratio = State 3 rate / State 4 rate.

Parameter	Control	NPX
State 4 (nmol O_2/min per mg protein)	18.6 ± 1.4	19.7 ± 1.0
State 3 (nmol O_2/min per mg protein)	27.0 ± 2.8	41.7 ± 1.5*
RCR	1.88 ± 0.02	3.16 ± 0.10*

*Significantly different ($P<0.05$) from the corresponding value in mitochondria from control rats.

Proteomics results

To further explore mitochondrial energetics data (enzyme activities and respiration), a proteomics analysis of mitochondria from control and NPX rats was conducted to obtain an overview of mitochondrial protein levels. Using the SEQUEST and X!Tandem search engines, a total of 117 proteins were identified with ≥ 99% probability. Using the Mascot search engine, a total of 72 proteins were identified with ≥ 95% probability, of which 25 proteins were quantitated. For each protein, relative quantitation was calculated. As shown in **Table 4-5**, all the numbers in bold print signify a 1.5-fold or higher difference.

In order to facilitate interpretation of mitochondrial proteomics data, we divided mitochondrial proteins into different categories and defined proteins belonging to the respective categories. The energy production category involves proteins that are involved in ATP synthesis and many metabolic pathways such as the tricarboxylic acid cycle, electron transport chain, amino acid, fatty acid, ketone body and drug metabolism. The apoptosis category is composed of proteins known to play a role in mitochondrial stress response. The data show an increase in expression of proteins that are involved in ATP synthesis, stress response, tricarboxylic acid (citric acid) cycle, respiratory electron transport chain and various metabolic pathways including amino acid, fatty acid and ketone body metabolism in the NPX group, further suggesting that a hypermetabolic state exists after uninephrectomy and compensatory renal growth.

Table 4-5. Mitochondrial Proteomics.

All the numbers in bold print signify a 1.5 fold or higher difference.

Relative quantitation: average signal intensity (NPX) / average signal intensity (Control)

Accession		NPX/Con
	ATP Synthesis, Transport and Metabolic Processes	
P10719	ATP synthase subunit beta	1.2
Q98QB6	ATP synthase subunit beta 2 (ATP synthase F1 sector subunit beta 2)	**1.5**
P15999	ATP synthase subunit alpha	**1.5**
P05141	ADP/ATP translocase 2 (ADP,ATP carrier protein 2)	0.8
	Stress Response Proteins	
Q64433	10 kDa heat shock protein (Hsp10)	1.4
P63038	Heat shock protein 60 (HSP-60)	**1.7**
	Tricarboxylic acid cycle (Citrate Cycle)	
P56574	Isocitrate dehydrogenase [NADP], (Oxalosuccinate decarboxylase)	**1.6**
Q9ER34	Aconitate hydratase, (Aconitase)	**2.5**
	Respiratory Electron Transport Chain	
Q52V09	Cytochrome c	1.4
P13803	Electron transfer flavoprotein subunit alpha	1.0

Q66HF1	NADH-ubiquinone oxidoreductase 75 kDa subunit	**1.9**
	Amino Acid and Fatty Acid Metabolic Pathways	
P50442	Glycine amidinotransferase, (Transamidinase)	**1.9**
Q64565	Alanine-glyoxylate aminotransferase 2, (Beta-alanine-pyruvate aminotransferase)	**2.1**
Q02253	Methylmalonate-semialdehyde dehydrogenase (Malonate-semialdehyde dehydrogenase)	1.3
P08503	Medium-chain specific acyl-CoA dehydrogenase	**2.6**
Q64428	Trifunctional enzyme subunit alpha, (3-hydroxyacyl-CoA dehydrogenase)	0.7
P26443	Glutamate dehydrogenase 1	**1.9**
	Ketone Metabolism	
Q9D0K2	Succinyl-CoA:3-ketoacid-coenzyme A transferase 1, (3-oxoacid CoA-transferase 1)	**1.5**
	Drug Metabolism	
Q64573	Kidney microsomal carboxylesterase (Liver carboxylesterase 3)	**1.5**
	Anion Transport (Transmembrane Transport)	
Q9Z2L0	Voltage-dependent anion-selective channel protein 1 (VDAC-1)	1.1
	Amino acid Transport	

Q64319	Neutral and basic amino acid transport protein rBAT (B(0,+)-type amino acid transport protein)	1.0
	Oxidoreductase Activity	
Q6AYT0	Quinone oxidoreductase (Zeta-crystallin)	1.2
Q07523	Hydroxyacid oxidase 2	1.0
Q68FT3	Probable oxidoreductase C10orf33 homolog	**1.9**
Q9DBF1	Aldehyde dehydrogenase family 7 member A1 (Antiquitin-1)	0.9

Discussion

The basic concept of the hypermetabolic state that is suggested to exist in compensatory renal hypertrophy is that the remnant renal tissue must work harder to try and make up for the lost function. The principal means to accomplish this is through increased generation of ATP by the mitochondria, which is tightly regulated in the kidneys according to the need for metabolic energy (Soltoff, 1986). In the present study, evidence for increased rates of mitochondrial metabolism were the significant increases in activities of malic, glutamate, and succinate dehydrogenases and State 3 rates of succinate-dependent respiration. We also observed significantly higher protein expression of the $(Na^{+}+K^{+})$-ATPase in kidneys from NPX rats, which agrees with our previous observation of higher enzymatic activity in renal PT cells from NPX rats (Lash et al., 2001b). Because this protein is one of the primary consumers of ATP in the renal PT cell (Soltoff, 1986), its higher expression and activity in kidneys from NPX rats as compared to those from control rats provide further support for the conclusion that compensatory renal hypertrophy generates a hypermetabolic state in the remnant renal cell due to increased energy demands.

In this study, we applied proteomics for relative quantification of mitochondrial proteins and analyzed the main pathways of mitochondrial activity for energy metabolism and stress response. Consistent with mitochondrial enzyme and respiration data, mitochondrial proteomics data also suggest the existence of a hypermetabolic state and stress in mitochondria from hypertrophied kidney. As mitochondrial proteins are central to various metabolic activities, disturbance of mitochondrial proteins is also often associated with a variety of diseases or various pathological states such as respiratory chain defects, fatty acid oxidation deficiencies and neurodegenerative

disease (Chan, 2006; Janssen et al., 2004; Gregersen et al, 2004; Kwong et al., 2006). This assessment of mitochondrial proteins provides specific, mechanistic information about molecular changes that influence cellular metabolism in mitochondria from both hypertrophied and normal kidney.

Overall, our enzyme, respiration and proteomics data suggested a hypermetabolic state in hypertrophied kidney. As mitochondria are the major organelles to produce superoxide anion in cells, increased mitochondrial respiration and mitochondrial function also suggests potential increase in reactive oxygen species (ROS) formation, which in turn possibly lead to a higher basal state of oxidant stress as compared to mitochondria from normal rat kidneys. In addition, the upregulation of mitochondrial proteins that are involved in metabolic pathways and apoptosis might be a way for cells to cope with potential basal oxidative stress during compensatory renal hypertrophy.

Assessment of basal and toxicant-induced oxidative stress in renal mitochondria

Results

The hypermetabolic state of renal mitochondria from NPX rats, and the evidence of renal dysfunction, suggest that a higher state of oxidative stress exists that may contribute to higher susceptibility to chemically induced injury. To compare basal and toxicant induced oxidative stress between renal mitochondria from control and NPX rats, we analyzed lipid peroxidation by using two assays (one assay based on MDA formation and one based on degradation of cis-parinaric acid) and measured aconitase activity as a marker for mitochondrial oxidative stress. We also examined two types of protein adducts as oxidative stress markers, 3-NT (3-nitrotyrosine) and HNE (4-hydroxy-2-nonenal).

The results of the MDA assay show that there is no significant difference in renal mitochondrial lipid peroxidation between control and NPX rats under either basal conditions or when mitochondria are challenged by exposure to tBH (**Figure 4-3A**). The naturally occurring polyunsaturated fatty acid cis-parinaric acid is used in eukaryotic cells as a very sensitive marker for the initial stages of lipid peroxidation (Tribble et al., 1994). When double bonds of cis-parinaric acid are broken in lipid peroxidation reactions, decay in fluorescence is used to indirectly monitor the degree of membrane lipid peroxidation. Under anaerobic conditions (N_2 + Fe^{2+}), there was no significant difference in either basal or tBH-induced mitochondrial lipid peroxidation between control and NPX rats (**Figure 4-3B**).

Because mitochondrial aconitase activity is a sensitive indicator of redox homeostasis and its activity is uniquely sensitive to various physiological and pathological conditions (James et al., 2002), it is frequently viewed as a marker of oxidative stress in biological systems. The underlying mechanism is believed to be the facile inactivation of its iron–sulfur prosthetic group by toxicants such as peroxides (Han et al., 2003; James et al., 2002; Gardner et al., 1994). As shown in **Figure 4-3C**, renal aconitase activity was significantly lower in mitochondria from NPX rats relative to control rats even without any exogenous toxicant, suggesting that renal compensatory hypertrophy does cause an increase in underlying mitochondrial oxidative stress. The progressive oxidative stress in animals with renal insufficiency can lead to oxidation of proteins, carbohydrates, nucleic acids, lipids and accumulation of harmful byproducts in various tissues (Himmelfarb et al., 2002; Vaziri, 2004). As a further assessment of mitochondrial redox status, we analyzed protein adducts of two oxidative stress markers, 3-NT and HNE, by Western blot analysis in renal mitochondria. No differences were observed in blots for 3-NT modified proteins (data not shown). However, assessment of HNE-adducted proteins showed significantly higher staining in renal mitochondria from NPX rats, with the most prominent staining at 45 kDa and 52 kDa (**Figure 4-3D**).

To analyze the effect of toxicant (tBH) on mitochondrial protein levels, we performed proteomic analyses on mitochondrial samples from control and NPX groups. Using the Mascot search engine, a total of 72 proteins were identified with ≥ 95% probability, of which 25 proteins were quantitated. For each protein, relative quantitation was calculated. As shown in **Table 4-6**, all the numbers in bold print signify a 1.5-fold or higher difference and a 0.5-fold or lower difference.

The comparison of NPX-tBH/Control-tBH protein expression cannot clearly suggest if changes are due to the effects of nephrectomy or toxicant-treatment. To further explore these data, we also analyzed the protein fold change using NPX-tBH/NPX and Control-tBH/Control comparisons. The data show that tBH treatment caused a significant decrease in expression of proteins in mitochondria from both control (Control-tBH/Control) and NPX (NPX-tBH/NPX) groups. This lower protein expression may be a result of cellular toxicity due to too high a concentration of or exposure time to tBH. In addition, tBH treatment had similar effects on mitochondrial proteins from both control and NPX groups that are involved in the citric acid cycle, electron transport chain, amino acid, fatty acid, ketone and drug metabolism.

Figure 4-3. Assessment of effects of compensatory renal growth on basal and toxicant-induced oxidative stress in renal mitochondria.

A. Basal and tBH-induced lipid peroxidation in renal mitochondria from CON and NPX rats was measured using malondialdehyde (MDA) formation, as determined with 1-methyl-2-phenylindole. Renal mitochondrial samples from CON and NPX rats were incubated with buffer or 500 µM tBH for 1h. Results are means ± SEM of three separate samples from each group. *Significantly different ($P < 0.05$) from the corresponding untreated samples.

B. Basal and tert-butyl hydroperoxide (tBH)-induced lipid peroxidation in renal mitochondria from control (CON) and uninephrectomized (NPX) rats was measured using fluorescent cis-parinaric acid. Renal mitochondrial samples were incubated with 6.4 mM cis-parinaric acid + 5 mM hemin and treated with either 200 µM or 500 µM tBH. Results are means ± SEM of three separate samples from each group. *Significantly different ($P < 0.05$) from the corresponding untreated samples.

C. Mitochondrial aconitase activity in renal mitochondria from CON and NPX rats was measured as NADPH formation at A_{340}. Results are means ± SEM of three separate samples from each group. *Significantly different ($P < 0.05$) from the value in mitochondria from CON rats.

D. Adducts of 4-hydroxy-2-nonenal (HNE) with mitochondrial proteins were determined by Western blot analysis. VDAC protein was used as a mitochondrial loading control. Blots were quantified by densitometry using GelEval 1.22 software. Data are presented as means ± SEM of three separate samples from each group. *Significantly different ($P < 0.05$) compared to corresponding sample from CON rats.

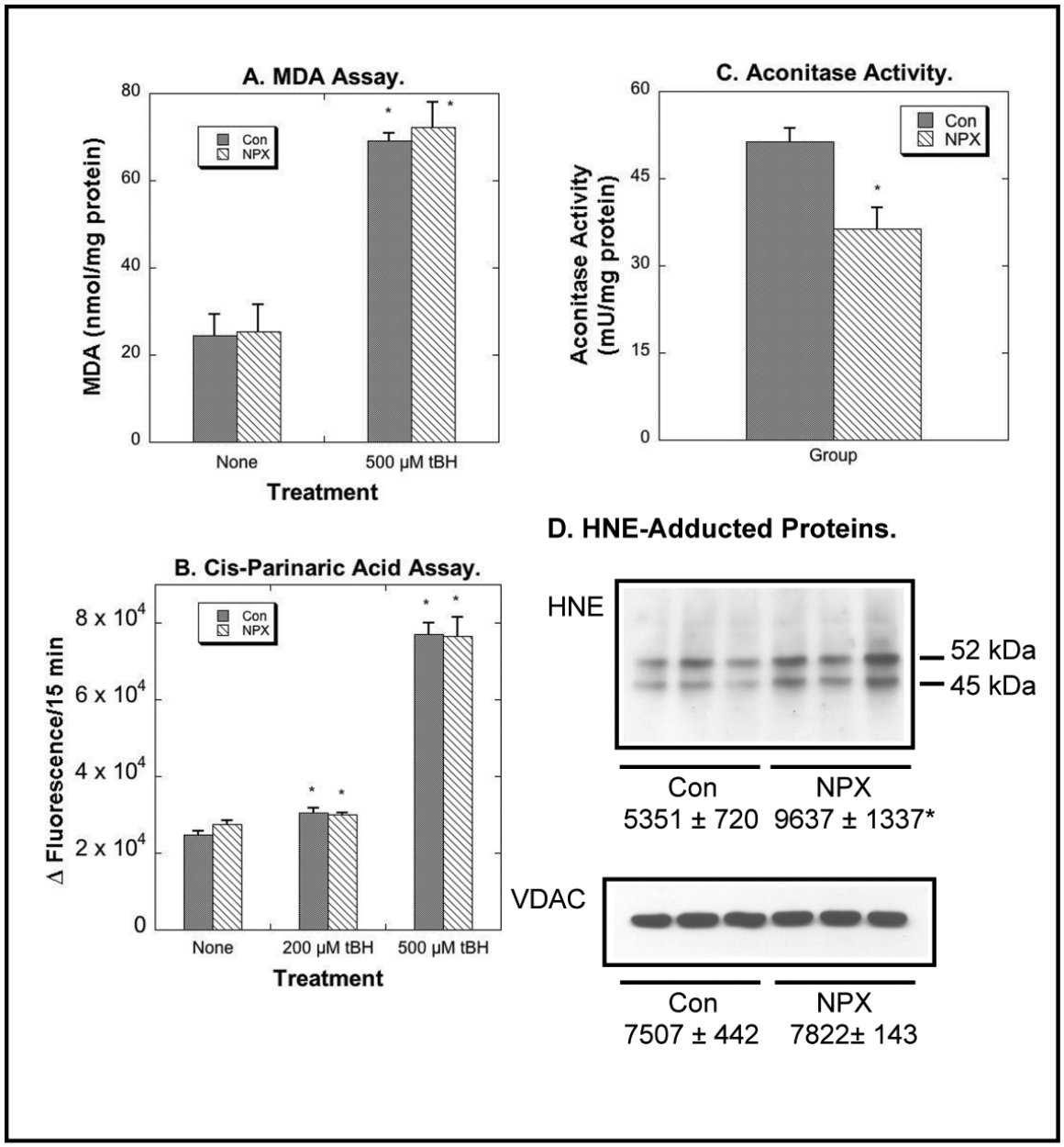
A. MDA Assay.
MDA (nmol/mg protein)
Con
NPX
None
500 µM tBH
Treatment
C. Aconitase Activity.
Aconitase Activity (mU/mg protein)
Group
B. Cis-Parinaric Acid Assay.
Δ Fluorescence/15 min
None
200 µM tBH
500 µM tBH
Treatment
D. HNE-Adducted Proteins.
HNE
52 kDa
45 kDa
Con
NPX
5351 ± 720
9637 ± 1337*
VDAC
Con
NPX
7507 ± 442
7822± 143

Table 4-6. Effect of toxicant (tBH) on mitochondrial protein expression during compensatory renal hypertrophy.

All the numbers in bold print signify a 1.5-fold or higher difference and a 0.5-fold or lower difference.

Relative quantitation: average signal intensity (NPX-tBH) / average signal intensity (NPX)

average signal intensity (Control-tBH) / average signal intensity (Control)

average signal intensity (NPX-tBH) / average signal intensity (Control-tBH)

Accession		**NPX-tBH/ NPX**	**Control-tBH/ Control**	**NPX-tBH/ Control-tBH**
	ATP Synthesis, Transport and Metabolic Processes			
P10719	ATP synthase subunit beta	0.9	0.6	**1.5**
Q98QB6	ATP synthase subunit beta 2 (ATP synthase F1 sector subunit beta 2)	1.2	**0.5**	**3.2**

P15999	ATP synthase subunit alpha	0.8	0.8	1.3
P05141	ADP/ATP translocase 2 (ADP,ATP carrier protein 2)	0.7	**0.4**	1.4
	Stress Response Proteins			
Q64433	10 kDa heat shock protein (Hsp10)	0.7	**0.4**	**2.4**
P63038	Heat shock protein 60 (HSP-60)	0.9	**0.5**	**1.6**
	Tricarboxylic acid cycle (Citrate Cycle)			
P56574	Isocitrate dehydrogenase [NADP], (Oxalosuccinate decarboxylase)	0.7	0.6	1.2
Q9ER34	Aconitate hydratase, (Aconitase)	0.6	0.7	1.1
	Respiratory Electron Transport Chain			
Q52V09	Cytochrome c	**0.5**	**0.3**	**2.3**
Q66HF1	NADH-ubiquinone oxidoreductase 75 kDa subunit	**0.2**	**0.1**	**0.4**

	Amino Acid and Fatty Acid Metabolic Pathways			
P50442	Glycine amidinotransferase, (Transamidinase)	1.1	1.2	1.4
Q64565	Alanine-glyoxylate aminotransferase 2, (Beta-alanine-pyruvate aminotransferase)	**0.5**	0.6	1.1
Q02253	Methylmalonate-semialdehyde dehydrogenase (Malonate-semialdehyde dehydrogenase)	0.7	**0.5**	**1.8**
P08503	Medium-chain specific acyl-CoA dehydrogenase	0.7	1.5	1.2
Q64428	Trifunctional enzyme subunit alpha, (3-hydroxyacyl-CoA dehydrogenase)	**0.5**	**0.5**	1.0
P26443	Glutamate dehydrogenase 1	**0.5**	0.6	1.4
P00507	Aspartate aminotransferase, mitochondrial precursor (Transaminase A)	**3.6**	**4.8**	0.6

	Ketone Metabolism			
Q9D0K2	Succinyl-CoA:3-ketoacid-coenzyme A transferase 1, (3-oxoacid CoA-transferase 1)	**0.5**	0.6	0.9
	Drug Metabolism			
Q64573	Kidney microsomal carboxylesterase (Liver carboxylesterase 3)	**0.3**	**0.4**	**1.5**
	Anion Transport (Transmembrane Transport)			
Q9Z2L0	Voltage-dependent anion-selective channel protein 1 (VDAC-1)	1.2	0.6	**1.9**
	Amino acid Transport			
Q64319	Neutral and basic amino acid transport protein rBAT (B(0,+)-type amino acid transport protein)	0.6	**0.5**	1.2

	Oxidoreductase Activity			
Q6AYT0	Quinone oxidoreductase (Zeta-crystallin)	0.8	0.9	1.1
Q07523	Hydroxyacid oxidase 2	0.6	**0.5**	1.3
Q68FT3	Probable oxidoreductase C10orf33 homolog	**0.3**	1.0	0.7
Q9DBF1	Aldehyde dehydrogenase family 7 member A1 (Antiquitin-1)	**1.7**	0.6	**4.6**

Discussion

Inasmuch as the mitochondria are the principal intracellular sites of oxygen consumption and increased rates of electron transport are believed to be associated with increased release of reactive oxygen species, we hypothesized that the consequence of these changes in mitochondrial function is an enhancement of basal oxidant stress (Lash et al., 2001a). The current studies pursued this further by assessing both basal and toxicant-stimulated lipid peroxidation using two well-established assays, formation of MDA and degradation of cis-parinaric acid. We also measured activity of mitochondrial aconitase, which, as noted above, is considered a highly sensitive indicator of oxidative stress due to the facile oxidation of its Fe-S cluster leading to inactivation (Han et al., 2003; James et al., 2002; Gardner et al., 1994).

Neither assessment of lipid peroxidation showed a significant difference between control and NPX kidneys, either in the absence or presence of toxicant. Expression of two important redox proteins in renal mitochondria, SOD2 and Trx2, were also unchanged after compensatory renal hypertrophy. An important consideration in evaluating such data, however, is the manner by which the measurements are normalized. In the present work, enzyme activities and levels of metabolites were normalized to total protein content, which was the only normalization parameter available and is the one that is most commonly used. Part of the compensatory hypertrophy response, however, is an increase in protein per cell (Meyer et al., 1996; Fine, 1986; Shirley and Walter, 1991; Wolf and Neilson, 1991). We previously illustrated the impact of this by normalizing activities in renal PT cell primary cultures derived from either control or NPX rats to both protein and DNA content (Lash et al., 2001b). Whereas the amount of total protein

per cell increases as a consequence of compensatory renal hypertrophy, the amount of DNA per cell does not change owing to the absence of a significant hyperplasia after a reduction in renal mass. Thus, lack of a difference between samples from control and NPX rats when normalized to protein equates to an increase, although one that is proportional to protein.

In contrast to the lipid peroxidation data, the mitochondrial aconitase activity data showed significant redox imbalance, suggesting an increase in mitochondrial oxidative stress in NPX kidney. To further support the conclusion that there is a degree of redox imbalance in renal mitochondria of NPX rats, we observed a significant increase in the amount of HNE-modified protein. The increase in Western blot density was 1.7-fold and was predominantly detected in two protein bands of molecular weight 52 kDa and 45 kDa. Although the identity of these modified proteins is currently unknown, their detection and the extent of the difference between renal mitochondria from control and NPX rats, suggest they may be important in determining the compensatory hypertrophy phenotype. Potential nitration of mitochondrial proteins was also assessed, but no difference between renal mitochondria from control and NPX rats was found, suggesting that increases in reactive nitrogen species were not a component of the compensatory hypertrophy phenotype.

The relative quantitation of proteins from mitochondrial pathways enabled the detection of toxicant-induced changes in mitochondria from hypertrophied kidney, suggesting alterations in susceptibility to mitochondrial toxicants. Overall, the proteomic analysis identified a number of

toxicant-induced changes during compensatory renal hypertrophy that could be involved in mediating mitochondrial toxicant-induced oxidative stress. Further exploration of these changes may provide insight into whether or not mitochondrial toxicant-induced stress response in hypertrophied kidney is due to cell death or any other mechanism. From our data, it is not clear if the similar effect of the toxicant, tBH, on mitochondrial proteins from both control and NPX groups is due to use of too high a concentration of tBH or too long an exposure. It would be interesting to treat the mitochondria with multiple concentrations of toxicants in multiple mitochondrial samples from control and NPX groups.

Effect of compensatory renal hypertrophy on mitochondrial size, number and membrane potential

Results

Effect of compensatory renal hypertrophy on mitochondrial size and number in renal PT cells

Based on contradictory data from previous studies (Cuppage et al., 1973; Hwang et al., 1990), our goal was to study basic properties of renal mitochondria after compensatory renal hypertrophy due to uninephrectomy. To label mitochondria, PT cells were incubated with MitoTracker^{TM} probes, which passively pass across plasma membranes and accumulate in metabolically active mitochondria. Our data showed a significant increase in mitochondrial staining with MitoTracker^{TM} dye in NPX rats, suggesting a possibility of either an increase in mitochondrial number (proliferation) or size (hypertrophy). To further explore these data, mitochondrial DNA and mitochondrial protein were measured. As shown in **Figure 4-5** and **Figure 4-6**, the data indicate no significant difference in mitochondrial DNA but significant increases in mitochondrial protein contents in the NPX group, suggesting renal mitochondrial hypertrophy in the NPX group.

Renal PT cells from NPX rats have higher basal mitochondrial membrane potential than those from control rats

To analyze mitochondrial membrane potential, PT cells were incubated with JC-1 (**Figure 4-4**). JC-1 is a cationic dye that exhibits membrane potential-dependent accumulation in mitochondria, indicated by shifting its fluorescence emission from green (~525 nm) to red (~590 nm). Polarized mitochondria are indicated by punctate red staining. The graphs represent average quantitation of three images and show a marked increase in JC-1 red punctate staining and no significant difference in JC-1 green staining. Overall, these data demonstrate an increase in JC-1 red punctate staining in kidneys of NPX rats, which is higher than the increase in MitoTracker^{TM} staining, suggesting a hyperpolarized state in the kidneys of NPX rats.

Figure 4-4. MitoTracker™ staining.

PT cells were grown on 35 mm dishes for 4 days and incubated with MitoTracker™ (50 nM) for 30 min. MitoTracker™ staining in PT cells from Control and NPX rats was measured using a Zeiss LSM 510 confocal microscope.

A) Images of MitoTracker™ staining were measured by confocal microscopy at 554 nm excitation and 576 nm emission. Magnification = 630x.

B) The graph represents average quantitation of three images. The integrated intensity of the entire image was done using Metamorph 7.1.7.0 Offline. *Significantly different ($P < 0.05$) from control cells.

A.

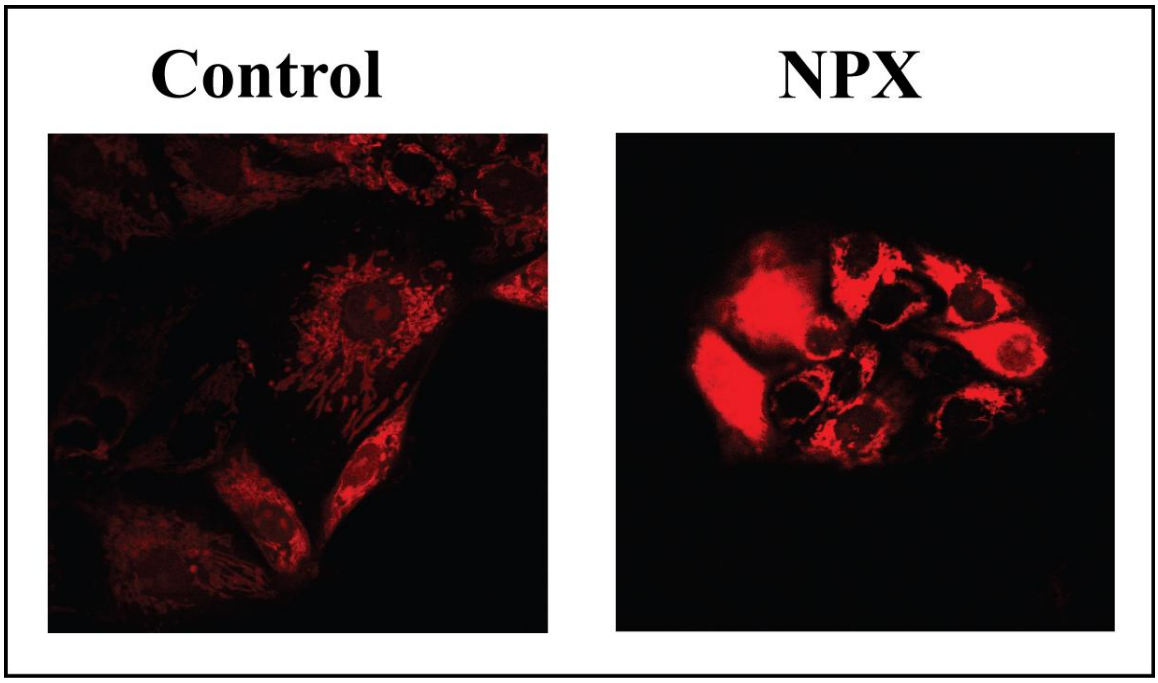
Control
NPX

B.

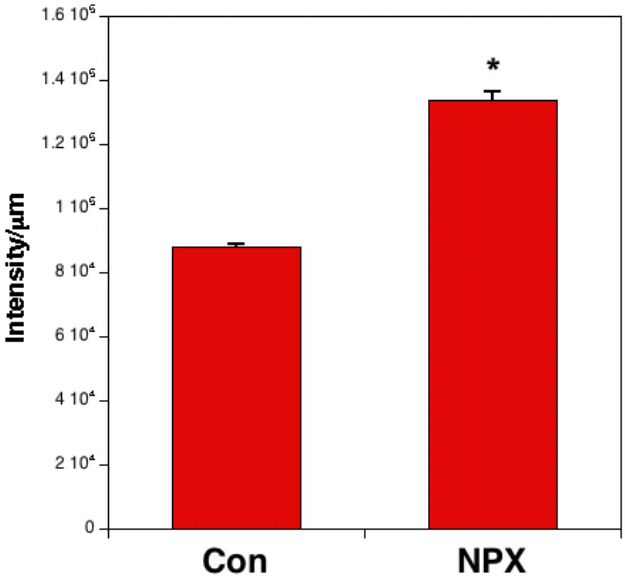
1.6 10⁵
1.4 10⁵
1.2 10⁵
1 10⁵
8 10⁴
6 10⁴
4 10⁴
2 10⁴
0
Intensity/µm
*
Con
NPX

Figure 4-5. Mitochondrial DNA.

Mitochondrial DNA was measured by DNA fluorescence assay. DAPI fluorescence was measured at 360 nm excitation and 450 nm emission. Results are means ± SEM of three separate samples from each group.

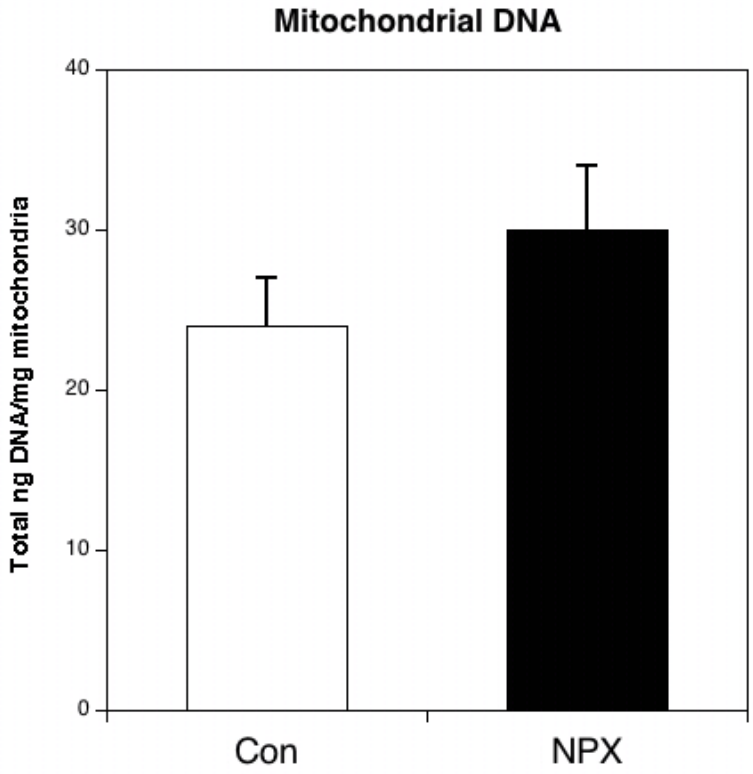

Figure 4-6. Mitochondrial protein.

Mitochondrial protein contents were measured by the BCA protein assay. *Significantly different ($P < 0.05$). Data are presented as means ± SEM of three separate samples from each group.

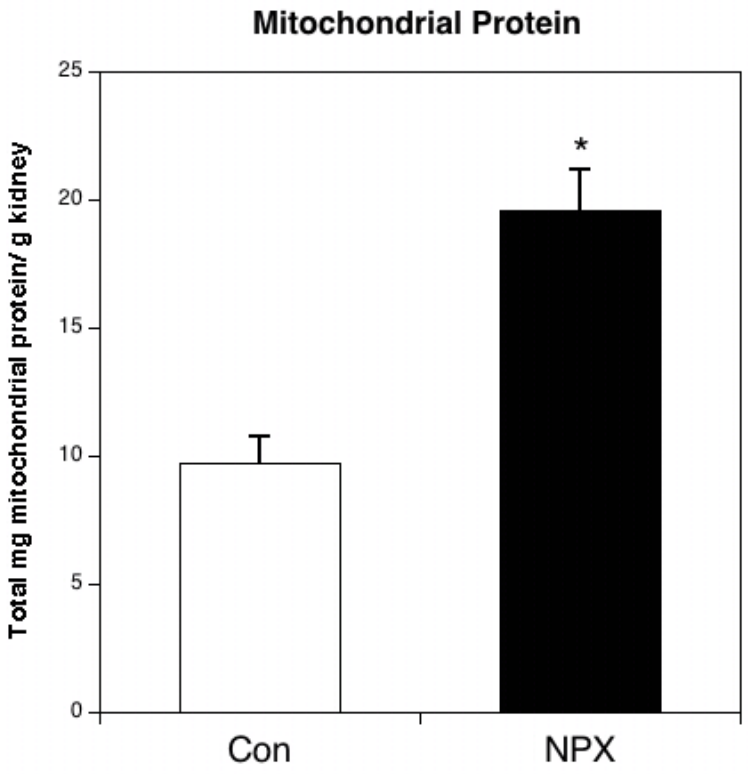

Figure 4-7. Measurement of mitochondrial membrane potential in PT cells from control and NPX rats.

PT cells were incubated with JC-1 (5 µg/ml) for 30 min. JC-1 fluorescence was measured by confocal microscopy using an overlay of red (488 nm excitation, 590 nm emission) and green (488 nm excitation, 525 nm emission) on a Zeiss LSM 510 confocal microscope.

A) JC-1 aggregate is indicated by red punctate staining (left panel). JC-1 monomer is indicated by green staining (middle panel). The overlay of both images is indicated by yellow color, which indicates co-localization of red and green (right panel). Magnification = 630x

B) The graphs represent average quantitation of three images. The integrated intensity of the entire image was measured by using Metamorph 7.1.7.0 Offline. *Significantly different ($P < 0.05$) from control cells.

A.

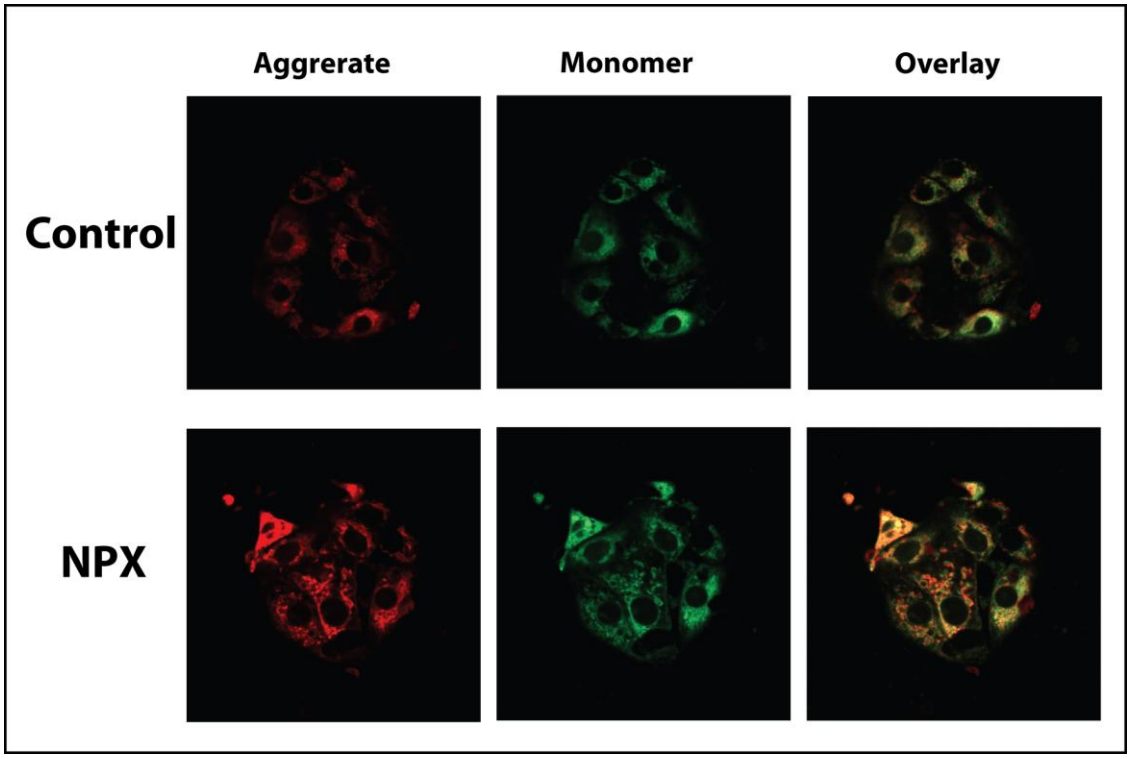
Aggrerate
Monomer
Overlay
Control
NPX

B.

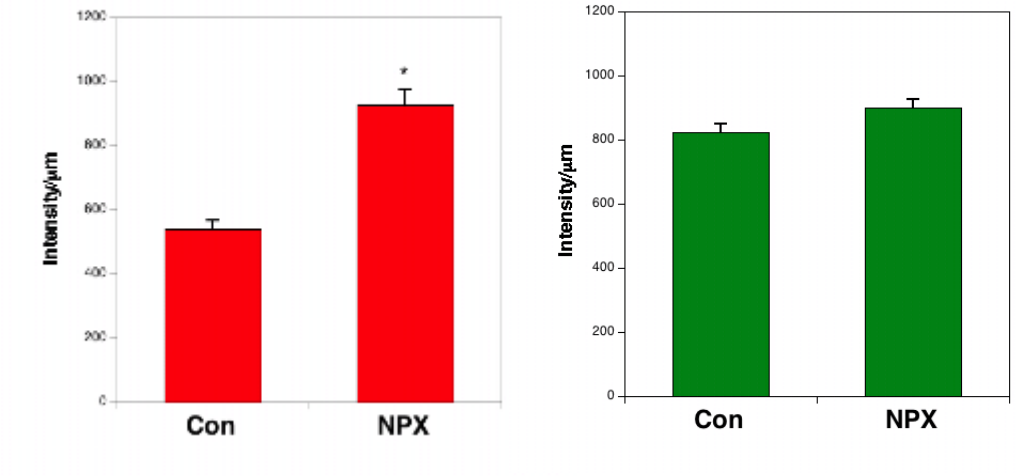
Intensity/µm
1200
1000
800
600
400
200
0
*
Con
NPX
Intensity/µm
1200
1000
800
600
400
200
0
Con
NPX

Discussion

In contrast to previous studies that suggested the existence of both renal mitochondrial proliferation and hypertrophy (Johnson and Amendola, 1969; Cuppage et al., 1973), Hwang's group (Hwang et al., 1990) concluded only mitochondrial hypertrophy of a fixed number of mitochondria in compensatory renal hypertrophy of renal PT cells. On the basis of these previous studies, which have suggested renal mitochondrial proliferation and hypertrophy, we analyzed properties of renal mitochondria after compensatory renal hypertrophy due to uninephrectomy. In the present study, we demonstrated the occurrence of renal mitochondrial hypertrophy following reduction in renal mass that was presumably to satisfy the greater need for energy metabolism (Benipal and Lash, 2011). This is consistent with data from the studies of Hwang and colleagues (Hwang et al., 1990).

The elevation in basal mitochondrial membrane potential suggested the existence of a hyperpolarized state, which is consistent with our previous data of higher rates of state 3 respiration in isolated renal mitochondria from NPX rats (Benipal and Lash, 2011). These data suggest that increased rates of electron flow and hyperpolarization by increased mitochondrial respiration further lead to increased reactive oxygen species formation, which potentially causes a significant degree of redox imbalance and basal oxidative stress in renal mitochondria, as suggested by our recent studies (Benipal and Lash, 2011), and increased susceptibility of PT cells from NPX rats to nephrotoxicants (Lash et al., 2006).

CHAPTER V. MODULATION OF MITOCHONDRIAL REDOX STATUS IN PT CELLS TO REDUCE THE RISK OF SUSCEPTIBILTY TO NEPHROTOXICANTS.

Influence of overexpression of the DIC on susceptibility to chemically induced toxicity by mitochondrial toxicants

Results

The overexpression of the DIC was confirmed by analyzing gene expression. As shown in **Table 5-1**, overexpression of DIC plasmids leads to a 7,806-fold increase in DIC gene expression. Acute cytotoxicity was assessed by measuring lactate dehydrogenase (LDH) release in renal PT cells from NPX rats. After transfection with the DIC plasmid, the PT cells were treated with either AA (1 μM, 10 μM), tBH (100 μM, 200 μM) or MVK (100 μM, 200 μM) without or with an overnight supplementation with 5 mM GSH. With endogenous GSH, overexpression of DIC did not cause any significant change in LDH release induced by AA (**Figure 5-1A**). However, after supplementation of PT cells with GSH, overexpression of DIC caused protection against the mitochondrial specific toxicant AA (**Figure 5-1B**). Furthermore, overexpression of DIC did not cause any protection against tBH or MVK with endogenous or supplemented GSH in PT cells from NPX rats (**Figure 5-1A** and **Figure 5-1B**).

Table 5-1. Analysis of DIC gene overexpression by RT-PCR in renal proximal tubular cells from NPX rats.

Primers for the DIC were designed with the aid of Oligo 6.76 and the cDNA sequences published in GenBank ™. An optimum cDNA concentration of 30–300 ng DNA/well was determined for each gene. All C_T values are based on triplicate measurements from total RNA from 3 renal PT cell preparations from NPX rats and are means ± SEM. GAPDH C_T values were used for correction: For control and DIC-transfected samples, GAPDH C_T values = 27.8 ± 0.2 for control and 31.7 ± 0.5 for DIC-transfected. Relative gene expression values were calculated by the formula: $2^{-\Delta CT\ (DIC\text{-}transfected)} / 2^{-\Delta CT\ (Control)}$, ΔC_T value is the difference between the C_T value for the gene of interest and that of GAPDH.

Control	**DIC-transfected**	**Relative Expression**
C_T mean ± SE	C_T mean ± SE	(DIC-transfected / Control)
30.3 ± 0.1	21.3 ± 0.2	7,806

Figure 5-1. Effect of overexpression of the DIC on sensitivity to chemical-induced toxicity.

A. Experiments were performed on day 6 of cell culture (72 h post-DIC transfection). Suspensions of PT cells isolated from NPX rats were treated with the indicated concentrations of AA, MVK or tBH for 4 h. After 4 h, aliquots were removed and LDH activity was measured. Values represent means ± SEM. Data shown here are the average of three experiments.

B. Experiments were performed on day 6 of cell culture (72 h post-DIC transfection). Suspensions of PT cells isolated from NPX rats were incubated with 5 mM GSH overnight prior to treatment with the indicated concentrations of AA, MVK or tBH for 4 h. After 4 h, aliquots were removed and LDH activity was measured. Values represent means ± SEM. Data shown here are the average of three experiments. *Significantly different ($P < 0.05$).

Figure 5-1A.

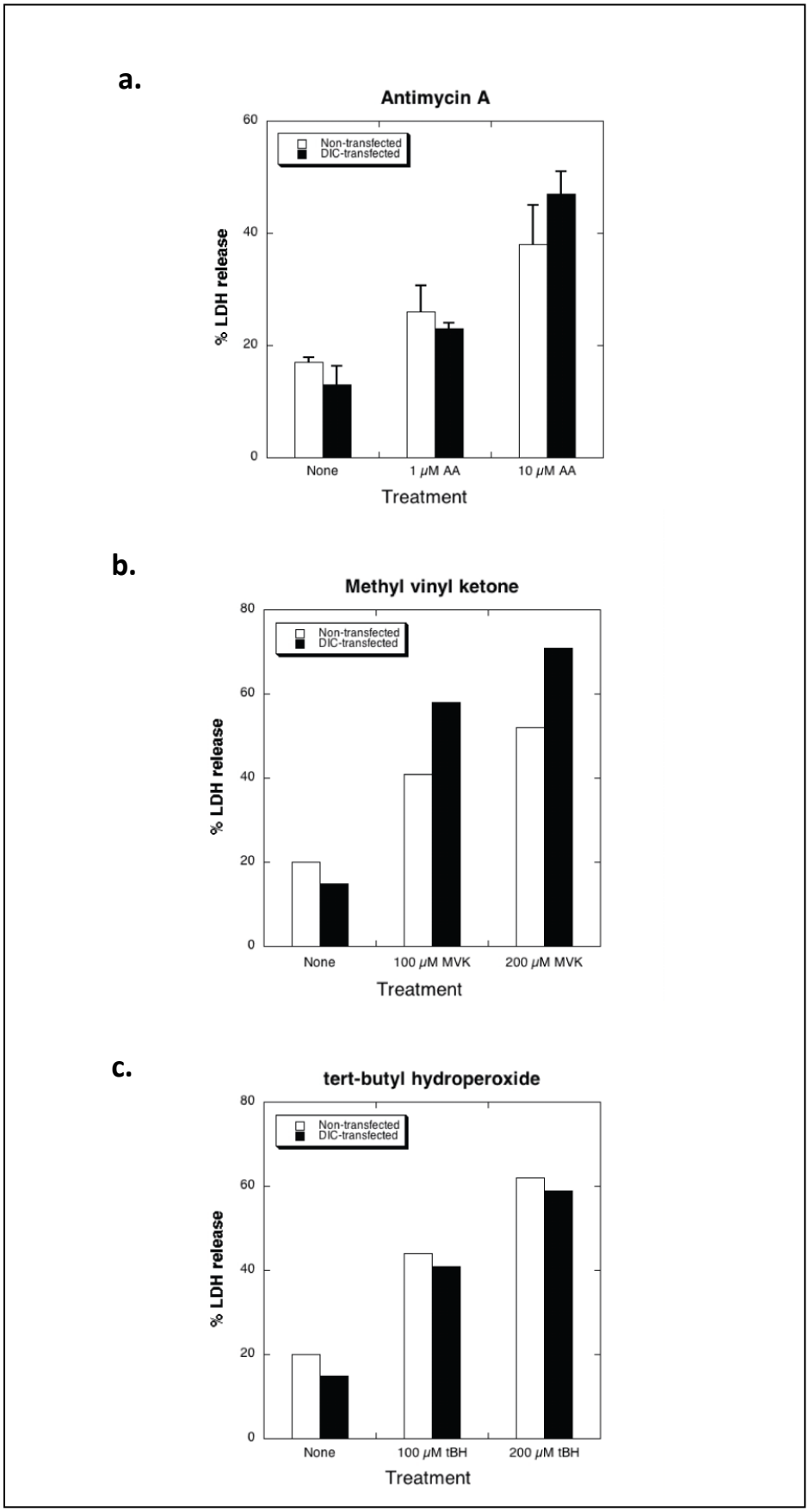
a.
Antimycin A
Non-transfected
DIC-transfected
% LDH release
60
40
20
0
None
1 μM AA
10 μM AA
Treatment
b.
Methyl vinyl ketone
Non-transfected
DIC-transfected
% LDH release
80
60
40
20
0
None
100 μM MVK
200 μM MVK
Treatment
c.
tert-butyl hydroperoxide
Non-transfected
DIC-transfected
% LDH release
80
60
40
20
0
None
100 μM tBH
200 μM tBH
Treatment

Figure 5-1B.

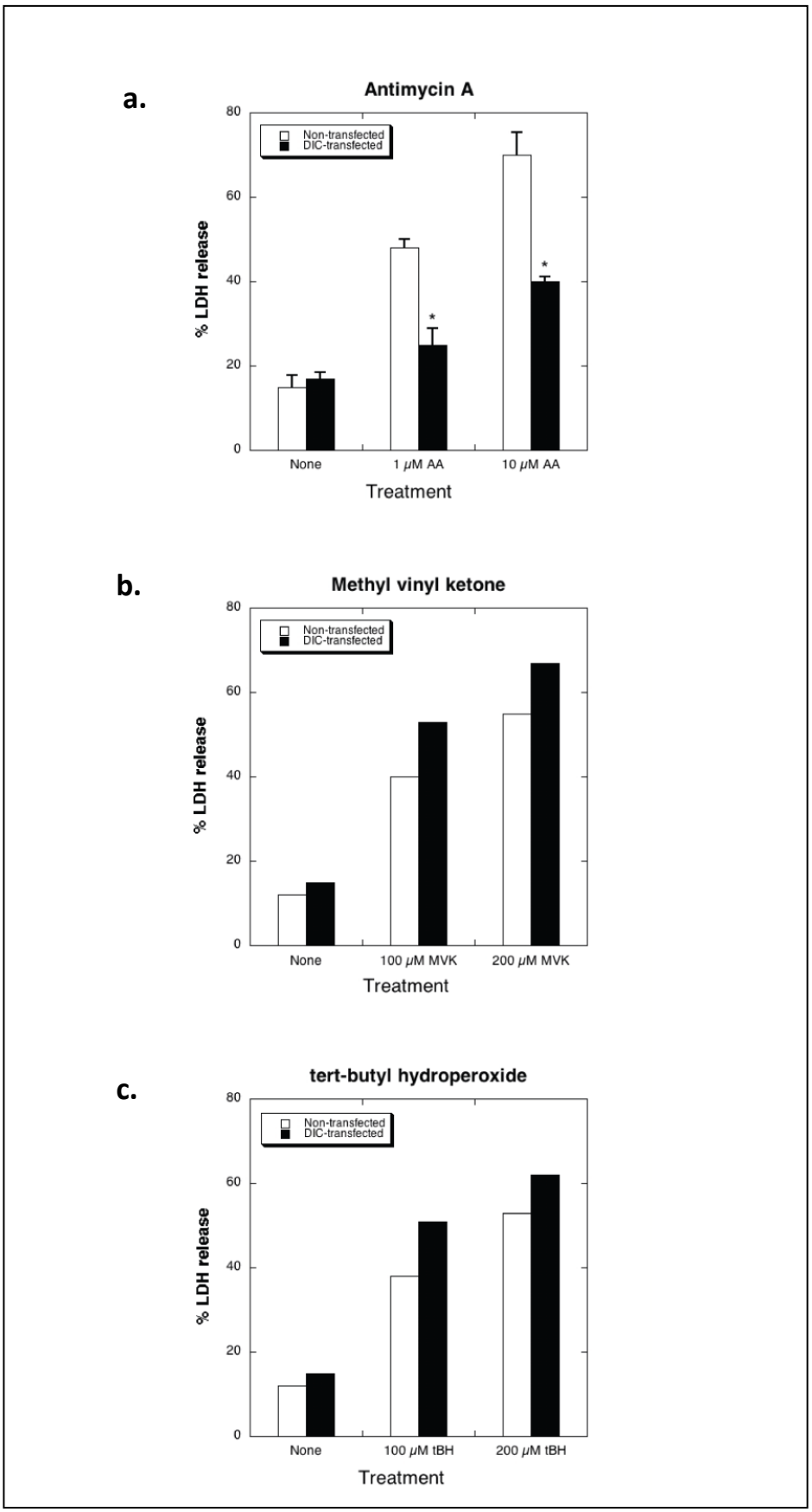
a.
Antimycin A
Non-transfected
DIC-transfected
% LDH release
80
60
40
20
0
None
1 μM AA
10 μM AA
Treatment
b.
Methyl vinyl ketone
Non-transfected
DIC-transfected
% LDH release
None
100 μM MVK
200 μM MVK
Treatment
c.
tert-butyl hydroperoxide
Non-transfected
DIC-transfected
% LDH release
None
100 μM tBH
200 μM tBH
Treatment

Influence of overexpression of the OGC on susceptibility to chemically induced toxicity by mitochondrial toxicants

Results

Overexpression of the OGC was confirmed by analyzing gene expression. As shown in **Table 5-2**, overexpression of OGC plasmids lead to a 5,007-fold increase in OGC gene expression. Acute cytotoxicity was assessed by measuring LDH release in PT cells from NPX rats. After transfection with the OGC plasmid, the PT cells were treated with either AA (1 μM, 10 μM), tBH (100 μM, 200 μM) or MVK (100 μM, 200 μM) without or with an overnight supplementation with 5 mM GSH. With endogenous GSH, overexpression of OGC did not cause any significant change in LDH release induced by AA (**Figure 5-2A**). However, after supplementation of PT cells with GSH, overexpression of OGC caused protection against the mitochondrial specific toxicant AA (**Figure 5-2B**). Furthermore, overexpression of OGC did not cause any protection against tBH or MVK with either endogenous or supplemented GSH (**Figure 5-2A and Figure 5-2B**) in PT cells from NPX rats.

Overall, these results suggest higher GSH transport activity by overexpression of DIC and OGC in renal PT cells of hypertrophied kidney markedly protected against toxicity and oxidative stress induced by the mitochondrial selective toxicant AA, indicating the significance of mitochondrial GSH transport in determining susceptibility to cytotoxic chemicals.

Table 5-2. Analysis of OGC gene overexpression by RT-PCR in renal proximal tubule cells of NPX rats.

Primers for the OGC were designed with the aid of Oligo 6.76 and the cDNA sequences published in GenBank ™. An optimum cDNA concentration of 30 to 300 ng DNA/well was determined for each gene. All C_T values are based on triplicate measurements from total RNA from 3 renal PT cell preparations from NPX rats and are means ± SEM. GAPDH C_T values were used for correction: For control and OGC-transfected samples, GAPDH C_T values = 27.8 ± 0.1 for control and 28.3 ± 0.2 for OGC-transfected. Relative gene expression values were calculated by the formula: $2^{-\Delta CT\ (OGC\text{-}transfected)} / 2^{-\Delta CT\ (Control)}$, ΔC_T value is the difference between the C_T value for the gene of interest and that of GAPDH.

Control	**OGC-transfected**	**Relative Expression**
C_T mean ± SE	C_T mean ± SE	(OGC-transfected / Control)
31.8 ± 0.3	20.0 ± 0.5	5,007

Figure 5-2. Effect of overexpression of the OGC on sensitivity to chemical-induced toxicity.

A. Experiments were performed on day 6 of cell culture (72 h post-OGC transfection). Suspensions of PT cells isolated from NPX rats were treated with the indicated concentrations of AA, MVK or tBH for 4 h. After 4 h, aliquots were removed and LDH activity was measured. Values represent means ± SEM. Data shown here are the average of three experiments.

B. Experiments were performed on day 6 of cell culture (72 h post-OGC transfection). Suspensions of PT cells isolated from NPX rats were incubated with 5mM GSH overnight prior to treatment with the indicated concentrations of AA, MVK or tBH for 4 h. After 4 h, aliquots were removed and LDH activity was measured. Values represent means ± SEM. Data shown here are the average of three experiments. *Significantly different ($P < 0.05$).

Figure 5-2A.

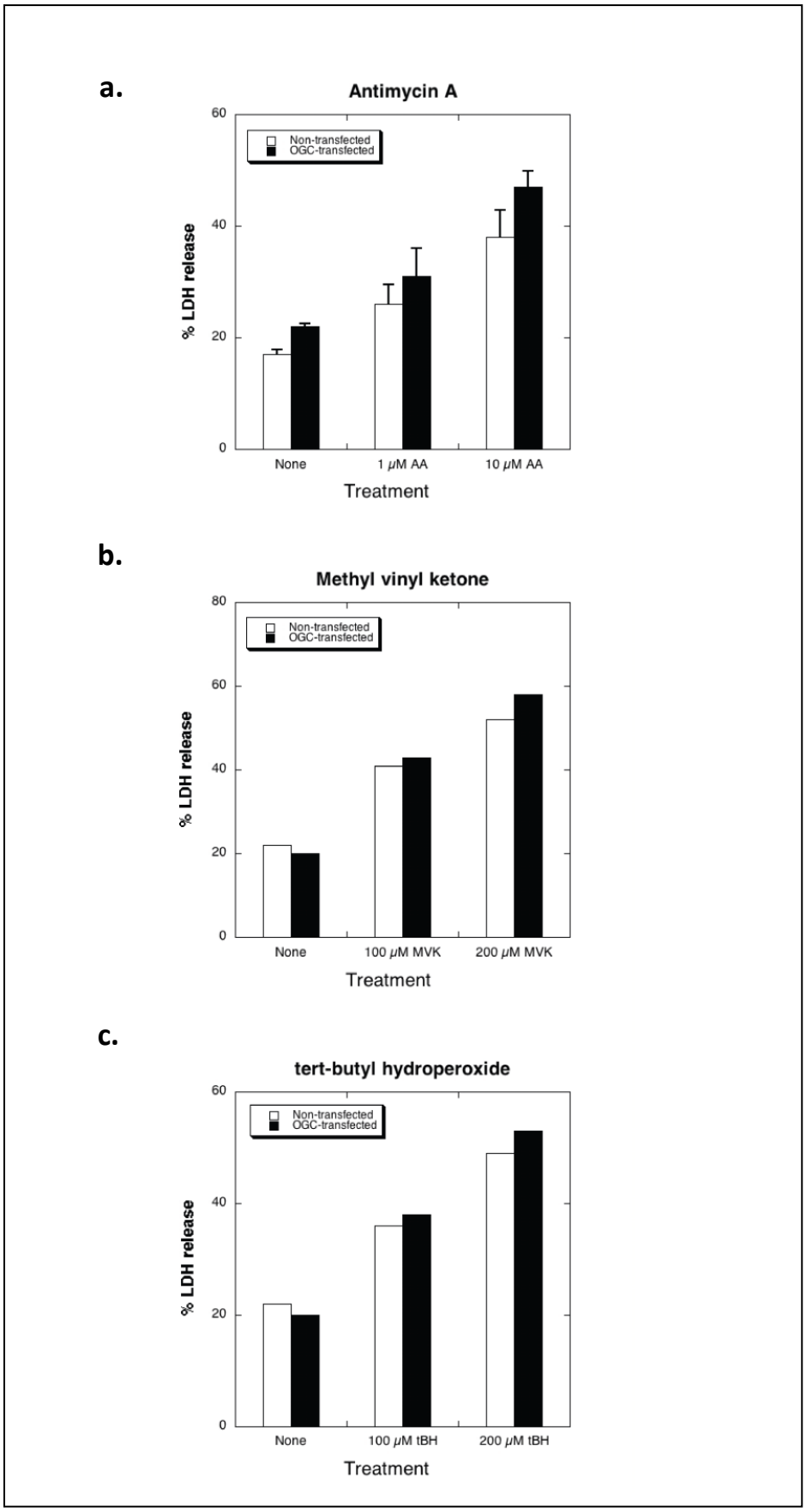
a.
Antimycin A
Non-transfected
OGC-transfected
% LDH release
60
40
20
0
None
1 μM AA
10 μM AA
Treatment
b.
Methyl vinyl ketone
Non-transfected
OGC-transfected
% LDH release
80
60
40
20
0
None
100 μM MVK
200 μM MVK
Treatment
c.
tert-butyl hydroperoxide
Non-transfected
OGC-transfected
% LDH release
60
40
20
0
None
100 μM tBH
200 μM tBH
Treatment

Figure 5-2B.

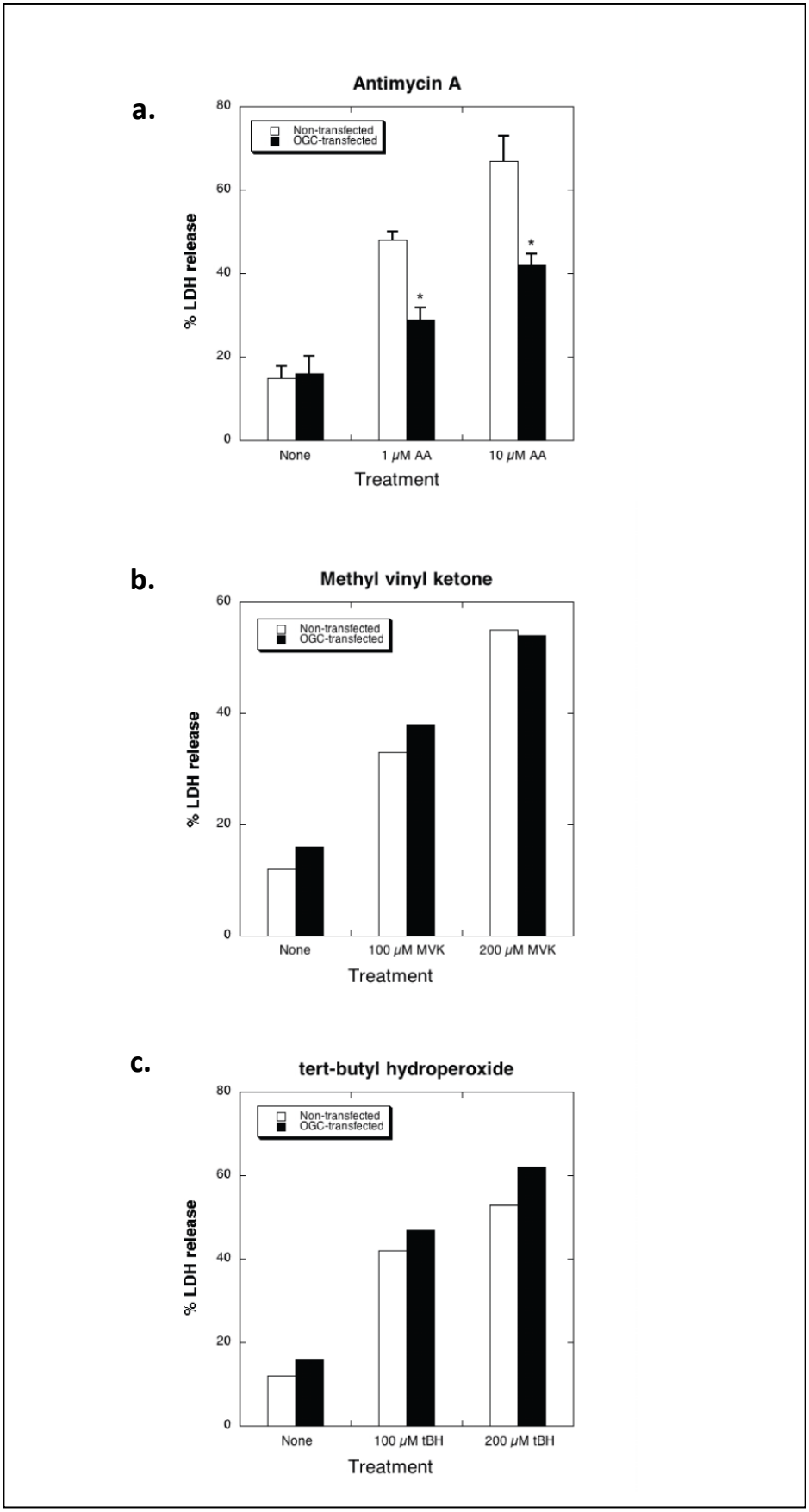
a.
Antimycin A
Non-transfected
OGC-transfected
% LDH release
0
20
40
60
80
None
1 μM AA
10 μM AA
Treatment
*
*
b.
Methyl vinyl ketone
Non-transfected
OGC-transfected
% LDH release
0
20
40
60
None
100 μM MVK
200 μM MVK
Treatment
c.
tert-butyl hydroperoxide
Non-transfected
OGC-transfected
% LDH release
0
20
40
60
80
None
100 μM tBH
200 μM tBH
Treatment

Discussion

Our previous reports showed a significant degree of redox imbalance and basal oxidative stress in renal mitochondria (Benipal and Lash, 2011) and an increased susceptibility of PT cells from NPX rats to nephrotoxicants (Lash et al., 2006). Furthermore, our lab also showed in NRK-52E cells that overexpression of mitochondrial GSH transporters protected against nephrotoxicants (Lash et al., 2002b; Xu et al., 2006). Taken together, these observations suggested that a threshold level of mitochondrial GSH is needed to counteract oxidative stress and susceptibility to toxicants in PT cells. Thus, we hypothesized that further increases in mitochondrial GSH levels in PT cells by overexpression of DIC and/or OGC will improve mitochondrial energetics and redox status and lower susceptibility to mitochondrial toxicants.

In this study, our approach was to increase GSH content in a subcellular organelle, mitochondria, by altering expression of the DIC and OGC to effect desired changes in mitochondrial GSH status. To investigate the toxicological consequences of altering mitochondrial GSH transport, we incubated renal PT cells from NPX rats with three mechanistically distinct mitochondrial toxicants, AA, tBH, and MVK. All three toxicants are unique in their mechanisms as shown in **Figure 5-3**. AA is a specific mitochondrial inhibitor that decreases mitochondrial electron transport chain activity and mitochondrial membrane potential leading to increases in reactive oxygen species. tBH is an oxidant that causes lipid peroxidation and GSH oxidation whereas MVK is an alkylating agent that causes GSH depletion by formation of GSH adducts.

Interestingly, assessment of cytotoxicity by LDH release demonstrated that overexpression of either of the mitochondrial GSH carriers, the DIC and OGC, only protected against AA. This

extensive protection against AA by overexpression of mitochondrial GSH transporters can be explained by a direct effect of AA on the mitochondrial electron transport chain. In other words, out of all three toxicants, AA specifically inhibits mitochondria and consequently, increased mitochondrial GSH by overexpression of GSH transporters decreases the oxidative stress induced by AA. Thus, consistent with our previous data in NRK-52E cells (Lash et al., 2002b; Xu et al., 2006), our present data also demonstrated that manipulation of mitochondria by overexpression of mitochondrial GSH carriers, DIC and OGC, reduced the risk of susceptibility to nephrotoxicants in hypertrophied kidney cells.

Overall, our data represent a significant analysis of the influence of modulation of renal mitochondrial GSH transport on the influence of compensatory renal hypertrophy on susceptibility of renal PT cells to mitochondrial toxicants. Furthermore, it would be interesting to extend this study by analyzing the effect of overexpression of the mitochondrial GSH transporters, DIC and OGC, on oxidative stress, proliferation and cellular GSH status. The ultimate goal of this study is to improve renal redox status after reduction in kidney mass by increasing mitochondrial GSH. This is then intended to reduce the risk of susceptibility to nephrotoxicants as reported by our previous studies (Lash et al., 2006; Lash et al., 2002b; Xu et al., 2006). Besides compensatory renal hypertrophy after reduction in kidney mass, GSH dysregulation is also associated with a number of toxic and pathological states. For example, lower cellular GSH levels are associated with diabetes, neurodegeneration and cardiovascular diseases (Ballatori et al., 2009) and depletion or oxidation of mitochondrial GSH is associated with cirrhosis, diabetic nephropathy and alcoholic liver disease (Fernandez-Checa et al., 1993; Krahenbuhl et al., 1992; Santos et al., 2003; Mastrocola et al., 2005). Towards this end, our

approach of improving cellular and subcellular (mitochondrial) GSH status might be applicable to not only compensatory renal hypertrophy but also to diseases that are associated with GSH dysregulation.

Figure 5-3. Mitochondrial toxicants.

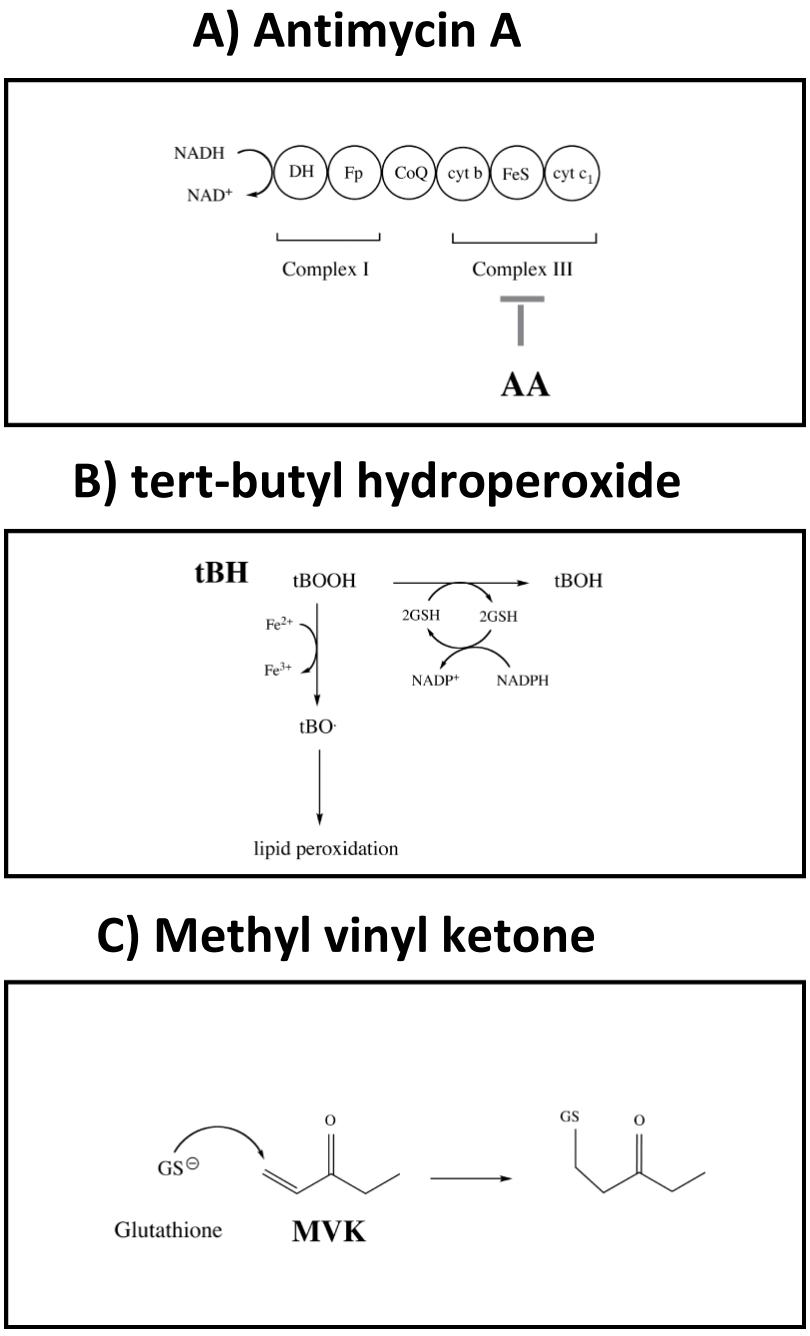

CHAPTER VI. SUMMARY AND CONCLUSIONS

The primary goal of this dissertation was to further characterize renal function and mitochondrial status during compensatory renal hypertrophy caused by uninephrectomy and to further expand on our previous studies of modulating renal mitochondrial redox status. We hypothesize that compensatory renal hypertrophy after uninephrectomy alters renal function and mitochondrial status and modulation of mitochondrial redox status alters susceptibility to nephrotoxicants in hypertrophied kidney cells. To study compensatory renal hypertrophy, we used the uninephrectomy rat model as this model has been reasonably well characterized as to the physiological and morphological changes that occur.

The analysis of renal physiological parameters suggested that the compensatory response of the remaining kidney after uninephrectomy is associated with modest impairment of renal function as assessed by blood and urinary parameters. The previous observations suggested that compensatory renal hypertrophy is associated with a significant increase in GSH content by higher activity of γ-glutamylcysteine synthetase (GCS). To further explore another potential mechanism for the increase in the cytoplasmic pool of GSH, we analyzed the expression of several plasma membrane carrier proteins that are responsible for GSH transport into PT cells to determine whether or not there is increased transport of GSH across the BLM. Our results showed significantly higher protein expression of Oat1 and Oat3, which play a role in GSH uptake, and higher protein expression of the $(Na^+ + K^+)$-stimulated ATPase, which provides the Na^+ ion gradient for secondary active transporters that ultimately help mediate the uptake of

GSH. Overall, these results suggested that higher intracellular accumulation of GSH is due to higher activity of GCS and increased GSH transport across the BLM.

After analyzing renal plasma membrane GSH transporters, the next goal was to see whether or not compensatory renal hypertrophy caused alterations in renal mitochondrial redox status, including GSH and the redox enzymes superoxide dismutase (Sod2) and thioredoxin2 (Trx2). The analysis of renal mitochondrial glutathione status showed modest but significant increases in both GSH and GSSG in renal mitochondria from NPX rats as compared to control rats. We next determined gene and protein expression of two inner mitochondrial carrier proteins, the DIC and OGC, which partially determine renal mitochondrial GSH status. In contrast to our expectations, neither gene nor protein expression of the DIC or OGC were increased and there were no changes in protein expression of the mitochondrial redox enzymes Sod2 and Trx2 after uninephrectomy. Hence, we concluded that the increase in mitochondrial GSH concentrations is due to mass action or changes in the kinetics of the mitochondrial GSH transporters, DIC and OGC, caused by a hypermetabolic state.

To analyze the impact of compensatory renal hypertrophy on functional characteristics of renal mitochondria, we analyzed activities of mitochondrial enzymes that are indicative of cellular energetics and redox status. To further explore mitochondrial energetics, we also looked at mitochondrial respiration and proteomics. All the results provided evidence for a hypermetabolic state in the NPX group signified by increases in activities of energetics enzymes, state 3 rates of

respiration and expression of proteins that are involved in various metabolic pathways. Overall, these observations suggest that to accommodate the increased energy demand caused by compensatory renal hypertrophy, there are increased rates of mitochondrial electron transport chain leading to the hypermetabolic state that can also lead to mitochondrial dysfunction due to increased ROS formation.

The evidence for renal dysfunction and a hypermetabolic state of renal mitochondria from NPX rats suggested that a higher state of mitochondrial oxidative stress exists that may also contribute to higher susceptibility to chemically induced renal injury. Hence, our next goal was to compare basal and toxicant-induced renal mitochondrial oxidative stress between control and NPX rats. We analyzed both basal and toxicant-stimulated lipid peroxidation and aconitase activity, which is a highly sensitive indicator of oxidative stress in biological systems. The assessment of basal and toxicant-induced lipid peroxidation data showed no significant difference between control and NPX kidneys. However, aconitase activity data suggested redox imbalance leading to increased mitochondrial oxidative stress, which is further supported by significant increases in the amount of HNE-adducted proteins in renal mitochondria from NPX rats.

Based on previous observations that were contradictory and suggested both renal mitochondrial proliferation and hypertrophy on the one hand and only mitochondrial hypertrophy on the other hand, our goal was to further explore the effect of compensatory renal hypertrophy on mitochondrial size and number in renal PT cells. We showed that mitochondrial hypertrophy of

renal PT cells follows reduction in renal mass to satisfy the need for energy metabolism during compensatory renal hypertrophy. Furthermore, elevation in basal membrane potential as shown by JC-1 staining suggested a hyperpolarized state in mitochondria from the NPX group. This suggested that hyperpolarization caused by increased mitochondrial respiration further leads to basal mitochondrial oxidative stress and increased susceptibility of PT cells to nephrotoxicants in the NPX group.

Finally, to test our hypothesis that increasing renal mitochondrial GSH reduces the risk of susceptibility to nephrotoxicants in hypertrophied kidney cells, we overexpressed two mitochondrial GSH carriers, the DIC and OGC, in PT cells from the NPX group. The basic idea was that overexpression of mitochondrial GSH transporters would decrease susceptibility to nephrotoxicants by increasing mitochondrial GSH levels caused by increased expression and transport activity of GSH transporters, the DIC and OGC. The assessment of cytotoxicity showed that after supplementation of PT cells with GSH, overexpression of mitochondrial GSH transporters protected against the mitochondrial specific toxicant antimycin A. These data supported our hypothesis that higher mitochondrial GSH transport activity by overexpression of the DIC and OGC in hypertrophied kidney cells markedly protected against toxicity, supporting the significance of mitochondrial GSH transport in determining susceptibility to toxicants.

In summary, we showed that in hypertrophied kidney there are alterations in physiological parameters suggesting modest renal dysfunction, higher expression of renal organic anion

transporters suggesting higher transport of GSH and higher transport of xenobiotics leading to an increase in susceptibility to nephrotoxicants, and alterations in hypertrophied mitochondria suggesting redox imbalance and increased basal oxidative stress. As shown in **Figure 6-1**, we conclude that in hypertrophied mitochondria, a hypermetabolic state caused by increases in citric acid cycle and electron transport chain activities lead to a hyperpolarized state and superoxide production, which further causes mitochondrial oxidative stress. Furthermore, the increase in mitochondrial GSH concentrations is due to mass action or a kinetic effect on mitochondrial GSH transporters. In addition, our data also provide evidence that manipulation of mitochondrial GSH transport modulates response to nephrotoxicants, supporting the toxicological significance of the mitochondrial GSH transport process in compensatory renal hypertrophy.

Figure 6-1. Summary scheme.

Abbreviations: DIC, dicarboxylate carrier; ROS, reactive oxygen species; O_2^-, superoxide anion; OGC, oxoglutarate carrier; 2-OG^{2-}, 2-oxoglutarate; Pi^{2-}, inorganic phosphate; TCA, tricarboxylic acid cycle.

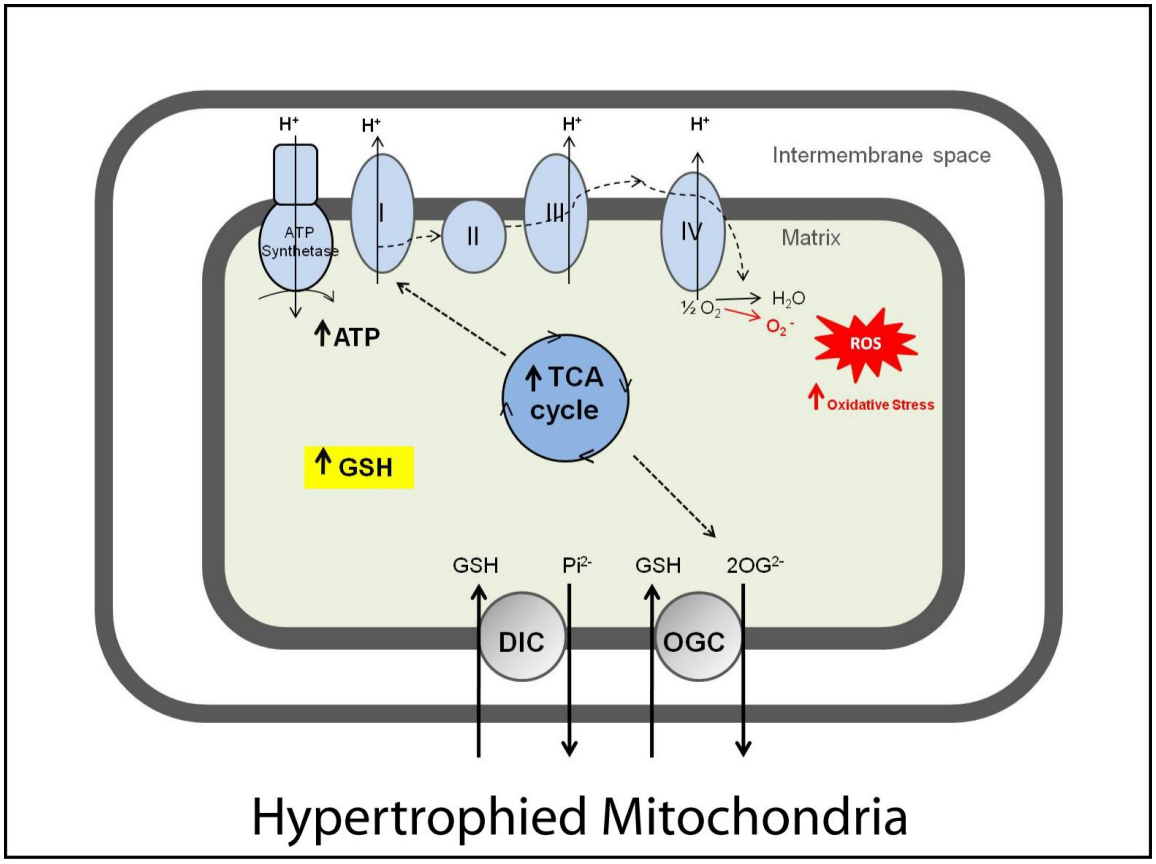

CHAPTER VII. OVERALL SIGNIFICANCE AND FUTURE DIRECTIONS

Reduction in renal mass and function afflicts millions of people worldwide as a consequence of several renal and non-renal diseases, infections, aging and surgery due to nephrectomy. Uninephrectomy, or surgical removal of one kidney, is performed for treatment in critical cases of renal diseases, injuries and for the purpose of kidney transplantation. Due to increasing incidence of reductions in kidney mass, high medical expenditures represent a significant challenge to public health care in the U.S. Although the remaining functional renal mass compensates for the loss of renal function, reduced kidney mass due to nephrectomy is a pathophysiologic process that is associated with alterations in renal hemodynamics, physiology and biochemistry.

Numerous human clinical and experimental animal studies have provided evidence that reduction in renal mass leads to proteinuria, hypertension, hyperfiltration, glomerulosclerosis and toxicological implications such as increased nephrotoxicity from many drugs. In this study using a uninephrectomized rat model, we showed that compensatory renal hypertrophy due to reduction in renal mass is associated with modest renal dysfunction, alterations in renal mitochondrial glutathione and energetics status and mitochondrial oxidative stress. Furthermore, we also expanded our previous studies of modulating renal mitochondrial redox status and showed that an increase in renal mitochondrial GSH status reduces the risk of susceptibility to cytotoxic chemicals. Thus, we have taken several comprehensive and diversified approaches to study the role of mitochondrial energetics and redox status in the compensatory renal

hypertrophy response including *in vivo*, *ex vivo* (isolated renal mitochondria), and *in vitro* (in primary cultures of PT cells).

Our particular focus on mitochondrial status is significant because alterations in mitochondrial function have been associated with numerous diverse pathologies. Changes in mitochondrial redox status likely underlie the regulation of mitochondrial and cellular energetics and cellular responses to many chemical exposures and pathological disease states. Mitochondrial GSH status is a critical determinant of cellular energetics and function and plays a critical role in determining susceptibility of cells to various toxicants. The ability to manipulate mitochondrial GSH status can provide a tool with which to probe mitochondrial function and modulate cellular injury upon exposure to various forms of mitochondrial toxicants. In this study, we used such an approach to alter one of the major GSH compartmentalization mechanisms in renal proximal tubules of the uninephrectomized rat model to produce protection from nephrotoxicants. Hence, further understanding of the regulation of mitochondrial GSH status and modulation of GSH levels in renal mitochondria hold promise for the development of new therapeutic approaches for many kidney diseases and chemically induced toxicities.

The manipulation of mitochondrial GSH can also be used as a therapeutic target, not only for compensatory renal hypertrophy or in renal donors, but also for a number of diseases and pathological states that are associated with the depletion or oxidation of the mitochondrial GSH pool. For example, chronic ethanol ingestion and alcoholic liver disease are associated with decreased liver mitochondrial GSH content (Garcia-Ruiz et al., 1994, 1995; Fernandez-Checa et al., 1987, 1991, 1993, 2002), which also leads to an increase in susceptibility to toxicants (Zhao

and Slattery 2002; Zhao et al., 2002). Furthermore, cirrhosis and other forms of biliary obstruction have been associated with mitochondrial dysfunction caused by depletion of the matrix GSH pool (Krahenbuhl et al., 1992, 1995) and Type 2 diabetes has also been linked with depletion and oxidation of mitochondrial GSH in rat brain, heart and kidney (Santos et al., 2003; Mastrocola et al., 2005; Rosca et al., 2005), suggesting the importance of regulation of mitochondrial GSH. Clearly, it becomes apparent that it is important to design pharmacologically-based strategies aimed at specific targets in transport and catabolism of GSH as a potential therapeutic treatment against human kidney diseases, chemically induced toxicities and health complications in renal donors. Thus, reducing complications after nephrectomy will also directly increase the quality of life for a renal donor.

Overall, the observations in this study enabled us to more completely define the phenotype for compensatory renal hypertrophy both *in vivo* and in an *ex vivo* model using primary culture of PT cells. This in turn also helped us to understand the biochemistry and toxicology of compensatory renal hypertrophy and provided a basis to reduce the risk of mitochondrial dysfunction and susceptibility to toxicants due to reduction in functional renal mass. With the basic knowledge acquired in this study, further studies of the protective effects of enhancing mitochondrial redox status and reversing deleterious properties of hypertrophied PT cells might provide a basis for novel therapeutic approaches to counteract the increased potential for renal insufficiency due to reduced functional renal mass.

Future studies need to further explore the effect of overexpression of mitochondrial GSH transporters on oxidative stress, proliferation and cellular GSH status. Furthermore, it would be

interesting to examine a more comprehensive range of transporter expression and activity by also decreasing the expression and activity of the two mitochondrial GSH transporters, the DIC and OGC.

REFERENCES

Anderson, M.E., Bridges, R.J., and Meister, A. (1980). Direct evidence for inter-organ transport of glutathione and that the non-filtration renal mechanism for glutathione utilization involves gamma-glutamyl transpeptidase. Biochem Biophys Res Commun *96*, 848-853.

Aw, T.Y., Wierzbicka, G., and Jones, D.P. (1991). Oral glutathione increases tissue glutathione in vivo. Chem Biol Interact *80*, 89-97.

Azar, S.A., Nakhjavani, M.R., Tarzamni, M.K., Faragi, A., Bahloli, A., and Badroghli, N. (2007). Is living kidney donation really safe? Transplant Proc *39*, 822-823.

Ballatori, N., and Dutczak, W.J. (1994). Identification and characterization of high and low affinity transport systems for reduced glutathione in liver cell canalicular membranes. J Biol Chem *269*, 19731-19737.

Ballatori, N., Krance, S.M., Notenboom, S., Shi, S., Tieu, K., Hammond, C.L. (2009). Glutathione dysregulation and the etiology and progression of human diseases. Biol Chem *390*, 191-214.

Barrows, C.H., Jr., Roeder, L.M., and Olewine, D.A. (1962). Effect of age on renal compensatory hypertrophy following unilateral nephrectomy in the rat. J Gerontol *17*, 148-150.

Bellomo, G., Mirabelli, F., DiMonte, D., Richelmi, P., Thor, H., Orrenius, C., and Orrenius, S. (1987). Formation and reduction of glutathione-protein mixed disulfides during oxidative stress. A study with isolated hepatocytes and menadione (2-methyl-1,4-naphthoquinone). Biochem Pharmacol *36*, 1313-1320.

Berber, I., Tellioglu, G., Kilicoglu, G., Ozgezer, T., Canbakan, M., Gulle, S., Yigit, B., and Titiz, I. (2008). Medical risk analysis of renal transplant donors. Transplant Proc *40*, 117-119.

Bertani, T., Cutillo, F., Zoja, C., Broggini, M., and Remuzzi, G. (1986). Tubulo-interstitial lesions mediate renal damage in adriamycin glomerulopathy. Kidney Int *30*, 488-496.

Blantz, R.C., Peterson, O.W., Blantz, E.R., and Wilson, C.B. (1988). Sexual differences in glomerular ultrafiltration: effect of androgen administration in ovariectomized rats. Endocrinology *122*, 767-773.

Bradford, M.M. (1976). A rapid and sensitive method for the quantitation of microgram quantities of protein utilizing the principle of protein-dye binding. Anal Biochem *72*, 248-254.

Brandt, J.T., Pierce, D.A., and Fausto, N. (1972). Ornithine decarboxylase activity and polyamine synthesis during kidney hypertrophy. Biochim Biophys Acta *279*, 184-193.

Campbell, N.A., and Reece, J.B. (2005). Biology, 7th edition, Pearson Education, Inc. Ch.44, pp. 882-884.

Caramelo, C., Tsai, P., Okada, K., and Schrier, R.W. (1988). Protein kinase C activity in compensatory kidney growth. Biochem Biophys Res Commun *152*, 315-321.

Chan, D.C. (2006). Mitochondria: dynamic organelles in disease, aging, and development. Cell *125*, 1241–1252.

Chen, Z., and Lash, L.H. (1998). Evidence for mitochondrial uptake of glutathione by dicarboxylate and 2-oxoglutarate carriers. J Pharmacol Exp Ther *285*, 608–618.

Chen, Z., Putt, D.A., and Lash, L.H. (2000). Enrichment and functional reconstitution of glutathione transport activity from rabbit kidney mitochondria: further evidence for the role of the dicarboxylate and 2-oxoglutarate carriers in mitochondrial glutathione transport. Arch Biochem Biophys *373*, 193-202.

Coe, F.L., and Korty, P.R. (1967). Protein synthesis during compensatory renal hypertrophy. Am J Physiol *213*, 1585-1589.

Cuppage F.E., Chiga M., and Tate A. (1973). Mitochondrial proliferation within the nephron. I. Comparison of mitochondrial hyperplasia of tubular regeneration with compensatory hypertrophy. Am J Pathol *70*, 119-130.

Evers, R., de Haas, M., Sparidans, R., Beijnen, J., Wielinga, P.R., Lankelma, J., and Borst, P. (2000). Vinblastine and sulfinpyrazone export by the multidrug resistance protein MRP2 is associated with glutathione export. Br J Cancer *83*, 375-383.

Fernandez-Checa, J.C., Ookhtens, M., and Kaplowitz, N. (1987). Effect of chronic ethanol feeding on rat hepatocytic glutathione. Compartmentation, efflux, and response to incubation with ethanol. J Clin Invest *80*, 57-62.

Fernandez-Checa, J.C., Garcia-Ruiz, C., Ookhtens, M., and Kaplowitz, N. (1991). Impaired uptake of glutathione by hepatic mitochondria from chronic ethanol-fed rats. Tracer kinetic studies in vitro and in vivo and susceptibility to oxidant stress. J Clin Invest *87*, 397-405.

Fernandez-Checa, J.C., Hirano, T., Tsukamoto, H., and Kaplowitz, N. (1993). Mitochondrial glutathione depletion in alcoholic liver disease. Alcohol *10*, 469-475.

Fernandez-Checa, J.C., Colell, A., and Garcia-Ruiz, C. (2002). S-Adenosyl-L-methionine and mitochondrial reduced glutathione depletion in alcoholic liver disease. Alcohol *27*, 179-183.

Fine, L. (1986). The biology of renal hypertrophy. Kidney Int *29*, 619-634.

Fine, L.G., and Norman, J.T. (1992). Renal growth responses to acute and chronic injury: routes to therapeutic intervention. J Am Soc Nephrol *2*, S206-211.

Flagg, E.W., Coates, R.J., Eley, J.W., Jones, D.P., Gunter, E.W., Byers, T.E., Block, G.S., and Greenberg, R.S. (1994). Dietary glutathione intake in humans and the relationship between intake and plasma total glutathione level. Nutr Cancer *21*, 33-46.

Fleischer, S., and Fleischer, B. (1967). Removal and binding of polar lipids in mitochondria and other membrane systems. In: Methods in Enzymology, edited by Estabrook, R.W., and Pullman, M.E. New York: Academic *X*, 406–433.

Franch, H.A., Shay, J.W., Alpern, R.J., and Preisig, P.A. (1995). Involvement of pRB family in TGF beta-dependent epithelial cell hypertrophy. J Cell Biol *129*, 245-254.

Franch, H.A., Curtis, P.V., and Mitch, W.E. (1997). Mechanisms of renal tubular cell hypertrophy: mitogen-induced suppression of proteolysis. Am J Physiol *273*, C843-851.

Franco, R., Schoneveld, O.J., Pappa, A., and Panayiotidis, M.I. (2007). The central role of glutathione in the pathophysiology of human diseases. Archives of Physiology and Biochemistry. *113*, 234-258.

Fujita, H., Omori, S., Ishikura, K., Hida, M., and Awazu, M. (2004). ERK and p38 mediate high-glucose-induced hypertrophy and TGF-beta expression in renal tubular cells. Am J Physiol Renal Physiol *286*, F120-126.

Garcia-Ruiz, C., Morales, A., Ballesta, A., Rodes, J., Kaplowitz, N., and Fernandez-Checa, J.C. (1994). Effect of chronic ethanol feeding on glutathione and functional integrity of mitochondria in periportal and perivenous rat hepatocytes. J Clin Invest *94*, 193-201.

Garcia-Ruiz, C., Morales, A., Colell, A., Ballesta, A., Rodes, J., Kaplowitz, N., and Fernandez-Checa, J.C. (1995). Feeding S-adenosyl-L-methionine attenuates both ethanol-induced

depletion of mitochondrial glutathione and mitochondrial dysfunction in periportal and perivenous rat hepatocytes. Hepatology *21*, 207-214.

Gardner, P.R., Nguyen, D.D., and White, C.W. (1994). Aconitase is a sensitive and critical target of oxygen poisoning in cultured mammalian cells and in rat lungs. Proc Natl Acad Sci U S A *91*, 12248-12252.

Gérard-Monnier, D., Erdelmeier, I., Regnard, K., Moze-Henry, N., Yadan, J.C., and Chaudiere, J. (1998). Reactions of 1-methyl-2-phenylindole with malondialdehyde and 4-hydroxyalkenals. Analytical applications to a colorimetric assay of lipid peroxidation. Chem Res Toxicol *11*, 1176-1183.

Gotoh, Y., Suzuki, H., Kinoshita, S., Hirohashi, T., Kato, Y., and Sugiyama, Y. (2000). Involvement of an organic anion transporter (canalicular multispecific organic anion transporter/multidrug resistance-associated protein 2) in gastrointestinal secretion of glutathione conjugates in rats. J Pharmacol Exp Ther *292*, 433-439.

Gregersen, N., Bross, P., and Andresen, B.S. (2004). Genetic defects in fatty acid beta-oxidation and acyl-CoA dehydrogenases. Molecular pathogenesis and genotype-phenotype relationships. Eur J Biochem. *271*, 470–482.

Griffith, O.W., and Meister, A. (1979a). Glutathione: interorgan translocation, turnover, and metabolism. Proc Natl Acad Sci U S A *76*, 5606-5610.

Griffith, O.W., and Meister, A. (1979b). Translocation of intracellular glutathione to membrane-bound gamma-glutamyl transpeptidase as a discrete step in the gamma-glutamyl cycle: glutathionuria after inhibition of transpeptidase. Proc Natl Acad Sci U S A *76*, 268-272.

Haberle, D., Wahllander, A., and Sies, H. (1979). Assessment of the kidney function in maintenance of plasma glutathione concentration and redox state in anaesthetized rats. FEBS Lett *108*, 335-340.

Habig, W.H., Pabst, M.J., and Jakoby, W.B. (1974). Glutathione S-transferases. The first enzymatic step in mercapturic acid formation. J Biol Chem *249*, 7130-7139.

Hagen, T.M., Aw, T.Y., and Jones, D.P. (1988). Glutathione uptake and protection against oxidative injury in isolated kidney cells. Kidney Int *34*, 74-81.

Hagen, T.M., Wierzbicka, G.T., Sillau, A.H., Bowman, B.B., and Jones, D.P. (1990). Bioavailability of dietary glutathione: effect on plasma concentration. Am J Physiol *259*, G524-529.

Halliburton, I.W., and Thomson, R.Y. (1965). Chemical aspects of compensatory renal hypertrophy. Cancer Res *25*, 1882-1887.

Han, D., Canali, R., Rettori, D., and Kaplowitz, N. (2003). Effect of glutathione depletion on sites and topology of superoxide and hydrogen peroxide production in mitochondria. Mol Pharmacol *64*, 1136-1144.

Harris, D.C., Chan, L., and Schrier, R.W. (1988). Remnant kidney hypermetabolism and progression of chronic renal failure. Am J Physiol *254*, F267-276.

Hayslett, J.P. (1979). Functional adaptation to reduction in renal mass. Physiol Rev *59*, 137-164.

Henry, M.A., Sweet, R.S., and Tange, J.D. (1983). A new reproducible experimental model of analgesic nephropathy. J Pathol *139*, 23-32.

Himmelfarb, J., Stenvinkel, P., Ikizler, T.A., and Hakim, R.M. (2002). The elephant in uremia: oxidant stress as a unifying concept of cardiovascular disease in uremia. Kidney Int *62*, 1524-1538.

Hise, M.K., Harris, R.H., and Mansbach, C.M., 2nd (1984). Regulation of de novo phosphatidylcholine biosynthesis during renal growth. Am J Physiol *247*, F260-266.

Hissin, P.J., and Hilf, R. (1976). A fluorometric method for determination of oxidized and reduced glutathione in tissues. Anal Biochem *74*, 214-226.

Holcomb, S.S. (2005). Evaluating chronic kidney disease risk. Nurse Pract *30*, 12-14, 17-18, 23-15; quiz 25-17.

Hostetter, T.H., Meyer, T.W., Rennke, H.G., and Brenner, B.M. (1986). Chronic effects of dietary protein in the rat with intact and reduced renal mass. Kidney Int *30*, 509-517.

Hostetter, T.H., Olson, J.L., Rennke, H.G., Venkatachalam, M.A., and Brenner, B.M. (2001). Hyperfiltration in remnant nephrons: a potentially adverse response to renal ablation. J Am Soc Nephrol *12*, 1315-1325.

Houser, M.T., and Berndt, W.O. (1986). The effect of unilateral nephrectomy on the nephrotoxicity of mercuric chloride in the rat. Toxicol Appl Pharmacol *83*, 506-515.

Humphreys, M.H., Etheredge, S.B., Lin, S.Y., Ribstein, J., and Marton, L.J. (1988). Renal ornithine decarboxylase activity, polyamines, and compensatory renal hypertrophy in the rat. Am J Physiol *255*, F270-277.

Hwang, S., Bohman, R., Navas, P., Norman, J.T., Bradley, T., and Fine, L.G. (1990). Hypertrophy of renal mitochondria. J Am Soc Nephrol *1*, 822-827.

Igawa, T., Kanda, S., Kanetake, H., Saitoh, Y., Ichihara, A., Tomita, Y., and Nakamura, T. (1991). Hepatocyte growth factor is a potent mitogen for cultured rabbit renal tubular epithelial cells. Biochem Biophys Res Commun *174*, 831-838.

James, E.A., Gygi, S.P., Adams, M.L., Pierce, R.H., Fausto, N., Aebersold, R.H., Nelson, S.D., and Bruschi, S.A. (2002). Mitochondrial aconitase modification, functional inhibition, and evidence for a supramolecular complex of the TCA cycle by the renal toxicant S-(1,1,2,2-tetrafluoroethyl)-L-cysteine. Biochemistry *41*, 6789-6797.

Janssen, R.J., Heuvel, L.P. Van Den., and Smeitink, J.A. (2004). Genetic defects in the oxidative phosphorylation (OXPHOS) system. Expert Rev Mol Diagn *4*, 143–156.

Johnson, H.A., and Vera Roman, J.M. (1966). Compensatory renal enlargement. Hypertrophy versus hyperplasia. Am J Pathol *49*, 1-13.

Johnson, H.A. (1969). Cytoplasmic response to overwork, in Compensatory renal hypertrophy, edited by Nowinski, W.W., and Goss, R.J., New York and London, Academic Press, 9–25

Johnson, H.A., and Amendola, F. (1969). Mitochondrial proliferation in compensatory growth of the kidney. Am J Pathol *54*, 35-45.

Jones, D.P., Sundby, G.B., Ormstad, K., and Orrenius, S. (1979). Use of isolated kidney cells for study of drug metabolism. Biochem Pharmacol *28*, 929-935.

Kaplowitz, N., Aw, T.Y., and Ookhtens, M. (1985). The regulation of hepatic glutathione. Annu Rev Pharmacol Toxicol *25*, 715-744.

Kidd, P.M. (1997). Glutathione: Systemic Protectant against Oxidative and Free Radical Damage. Alt Med Rev *2*, 155-176.

Klingenberg, M. (1979). Overview of mitochondrial metabolite transport systems. Methods Enzymol *56*, 245-252.

Krahenbuhl, S., Stucki, J., and Reichen, J. (1992). Reduced activity of the electron transport chain in liver mitochondria isolated from rats with secondary biliary cirrhosis. Hepatology *15*, 1160-1166.

Krahenbuhl, S., Talos, C., Lauterburg, B.H., and Reichen, J. (1995). Reduced antioxidative capacity in liver mitochondria from bile duct ligated rats. Hepatology *22*, 607-612.

Kwong, J.Q., Beal, M.F., and Manfredi, G. (2006). The role of mitochondria in inherited neurodegenerative diseases. J Neurochem *97*, 1659–1675.

Lash, L.H., and Jones, D.P. (1983). Transport of glutathione by renal basal-lateral membrane vesicles. Biochem Biophys Res Commun *112*, 55-60.

Lash, L.H., and Jones, D.P. (1984). Renal glutathione transport. Characteristics of the sodium-dependent system in the basal-lateral membrane. J Biol Chem *259*, 14508-14514.

Lash, L.H., and Anders, M.W. (1987). Mechanism of S-(1,2-dichlorovinyl)-L-cysteine- and S-(1,2-dichlorovinyl)-L-homocysteine-induced renal mitochondrial toxicity. Mol Pharmacol *32*, 549-556.

Lash, L.H., Jones, D.P., and Anders, M.W. (1988). Glutathione homeostasis and glutathione-S-conjugate toxicity in kidney. Rev Biochem Toxicol *9*, 29-67.

Lash, L.H., and Tokarz, J.J. (1990). Oxidative stress in isolated rat renal proximal and distal tubular cells. Am J Physiol *259*, F338-347.

Lash, L.H., and Zalups, R.K. (1992). Mercuric chloride-induced cytotoxicity and compensatory hypertrophy in rat kidney proximal tubular cells. J Pharmacol Exp Ther *261*, 819-829.

Lash, L.H., and Zalups, R.K. (1994). Activities of enzymes involved in renal cellular glutathione metabolism after uninephrectomy in the rat. Arch Biochem Biophys *309*, 129-138.

Lash, L.H., Tokarz, J.J., Chen, Z., Pedrosi, B.M., and Woods, E.B. (1996). ATP depletion by iodoacetate and cyanide in renal distal tubular cells. J Pharmacol Exp Ther *276*, 194-205.

Lash, L.H., Visarius, T.M., Sall, J.M., Qian, W., and Tokarz, J.J. (1998). Cellular and subcellular heterogeneity of glutathione metabolism and transport in rat kidney cells. Toxicology *130*, 1-15.

Lash, L.H., Putt, D.A., and Zalups, R.K. (1999). Influence of exogenous thiols on inorganic mercury-induced injury in renal proximal and distal tubular cells from normal and uninephrectomized rats. J Pharmacol Exp Ther *291*, 492-502.

Lash, L.H., Putt, D.A., Horky, S.J., 3rd, and Zalups, R.K. (2001a). Functional and toxicological characteristics of isolated renal mitochondria: impact of compensatory renal growth. Biochem Pharmacol *62*, 383-395.

Lash, L.H., Putt, D.A., and Zalups, R.K. (2001b). Biochemical and functional characteristics of cultured renal epithelial cells from uninephrectomized rats: factors influencing nephrotoxicity. J Pharmacol Exp Ther *296*, 243-251.

Lash, L.H., Putt, D.A., Hueni, S.E., Cao, W., Xu, F., Kulidjian, S.J., and Horwitz, J.P. (2002a). Cellular energetics and glutathione status in NRK-52E cells: toxicological implications. Biochem Pharmacol *64*, 1533-1546.

Lash, L.H., Putt, D.A., and Matherly, L.H. (2002b). Protection of NRK-52E cells, a rat renal proximal tubular cell line, from chemical-induced apoptosis by overexpression of a mitochondrial glutathione transporter. J Pharmacol Exp Ther *303*, 476-486.

Lash, L.H. (2005). Role of glutathione transport processes in kidney function. Toxicol Appl Pharmacol *204*, 329-342.

Lash, L.H., Hueni, S.E., Putt, D.A., and Zalups, R.K. (2005). Role of organic anion and amino acid carriers in transport of inorganic mercury in rat renal basolateral membrane vesicles: influence of compensatory renal growth. Toxicol Sci *88*, 630-644.

Lash, L.H., Putt, D.A., and Zalups, R.K. (2006). Influence of compensatory renal growth on susceptibility of primary cultures of renal cells to chemically induced injury. Toxicol Sci *94*, 417-427.

Lash, L.H. (2006). Mitochondrial glutathione transport: physiological, pathological and toxicological implications. Chem Biol Interact *163*, 54-67.

Lash, L.H., Putt, D.A., Xu, F., and Matherly, L.H. (2007). Role of rat organic anion transporter 3 (Oat3) in the renal basolateral transport of glutathione. Chem Biol Interact *170*, 124-134.

Lash, L.H. (2009). Renal glutathione transport: Identification of carriers, physiological functions, and controversies. Biofactors *35*, 500-508.

Lash, L.H. (2010). Renal toxicology: Cytoprotective systems within the kidney. In Comprehensive Series in Toxicology, 2nd Ed., Vol. *7*: Kidney toxicology, (R.G. Schnellmann, ed.), Elsevier, Oxford, Ch.5, pp. 117-150.

Lash, L.H.., and Cummings, B.S. (2010). Mechanisms of toxicant-induced acute kidney injury. In Comprehensive Series in Toxicology, 2nd Ed., Vol. *7*: Kidney toxicology, (R.G. Schnellmann, ed.), Elsevier, Oxford, Ch.4, pp. 81-115.

Lawrence, R.A., and Burk, R.F. (1976). Glutathione peroxidase activity in selenium-deficient rat liver. Biochem Biophys Res Commun *71*, 952-958.

Li, L., Lee T.K., Meier P.J., and Ballatori, N. (1998). Identification of glutathione as a driving force and leukotriene C4 as a substrate for oatp1, the hepatic sinusoidal organic solute transporter. J Biol Chem *273*, 16184-16191.

Lou, H., Ookhtens, M., Stolz, A., and Kaplowitz, N. (2003). Chelerythrine stimulates GSH transport by rat Mrp2 (Abcc2) expressed in canine kidney cells. Am J Physiol Gastrointest Liver Physiol *285*, G1335-1344.

Mastrocola, R., Restivo, F., Vercellinatto, I., Danni, O., Brignardello, E., Aragno, M., and Boccuzzi, G. (2005). Oxidative and nitrosative stress in brain mitochondria of diabetic rats. J Endocrinol *187*, 37-44.

McIntyre, T.M., and Curthoys, N.P. (1980). The interorgan metabolism of glutathione. Int J Biochem *12*, 545-551.

McKernan, T.B., Woods, E.B., and Lash, L.H. (1991). Uptake of glutathione by renal cortical mitochondria. Arch Biochem Biophys *288*, 653-663.

Meyer, T.W., Baboolal, K., and Brenner, B.M. (1996). Nephron adaptation to renal injury. In: The Kidney, edited by Brenner, B.M. 5th ed. Philadelphia, PA: W.B Saunders Company; 2011-2048.

Mittur A., Wolkoff A.W., and Kaplowitz N. (2002). The thiol sensitivity of glutathione transport in sidedness-sorted basolateral liver plasma membrane and in Oatp1-expressing HeLa cell membrane. Mol Pharmacol *61*, 425-435.

Molland, E.A. (1976). Aspirin damage in the rat kidney in the intact animal and after unilateral nephrectomy. J Pathol *120*, 43-48.

Mujais, S.K., and Kurtzman, N.A. (1986). Regulation of renal Na-K-ATPase in the rat: effect of uninephrectomy. Am J Physiol *251*, F506-512.

Murphy, M.P., Echtay, K.S., Blaikie, F.H., Asin-Cayuela, J., Cocheme, H.M., Green, K., Buckingham, J.A., Taylor, E.R., Hurrell, F., Hughes, G., *et al.* (2003). Superoxide activates uncoupling proteins by generating carbon-centered radicals and initiating lipid peroxidation: studies using a mitochondria-targeted spin trap derived from alpha-phenyl-N-tert-butylnitrone. J Biol Chem *278*, 48534-48545.

Nagahara, H., Ezhevsky, S.A., Vocero-Akbani, A.M., Kaldis, P., Solomon, M.J., and Dowdy, S.F. (1999). Transforming growth factor beta targeted inactivation of cyclin E:cyclin-dependent kinase 2 (Cdk2) complexes by inhibition of Cdk2 activating kinase activity. Proc Natl Acad Sci U S A *96*, 14961-14966.

Nath, K.A., Croatt, A.J., and Hostetter, T.H. (1990). Oxygen consumption and oxidant stress in surviving nephrons. Am J Physiol *258*, F1354-1362.

Nowinski, W.W. (1969). Early history of renal hypertrophy. In Compensatory renal hypertrophy. Edited by Nowinski, W.W., and Goss, R.J., New York and London, Academic Press, 1–8

Ochoa, S. (1955). Malic dehydrogenase from pig heart. Methods Enzymol. *1*, 735-745.

Orlowski, M., and Meister, A. (1963). Gamma-Glutamyl-P-Nitroanilide: A New Convenient Substrate for Determination and Study of L- and D-Gamma-Glutamyltranspeptidase Activities. Biochim Biophys Acta *73*, 679-681.

Ouellette, A.J. (1983). Messenger RNA regulation during compensatory renal growth. Kidney Int *23*, 575-580.

Palmieri, F., Bisaccia, F., Capobianco, L., Dolce, V., Fiermonte, G., Iacobazzi, V., Indiveri, C., and Palmieri, L. (1996). Mitochondrial metabolite transporters. Biochim Biophys Acta *1275*, 127-132.

Palmieri, F. (2004). The mitochondrial transporter family (SLC25): physiological and pathological implications. Pflugers Arch *447*, 689-709.

Paulusma, C.C., van Geer, M.A., Evers, R., Heijn, M., Ottenhoff, R., Borst, P., and Oude Elferink, R.P. (1999). Canalicular multispecific organic anion transporter/multidrug resistance protein 2 mediates low-affinity transport of reduced glutathione. Biochem J *338 (Pt 2)*, 393-401.

Rebbeor, J.F., Connolly, G.C., and Ballatori, N. (2002). Inhibition of Mrp2- and Ycf1p-mediated transport by reducing agents: evidence for GSH transport on rat Mrp2. Biochim Biophys Acta *1559*, 171-178.

Remuzzi, G., Benigni, A., and Remuzzi, A. (2006). Mechanisms of progression and regression of renal lesions of chronic nephropathies and diabetes. J Clin Invest *116*, 288-296.

Rius, M., Nies, A.T., Hummel-Eisenbeiss, J., Jedlitschky, G., and Keppler, D. (2003). Cotransport of reduced glutathione with bile salts by MRP4 (ABCC4) localized to the basolateral hepatocyte membrane. Hepatology *38*, 374-384.

Rosca, M.G., Mustata, T.G., Kinter, M.T., Ozdemir, A.M., Kern, T.S., Szweda, L.I., Brownlee, M., Monnier, V.M., and Weiss, M.F. (2005). Glycation of mitochondrial proteins from diabetic rat kidney is associated with excess superoxide formation. Am J Physiol Renal Physiol *289*, F420-430.

Santos, D.L., Palmeira, C.M., Seica, R., Dias, J., Mesquita, J., Moreno, A.J., and Santos, M.S. (2003). Diabetes and mitochondrial oxidative stress: a study using heart mitochondria from the diabetic Goto-Kakizaki rat. Mol Cell Biochem *246*, 163-170.

Santos, L.S., Chin, E.W., Ioshii, S.O., and Tambara Filho, R. (2006). Surgical reduction of the renal mass in rats: morphologic and functional analysis on the remnant kidney. Acta Cir Bras *21*, 252-257.

Scalera, V., Huang, Y.K., Hildmann, B., and Murer, H. (1981). A simple isolation method for basal-lateral plasma membranes from rat kidney cortex. Membr Biochem *4*, 49-61.

Scherzer, P., Wald, H., and Czaczkes, J.W. (1985). Na-K-ATPase in isolated rabbit tubules after unilateral nephrectomy and Na+ loading. Am J Physiol *248*, F565-573.

Schlondorff, D., and Weber, H. (1976). Cyclic nucleotide metabolism in compensatory renal hypertrophy and neonatal kidney growth. Proc Natl Acad Sci U S A *73*, 524-528.

Schlondorff, D., Trizna, W., De Rosis, E., and Korth-Schutz, S. (1977). Effect of testosterone on compensatory renal hypertrophy in the rat. Endocrinology *101*, 1670-1675.

Schmidt, E., and Schmidt, F.W. (1983). Glutamate dehydrogenase. In: Bergmeyer HU (ed.), Methods of Enzymatic Analysis, Academic Press, New York and London. 3rd edn., *2*, 216–227.

Shan, X., Jones, D.P., Hashmi, M., and Anders, M.W. (1993). Selective depletion of mitochondrial glutathione concentrations by (R,S)-3-hydroxy-4-pentenoate potentiates oxidative cell death. Chem Res Toxicol *6*,75-81.

Shapiro, J.I., Elkins, N., Reiss, O.K., Suleymanlar, G., Jin, H., Schrier, R.W., and Chan, L. (1994). Energy metabolism following reduction of renal mass. Kidney Int Suppl *45*, S100-105.

Shirley, D.G., and Walter, S.J. (1991). Acute and chronic changes in renal function following unilateral nephrectomy. Kidney Int *40*, 62-68.

Sinuani, I., Averbukh, Z., Gitelman, I., Rapoport, M.J., Sandbank, J., Albeck, M., Sredni, B., and Weissgarten, J. (2006). Mesangial cells initiate compensatory renal tubular hypertrophy via

IL-10-induced TGF-beta secretion: effect of the immunomodulator AS101 on this process. Am J Physiol Renal Physiol *291*, F384-394.

Soltoff, S.P. (1986). ATP and the regulation of renal cell function. Annu Rev Physiol *48*, 9-31.

Sorger, T., and Germinario, R.J. (1983). A direct solubilization procedure for the determination of DNA and protein in cultured fibroblast monolayers. Anal Biochem *131*, 254-256.

Steer, K.A., Sochor, M., Gonzalez, A.M., and McLean, P. (1982). Regulation of pathways of glucose metabolism in kidney. Specific linking of pentose phosphate pathway activity with kidney growth in experimental diabetes and unilateral nephrectomy. FEBS Lett *150*, 494-498.

Tellioglu, G., Berber, I., Yatkin, I., Yigit, B., Ozgezer, T., Gulle, S., Isitmangil, G., Caliskan, M., Titiz, I. (2008). Quality of life analysis of renal donors. Transplant Proc *40*, 50-52.

Toback, F.G., Smith, P.D., and Lowenstein, L.M. (1974). Phospholipid metabolism in the initiation of renal compensatory growth after acute reduction of renal mass. J Clin Invest *54*, 91-97.

Tribble, D.L., van den Berg, J.J., Motchnik, P.A., Ames, B.N., Lewis, D.M., Chait, A., and Krauss, R.M. (1994). Oxidative susceptibility of low density lipoprotein subfractions is related to their ubiquinol-10 and alpha-tocopherol content. Proc Natl Acad Sci U S A *91*, 1183-1187.

Vaziri, N.D. (2004). Oxidative stress in uremia: nature, mechanisms, and potential consequences. Semin Nephrol *24*, 469-473.

Wesson, L.G. (1989). Compensatory growth and other growth responses of the kidney. Nephron *51*, 149-184.

Wolf, G., and Neilson, E.G. (1991). Molecular mechanisms of tubulointerstitial hypertrophy and hyperplasia. Kidney Int *39*, 401-420.

Wolf, G., Mueller, E., Stahl, R.A., and Ziyadeh, F.N. (1993). Angiotensin II-induced hypertrophy of cultured murine proximal tubular cells is mediated by endogenous transforming growth factor-beta. J Clin Invest *92*, 1366-1372.

Xu, F., Putt, D.A., Matherly, L.H., and Lash, L.H. (2006). Modulation of expression of rat mitochondrial 2-oxoglutarate carrier in NRK-52E cells alters mitochondrial transport and accumulation of glutathione and susceptibility to chemically induced apoptosis. J Pharmacol Exp Ther *316*, 1175-1186.

Zalups, R.K., and Diamond, G.L. (1987). Mercuric chloride-induced nephrotoxicity in the rat following unilateral nephrectomy and compensatory renal growth. Virchows Arch B Cell Pathol Incl Mol Pathol *53*, 336-346.

Zalups, R.K., and Lash, L.H. (1990). Effects of uninephrectomy and mercuric chloride on renal glutathione homeostasis. J Pharmacol Exp Ther *254*, 962-970.

Zalups, R.K., and Henderson, D.A. (1992). Cellular morphology in outer medullary collecting duct: effect of 75% nephrectomy and K^+ depletion. Am J Physiol *263*, F1119-1127.

Zalups, R.K., Gelein, R.M., and Cherian, M.G. (1992). Shifts in the dose-effect relationship for the nephropathy induced by cadmium-metallothionein in rats after a reduction in renal mass. J Pharmacol Exp Ther *262*, 1256-1266.

Zalups, R.K. (1997). Reductions in renal mass and the nephropathy induced by mercury. Toxicol Appl Pharmacol *143*, 366-379.

Zhao, P., and Slattery, J.T. (2002). Effects of ethanol dose and ethanol withdrawal on rat liver mitochondrial glutathione: implication of potentiated acetaminophen toxicity in alcoholics. Drug Metab Dispos *30*, 1413-1417.

Zhao, P., Kalhorn, T.F., and Slattery, J.T. (2002). Selective mitochondrial glutathione depletion by ethanol enhances acetaminophen toxicity in rat liver. Hepatology *36*, 326-335.

ABSTRACT

COMPENSATROY RENAL HYPERTROPHY, MITOCHONDRIA AND REDOX STATUS

by

BAVNEET BENIPAL

December 2011

Advisor: Dr. Lawrence H. Lash

Major: Pharmacology

Degree: Doctor of Philosophy

A reduction in functional renal mass occurs in humans during aging and severe kidney damage from diseases, injuries, infections and congenital conditions and after nephrectomy. Nephrectomy, or surgical removal of a kidney or a section of a kidney, is performed for treatment of unilateral secondary renal cancer, infections and for kidney transplantation. As a result, the remaining renal tissue undergoes compensatory growth due primarily to hypertrophy, in which both the size and functional capacity of the remaining kidney are increased. Renal compensatory hypertrophy is associated with a series of physiological, morphological and biochemical changes that also have toxicological implications.

Previous studies have shown that compensatory renal cellular hypertrophy after uninephrectomy resulted in a hypermetabolic state, increased glutathione (GSH) content, but higher renal oxidative stress. These changes are also associated with increased susceptibility of renal proximal tubule cells to several drugs and environmental chemicals. Furthermore, our lab

also showed that overexpression of mitochondrial GSH transporters, the dicarboxylate (DIC, *Slc25a10*) and 2-oxoglutarate (OGC, *Slc25a11*) carriers, in NRK-52E cells, which are derived from normal rat kidney proximal tubules, exhibited increased mitochondrial GSH uptake, contents of GSH and protection from chemically induced apoptosis from exposure to nephrotoxicants.

Based on these previous observations, we hypothesized that compensatory renal hypertrophy after uninephrectomy alters renal function *in vivo* and mitochondrial status and modulation of mitochondrial redox status alters susceptibility to nephrotoxicants in the remnant kidney. In this study, we used a uninephrectomized (NPX) rat model to induce compensatory renal growth. Our results show alterations in renal physiological parameters consistent with modest renal injury, altered renal cellular energetics, upregulation of certain renal plasma membrane transporters, including some that have been observed to transport GSH, and evidence of increased oxidative stress in mitochondria from the remnant kidney of NPX rats. Our present results provide further evidence that compensatory renal hypertrophy is associated with mitochondrial hypertrophy and hyperpolarization and manipulation of mitochondrial GSH transporters in PT cells of hypertrophied kidney alters susceptibility to chemically induced injury. These studies provide additional insight into the molecular changes that occur in compensatory renal hypertrophy and should help in the development of novel therapeutic approaches for patients with reduced renal mass.

AUTOBIOGRAPHICAL STATEMENT

BAVNEET BENIPAL

EDUCATION:

Bachelors of Science, 2006

University of Michigan-Dearborn

Concentration: Biochemistry

Ph.D., 2011

Wayne State University, School of Medicine

Concentration: Pharmacology

Minor: Interdisciplinary Biological Sciences

Clinical Pharmacology Certification – National Institutes of Health

PUBLICATIONS:

Benipal, B, and Lash, L.H. Influence of renal compensatory hypertrophy on mitochondrial energetics and redox status. *Biochemical Pharmacology*. 2011 Jan 15;81(2):295-303.

Tiquia SM, Schleibak M, Schlaff J, Floyd C, **Benipal B**, Zakhem E, Murray KS. Microbial community profiling and characterization of some heterotrophic bacterial isolates from river waters and shallow groundwater wells along the Rouge River, southeast Michigan. *Environ Technol*. 2008 Jun;29(6):651-63.